AN ENERGY FLOW APPROACH TO PROGRESSIVE COLLAPSE

By

JOHN ROBERT WILKES

A DISSERTATION PRESENTED TO THE GRADUATE SCHOOL
OF THE UNIVERSITY OF FLORIDA IN PARTIAL FULFILLMENT
OF THE REQUIREMENTS FOR THE DEGREE OF
DOCTOR OF PHILOSOPHY

UNIVERSITY OF FLORIDA

2016

To Andrea

ACKNOWLEDGMENTS

The author is indebted to his adviser, the Theodore R. Crom Professor of Civil Engineering, Ted Krauthammer—the director of the research presented herein, as well as all preceding CIPPS studies on which this work is based.

TABLE OF CONTENTS

page

LIST OF TABLES

LIST OF FIGURES

LIST OF ABBREVIATIONS

ACI	American Concrete Institute
AISC	American Institute of Steel Construction
ANSI	American National Standards Institute
ASCE	American Society of Engineers
BMSP	Blast Mitigation for Structures Program
BO	Boston
BOCA	Building Officials and Code Administrators International, Inc.
BPAT	Building Performance
CIPPS	Center for Infrastructure Protection and Physical Security
D	Dead Load
DHS	Department of Homeland Security
DOD	Department of Defense
DSAS	Dynamic Structural Analysis Suite
DTRA	Defense Threat Reduction Agency
E	Energy Flow
$\dot{E}$	Rate of Energy Flow
EFA	Energy Flow Approach
FEMA	Federal Emergency Management Association
GSA	General Services Administration
ICC	International Code Council
JV	Joint Venture
L	Live Load
LS	Linear Static
LVBIED	Large Vehicle-Borne Improvised Explosive Device

MM-ALE	Multi-Material Arbitrary Lagrangian Eulerian
NBCC	National Building Code of Canada
NBS	National Bureau of Standards
ND	Nonlinear Dynamic
NS	Nonlinear Static
OSHA	Occupational Safety and Health Administration
PBS	Public Building Service
PC	Progressive Collapse
PCA	Portland Cement Association
PCI	Prestressed Concrete Association
SAC	Structural Engineers Association of California (SEAOC), Applied Technology Council (APC), and California Universities for Research in Earthquake Engineering (CUREe)
SEI	Structural Engineering Institute
TNT	Trinitrotoluene
UBC	Unified Building Code
UFC	United Facilities Criteria
WTC	World Trade Center
WUF-B	Welded Unreinforced Flange with a Bolted web

Abstract of Dissertation Presented to the Graduate School
of the University of Florida in Partial Fulfillment of the
Requirements for the Degree of Doctor of Philosophy

AN ENERGY FLOW APPROACH TO PROGRESSIVE COLLAPSE

By

John Robert Wilkes

August 2016

Chair: Theodor Krauthammer
Major: Civil Engineering

To advance understanding and mitigation of progressive collapse (PC), a novel approach is offered—an amalgamated derivation of Newton's second law, the conservation of mechanical energy, and three antecedent studies performed by researchers at Center for Infrastructure Protection and Physical Security.

The first of the antecedent studies revealed an energy – collapse relationship by demonstrating failure did not progress when the sum of energies from failed member(s) and the stored potential energy was fully absorbed/converted into the internal, or strain, energy in adjacent structural members (Szyniszewski and Krauthammer, 2012). Potential, or gravitational, energy is released through displacement, or collapse. Conversely, collapse progresses if strain energy is unable to absorb fully the released potential and excess kinetic energy. The second study quantified the contribution of connections to PC (Yim and Krauthammer, 2009). The third examined energy flow—yielding an energy-based load-impulse threshold for structural elements (Tsai and Krauthammer, 2015)—further substantiating the conclusions from the first study—an energy approach is superior to current force-based methods for determining damage.

A methodology is presented for an energy flow-based PC assessment of multi-story moment resisting frame buildings—an extension of the energy approach by Szyniszewski and

Krauthammer (2012), an expansion of modeling methods of steel connections by Yim and Krauthammer (2010), and inclusion of energy flow rate characterization by Tsai and Krauthammer (2015).

This research explains the contributions of *energy flow and the rate energy flow* to the susceptibility of collapse for mid-rise steel framed buildings. Energy-time histories of structural members were analyzed to determine energy flow throughout the structural system. All structural elements—including *all* connections—were represented numerically to determine the building's susceptibility to PC, including the sequence of failing members. Assessing PC susceptibility with the *incorporation of the rate of energy flow* for a structure that *accounts for the effects of connection strength* constitutes a novel approach. Advanced analytical methods, namely nonlinear transient dynamic finite element simulations were used to reveal the energy flow – energy flow rate – failure relationship. In addition, the efficacy of the Alternate Path method and the extent of redistribution required to accommodate blast-induced damage was examined.

CHAPTER 1
INTRODUCTION

1.1 Problem Statement

Progressive collapse is a phenomenon whereby localized failure(s) propagates to collapse of an entire multi-story structure, or a significant portion thereof. PC is a life safety issue, and although it can be initiated from a variety of loads, explosive effects are of significant concern and thus considered exclusively herein. The following statements by two demolition experts articulate well the motivations for this research (Loizeaux and Osborn, 2007): "It is important to provide sufficient energy absorption and load transfer mechanisms into [our] building structures so [that] they never gain adequate momentum to result in catastrophic failure. Ultimately, we envision [that] energy equilibrium calculation methods will play an important role in the design of structures to resist progressive collapse and we suggest [that] future research be focused in the area of energy equilibrium design methods."

Engineers practicing in the field of protective design need an accurate, efficient, and reliable method to assess PC susceptibility. Design manual provisions addressing PC incorporate an approach known as the Alternate Path method, which includes multiple notional single column removals under prescribed factored load combinations. Unfortunately, this method is inefficient, requiring an inordinate number of analyses due to a multitude of notional column removals. The Alternate Path method assures minimal redundancy of the vertical loading carrying system only, and given a lack of correlation with damage resulting from realistic air blasts, the efficacy of this approach for designing a PC-resistant structure is questionable. Hence, there are no design guidelines offering an efficient and reliable means to perform PC assessments.

1.2 Research Significance

It is widely known that fundamental energy principles govern the behavior of physical systems. Preliminary attempts were made to explore possible energy based methods for PC assessment, and a recent study showed that a threshold energy level could be associated with failures of specific structural elements. Nevertheless, characterizing the correlation between energy flow (magnitude and rate) and PC arguably constitutes a seminal contribution to the understanding of structural behavior under PC conditions. The Energy Flow Approach (EFA) presented here provides fundamental insight into the PC phenomenon, which the authors hope will lead to the development of an accurate, expedient, reliable, and effective method for assessing a building's susceptibility to PC. By using the EFA presented here, engineers can identify the most economical means for improving structural robustness, prioritize protective measures with utmost prudence, and quantify the maximum sustainable threat, or conversely, the minimum threat capable of initiating PC. The EFA presented is an accurate and rational energy flow based analytical procedure for PC of significant value to the structural engineering community, and may directly contribute to the current efforts in developing a performance-based disproportionate collapse design approach by the Structural Engineering Institute (SEI) of American Society of Civil Engineers (ASCE).

1.3 Objectives

In the context of assessing a structure's PC susceptibility, the work presented here demonstrates an EFA can represent the behavior of a typical mid-rise steel building in response to localized member failure(s), with repeatable accuracy. By analyzing energy-time histories from nonlinear transient dynamic finite element simulations, the results from this study correlate energy flow with member failure, and with subsequent effort, can evolve into an efficient

pragmatic approach for practicing engineers capable of accurately predicting the progression of collapsing members, i.e. PC.

1.4 Scope

The research presented here includes studying mechanical energy flow through structural steel frames to demonstrate the viability of an EFA for characterizing PC, by identifying how and where PC is initiated, and the manner and paths in which failure propagates throughout the structure. A ten-story moment-resisting steel frame (Appendix B), considered representative of typical mid-rise office buildings, was analyzed using the nonlinear transient dynamic finite element simulations software code LS-DYNA (Hallquist, 2014). Initially, the structure was analyzed under gravity loads per requirements of the United Facilities Criteria (UFC) 4-023-03 guideline (2013). The structure (under the same gravity loads) was then analyzed a second time after removing a single column on the first floor. Unlike the procedure defined in UFC 4-230-03 that requires performing several assessments with single column removals, this research entailed incrementally removing additional structural members (each additional member removal requiring a unique nonlinear transient dynamic finite element simulations) to examine if and when PC is initiated. The sequence of member removal was determined with a separate computer program capable of determining blast-induced structural damage (DSAS, 2012). Energy-time histories from the PC-inducing simulations were processed to confirm and quantify the energy flow-member failure correlation. Patterns emerging during these analyses demonstrated the energy – failure correlation. Displacement-, stress-, and strain-time histories were reviewed to confirm failure, as defined by UF guidelines. For select simulations, i.e. damage conditions, force time-histories were recorded and reviewed (for a predetermined set of members) to determine the accuracy and reliability of the EFA presented in comparison traditional force-based methods.

CHAPTER 2
BACKGROUND

Progressive collapse (PC) is the propagation of localized failure(s) through a structural system, ultimately resulting in failure of the entire building or of a significant portion thereof. Disproportionate collapse refers to a collapse event in which the scale of the final collapsed state is disproportionately larger than the loading event. PC is often confused with DC. For example, the final collapsed state of World Trade Center Towers 1 (North) and 2 (South) were disproportionate to the Boeing 767 and Boeing 757 impacts, respectively. In contrast, the final destructed state of the Alfred P. Murrah Federal Building can be considered commensurate, or proportional, to the detonation, understanding the charge weight and associated level of explosive energy of the detonation—approximately 4,000 lbs. of trinitrotoluene (TNT) (FEMA/ASCE, 1996). Several extensive discussions of collapse terminology, including the difference between progressive and disproportionate collapse, are available (Arup, 2011; Cormie et al., 2009; Starossek and Haberland, 2010). PC is the exclusive focus of this research.

PC mitigation efforts are categorized as either event control, addressing the loading event, or design methods (direct and indirect), which address the structural system. Items outside of the structure are often outside of the engineer's scope of work, e.g. social and/or political measures, control of hazardous substance access, etc. Focusing on the (the probability of) occurrence of abnormal loading, event control measures may be preferred, but are more often infeasible; e.g. increasing standoff distance in urban settings. Although instrumental and often the most effective, event control measures fall outside of the scope of this work, mentioned only to give the reader an understanding that a broad spectrum of non-structure related 'design' procedures are available.

Of the two design method options, indirect design improves a building's robustness implicitly. Three examples of such measures are given in the pending discussion of reactionary code development following catastrophic failures—ductility and continuity (1968: gas explosion in the Ronan Point apartments), perimeter column loss and reinforcement for reverse bending (1995: bombing of the Alfred P. Murrah Federal building), and fireproofing (2011: explosive airliner impacting World Trade Center Towers 1 and 2). Direct design mitigates PC through explicit measures. Specifically, direct design methods address the provision of minimum levels of strength, ductility, and continuity, as well as tie force methods (for both vertical and horizontal ties). Examples of such methods include the Alternate Path method and specific load resistance method. The EFA presented is categorized as a direct design method.

Additional nomenclature includes threat-specific, or threat-dependent, design, which falls in the direct design category. Threat-dependency means specified threats are considered. Non-specific threat, or threat-independent, designs consider—in a loose conceptual sense—but do not identify, or quantify, a threat. A nominal level of protection or damage is chosen, hopefully on a rational basis, but not necessarily as prescriptive design specifics are not required. For example, the Alternate Path method is the notional removal of a single column, which is threat-independent and unfortunately not rationally based on known blast loading events. Kirk Marchand and others have provided the pithiest descriptions—defining threat-dependent with, "when events and effects are quantified", and with threat-independent with, "events and/or effects are not quantified" (2008a; 2008b).

Further categorizing nomenclature includes either prescriptive or performance-based design. Prescriptive, specification, code, or provisional design uses known safety enhancing features. For example, afore mentioned seismic design requirements. Such methods are based

on experience and limited to the more traditional and regular building types. Performance-based design satisfies specific response criteria for defined threats. In contrast to prescriptive methods, this (performance-based) approach lends itself to atypical, non-traditional and irregular, buildings. Being so versatile to the considered threat, this approach can be threat-dependent or – independent, and designed indirectly or directly (Haberland and Starossek, 2009).

To conclude this review of PC-related nomenclature, design guidelines published over the last decade allows engineers to use one of four analytical methods. Increasing in complexity, these analyses are static – linear, static – nonlinear, dynamic – linear, and dynamic – nonlinear. Typical of design codes, simpler methods are inherently more conservative due to (load) increasing and (strength) reduction factors. Detailed discussions of these four analytical methods are available (Marjanishvili, 2004; Marjanishvili and Agnew, 2006).

2.1 A Review of PC: Seminal Events, Publications, and Regulatory Provisions

PC originated with the skyscraper, a consequence of advances in structural steel and elevator systems. In the United States (US), "high-rise" construction began in Chicago and New York City shortly after the civil war. Erection of early 'skyscrapers', as referred to at the time, increased from approximately 100 ft. – 150 ft. prior to the turn of the century, to approximately 300 ft. – 800 ft. during the first two decades of the twentieth century. Advances in (steel and concrete) material production, fabrication machinery, erection methods, elevator safety, electrical lighting, and indoor plumbing yielded technologies resulting in the creation infrastructure capable of accommodating significantly higher population densities, thereby satisfying the increasing work force demands. In broader terms, the industrial revolution allowed for vertical expansion of the built environment, and vice-versa. The result was the first generation infrastructure of modern day megalopolises—the most densely populated cities in world history.

Most common in developing countries, building collapses have and continue to occur in relative proportion to high-rise construction, e.g. Pemberton Mill (1860), Grover shoe factory (1905), and College Hall (1918) during America's Industrial Revolution. Although building codes were in development in the second half of the 1800's, provisions were limited in scope to fire protection and in jurisdiction to smaller areas, e.g. Baltimore's 1859 building code. Fortunately, design codes were developed for nationwide implementation at the turn of the century. American Concrete Institute (ACI) and American Institute of Steel Construction (AISC) began prescribing design regulations in 1910 and 1923, respectively. With the Chrysler and Empire State Buildings being the two notable exceptions, the great depression curtailed high-rise construction for several years, indirectly retarding advances in understanding the PC phenomenon. To elucidate—despite the ACI and AISC design codes continually improved since their respective inceptions at a rate (typically) no less than twice a decade—engineers did not distinguish between collapse and PC until WWII, i.e. the PC phenomenon was not even identified until the mid-20th century.

Prior WWII, and even until the advent of modern computing decades later, the understanding of such complex phenomena was constrained to hand calculations derived from theoretical formulations—analytical methods incapable of quantifying physical phenomenon as complex as the PC of a multifaceted 3-D structure. Hence, these classical tools were *extremely* limited relative to the computational tools of today, e.g. simulating explosions with state of the art finite element (FE) and computational fluid dynamic codes. With minimal advances in earthquake loading, design codes considered 'traditional loads' only—dead and live loads such as self-weight and human occupants, respectively. Complementary to traditional loads, abnormal loads were not incorporated into design standards until several decades after WWII. A

thorough treatment of abnormal loads for occupied building structures is available (Wright et al., 1973).

Focus on PC (which yielded publications) began during WWII. Initial advances were made by engineers in the United Kingdom (UK), namely John Baker and others, due to the abundance of bombarded buildings (primarily) within metropolitan London. Engineers learned a great deal about the response of structures to explosive loadings after analyzing the damage incurred in correlation with the structural type and configuration. The two most significant contributions included the superior performance of masonry infill walls and the high vulnerability of connections in multi-story steel framed buildings. A seminal text, with additional contributions, is available (Baker et al., 1948). In broader terms, Baker's research efforts showed PC is not solely a function of the (typically uncontrollable) extreme loading event, but the structural system as well. Consequently, the two PC mitigating categories were formed—event control and design methods. The findings from Baker's research was extensive, providing engineers concerned with protecting buildings with a substantial amount of data, which was used to help form the foundation of the field of protective design two decades later. However, PC was still rare (for several reasons, primarily structure type, size, geometric proportionalities, as well as construction materials and methods), and so collapse-related research was not a priority within the structural engineering community (Smith et al., 2010). This lack of investigative activity was even more prevalent in the US, where PC research lost support with the decreasing probability of WWII extending to US soil.

Although understanding of PC improved during the 1950's and 60's, practicing engineers did not have guidelines until *after* a gas leak explosion in 1968 within the corner unit on the 18th story of the 22-story Ronan Point apartment tower in London caused a PC (Allen and Schriever,

1973; Pearson and Delatte, 2005). Unfortunately, a number of PC catastrophes causing multiple fatalities did occur prior to 1968, but did not garner international attention. For example, the PC of a building under construction at Aberdeen University killed five workers and injured three others two years prior to the Ronan Point collapse (Hendry, 1967; Unknown, 1966). Published documents of this PC as well as other pre-1968 events are essentially non-existent. This may be a result of Ronan Point being the first occupied high-rise to have experienced PC due to an explosive loading event.

In contrast to the lack of attention from the structural engineering community at Aberdeen University, the Ronan Point collapse provided the impetus for development of PC guidelines around the world (Figure 2-1). This seminal event yielded codes or standards in the UK, Australia/New Zealand, Canada, Western Europe, Hong Kong, Northern Ireland, Scotland, and the US (Ellingwood and Dusenberry, 2005). Furthermore, over 300 papers were published during the first decade after the collapse (Longinow and Ellingwood, 1998) and more have continued to be published throughout the past forty-seven years. The first sets of PC codes were established in 1970 with *The Fifth Amendment* in the UK. In the US, the ANSI Standard A58.1-1972 included a minimal reference to PC and a more comprehensive treatment was not published for another decade (A58.1-1982). US-based codes were developed due to the tragedy at Ronan Point apartments—at local, state, regional, national, and international levels from various industry-regulating bodies. Examples included, but were not limited to, Building Officials and Code Administrators International, Inc. (BOCA), American Society of Civil Engineers (ASCE), Portland Cement Association (PCA), Prestressed Concrete Institute (PCI), New York City building codes, Connecticut Building Codes, American Concrete Institute (ACI), International Code Council (ICC), and so on (Pearson and Delatte, 2005). Furthermore, Ronan Point-related

code updates continued for over thirty years in both the US and Canada (ASCE, 2002). For example, in Canada, codes were developed to account for PC shortly after Ronan Point (NBCC, 1970) and subsequently improved upon (NBCC, 1975) through research (Taylor, 1975). Although US codes did consider extreme loading events prior to Ronan Point, they were limited to fire and earthquakes.

The structural engineering community responded so strongly to the Ronan Point collapse because the building's structural system (Larsen-Nielsen) was used extensively throughout the UK and abroad (Systems, 1968), housing tens of thousands of residents at the time of the Ronan Point accident. In fact, Ronan Point was one of nine identical buildings in London alone. Following WWII, several governments, including the US, constructed large-scale housing developments to shelter the booming post-war population. For countries that experienced destruction (of significant portions) of housing infrastructure, expediently constructed housing was urgently needed. The Larsen-Nielsen system was advantageous because all structural components, except for the foundation and columns, were precast concrete built off site, yielding a very rapid erection schedule.

The engineering community made significant strides mitigating PC in response to the tragedy at Ronan Point. However, construction of mid- and high-rise buildings outpaced increased understanding of, and thus corresponding preventative measures for, PC in the following decades. Indicative of the dangers with high-rise construction, all documented PC events with multiple fatalities in the U.S. over the next twenty-seven years occurred during construction. Five of the most well-known and documented accidents are listed as follows:

1. On January 25, 1971, in Boston, Massachusetts, a poorly constructed sixteen-story building completely collapsed due to punching shear failure—killing four laborers and injuring another twenty workers (King and Delatte, 2004).

2. Premature removal of shoring killed fourteen and injured another thirty-four during construction of the Skyline Plaza in Fairfax County, Virginia (Burnett and Leyendecker, 1973).
3. Similarly, but exacerbated due to design errors, the entire five-story Harbour Cay Condominiums pancaked in Cocoa Beach, Florida, on March 07, 1981 due to punching shear of the under-designed and poorly constructed slabs, killing eleven and injuring another twenty-three workers (Lew et al., 1981).
4. December 19, 1985, the twenty-two story Wedbush building collapsed due to the falling of a girder from a crane onto an already overloaded floor, killing three workers.
5. Due to "sloppy construction practices", inadequate shoring and specifically, a loss of support from a lifting jack during placement of three slabs on upper levels, twenty-eight workers died on April 23, 1987 at the L 'Ambiance Plaza (Martin and Delatte, 2000).

Although not exclusive to PC, Occupational Safety and Health Administration (OSHA) investigated *ninety-six* collapses during construction that involved fatalities and injuries between 1990 & 2008 (Arup, 2011).

Tens of fatal PC tragedies occurring in the US during construction did not garner major media attention for nearly three decades. This ended with the bombing of the Alfred P. Murrah Federal Building in Oklahoma City on April 19, 1995 (Figure 2-2). One-hundred sixty-eight people were killed, including nineteen children under the age of six and more than six-hundred eighty were injured (Mlakar et al., 1998). Although several US occupied structures were attacked prior to 1995, these tragedies occurred on foreign soils. Thus, this bombing of the Alfred P. Murrah Federal Building was the first seminal event on US soil that caused improvements in the existing, or developments of new, PC codes, guidelines, and specifications (FEMA/ASCE, 1996). This tragic event is considered by many in the community of protection engineering as a turning point toward a new era of terrorism.

Despite being designed and built in accord with all codes and provision at the time of construction—in 1977 (Corley et al., 1998), approximately half of the entire Alfred P. Murrah Federal Building collapsed in a *rapid* and catastrophic manner. This horrific event revealed that the existing codes and provisions did not sufficiently address PC. Following the bombing,

Federal Emergency Management Agency's (FEMA) Building Performance Assessment Team (BPAT) investigated the tragedy and subsequently published "The Oklahoma City bombing: Improving building performance through multi-hazard mitigation" (FEMA, 1996). Hinman and Hammond, among others, provided several recommendations based upon the findings from this report.

In addition to detailing the bombing, including, but not limited to, the progression of the collapse, this FEMA report focused on using seismic detailing to aid in mitigating PC—an explicit responsibility assigned to the BPAT. Although many of the findings from this report were specific to the event—the structure, site, charge weight, and charge location, the recommendations from this report were consequently applied to circumstances outside of appropriate applicability. To elaborate, the Alfred P. Murrah Federal Building had a unique design in that it had a very large transfer beam located on the second story—a non-redundant and vulnerable frame. In addition, the side of the building with this transfer beam had virtually no standoff from the street, allowing the terrorist to park the Large Vehicle-Borne Improvised Explosive Device (LVBIED) directly adjacent the building's exterior. Lastly, and although repeatable, the quantity of the explosive material would be very difficult for potential terrorists to acquire following this event without garnering significant attention from national security agencies. Due to these structural aspects specific to the Alfred P. Murrah Federal Building, the significant charge weight—approximately 2,000 of TNT equivalent, and detonation location, an offset distance roughly equivalent to the width of a sidewalk, the recommendations of the BPAT should have been provided with more extensive qualifications.

To summarize, BPAT found, "Many of the techniques used to upgrade the seismic resistance of buildings also improve a building's ability to resist the extreme loads of a blast and

reduce the likelihood of progressive collapse following an explosion" (FEMA, 1996). Again, although correct, many of the findings from this study were case-specific. Unfortunately, some of the protective design community misused these seismic-based design recommendations, and continue to do so, since the publication of the FEMA report.

Unfortunately, the misapplication of seismic design methods to mitigate the effects from blast loading events occurred again the Northridge earthquake. Many in the seismic design community leveraged earthquake-induced structural failures to promote seismic design and retrofit methods, regardless of their respective efficacies. Again, broad language stimulated many engineers, as well as researchers in academia, to over-state the applicability and efficacy of seismic design for PC mitigation—yielding misguided efforts through oversimplification of the PC phenomenon. Overstating the mitigating measures of seismic design resulted in practicing engineers inadequately addressing PC and arguably retarding understanding of PC. This problem was exacerbated with publications (Corley et al., 1998) and presentations (Corley, 2002) recommending the open-ended use of seismic design for PC mitigation. These publications did not stipulate the appropriate limitations of seismic design provisions for mitigating PC. Consequently, many engineers and industry entities proceeded with recommending seismic design for blast mitigation, often resulting in erroneous designs, i.e. yielding no mitigation against PC. For example, Portland Cement Association (PCA) provided a guide with specificity regarding the applicability of the seismic design codes for beams to blast loading events. In fact, some designs have not only been ineffective against blast loadings, but have unduly increased the likelihood of a catastrophic PC, e.g. inappropriate use of the bridging design approach.

In contrast, a few contributions from the seismic field have been applied astutely for use in blast mitigation, e.g. FEMA, 2010. However, there are significant differences between the two—seismic and blast loading events, many of which are mutually exclusive and require approaches specific to the time domain of the applied loading. In addition, other researchers have shown taking a seismic reinforcing approach to prevent PC, by means of a single case study of the Alfred P. Murrah Federal Building only, can be misleading and dangerous (Baldridge and Humay, 2003). "Some engineers have asserted that widespread adoption of earthquake engineering practices would be sufficient to mitigate risk from abnormal loads and PC. Such assertions must be viewed with skepticism" (Ellingwood, 2006). Other prudent engineers/researchers have reported seismic detailing, "…is not a complete solution" and importantly that seismic detailing is in "conflict" with blast resistant design—specifically, mechanical fusing of a building structure (Osteraas, 2006).

Fortunately, A few provisional codes have confirmed the fundamental differences between seismic and blast loading events. For example, "However, there are also significant differences between seismic and blast design, so seismic upgrades should only be used as a basis for blast resistant upgrades by engineers with blast design experience" (ASCE, 2011; ASCE 2011b). Additional differences were observed with continued research, e.g. "… it seems there is no concern about the occurrence of PC under seismic loading in a one column loss scenario for steel, special moment, resisting systems" (Tavakoli and Alashti, 2012). Despite the known differences between seismic and blast loading events, the ASCE's "41 Seismic Rehabilitation of Existing Buildings" (ASCE, 2008) procedures were adopted and modified for the GSA's "Alternate Path Analysis & Design Guidelines for Progressive Collapse Resistance" (GSA, 2013). In summary, the application of seismic design provisions to address PC were overstated

and overused following the bombing of the Alfred P. Murrah Federal building and the Northridge earthquake. With continued effort from informed engineers with blast experience, the misapplication of seismic methods for blast mitigation can be eliminated.

In contrast to the (relatively) more recently developed PC-mitigating guidelines, seismic codes have been under continued development since 1927, e.g. the Unified Building Code (UBC). Interestingly, and quite unfortunately, our society has been more reactive than proactive, and thus codes addressing seismic activity and PC share a fundamental commonality—both have been developed largely in response to catastrophic events; i.e. code development has been predominantly reactive. One limitation of this approach is that reaction-based code development typically yields an indirect design approach. Some of the more significant examples include provisions of sufficient ductility and continuity (Ronan Point), designing for loss of a perimeter column and provisions of sufficient reinforcement for reverse bending in beams and slabs (Alfred P. Murrah Building), and sufficient fireproofing protection of steel members (World Trade Center towers).

Current regulatory guidelines include indirect and direct design methods. Indirect design methods include measures such as providing minimum levels of strength, ductility and continuity, and tie force methods (for vertical and horizontal ties). Direct design methods include measures such as the Alternate Path method and specific load resistance method per the "Alternate Path Analysis & Design Guidelines for Progressive Collapse Resistance" (GSA, 2013) and the "Minimum Antiterrorism Standards for Buildings UFC 4-010-01" (DOD, 2000; 2007; 2013a).

Although a significant amount of guidelines were provided to engineers after the bombing of the Alfred P. Murrah Federal Building, and significantly more after the 9/11 attacks,

the efficacy of code provisions remain questionable. After the bombing in Oklahoma City, the Defense Threat Reduction Agency (DTRA) published the "Blast Mitigation for Structures" document under the Blast Mitigation for Structures Program (BMSP). The charge of this document was to, "reduce loss of life and injuries of the occupants of… buildings that are targets of terrorist attack" (Committee, 1999). However, this effort did not receive continued funding and the 1999 publication was the first and last edition. The following year, the US General Services Administration (GSA) published guidelines containing direct methods, although branded as a threat independent methodology, for assessing the potential for PC (GSA, 2000). This publication, the Public Building Service (PBS) Facilities Standards required one-member redundancy, with no correlation to susceptibility, vulnerability, or threat level. The Department of Defense (DOD) also provided guidance to practicing engineers the following year—prior to the September 11 attacks (DOD, 2001).

After collapse of both World Trade Center skyscrapers in New York City on September 11, 2001 (9/11), three different government agencies responded by publishing updated design guidelines. The US GSA updated the PBS Facilities Standards with another round of provisions containing threat-independent design methods with significant reference to previous manuals, which included general performance-based provisions only, (GSA, 2003). These guidelines were an evolution of the 2000 PBS Facilities Standards, but with an exemption for certain buildings from PC considerations, also with no correlation to susceptibility, vulnerability, or threat level. Again in 2003, the DOD published "Design of Buildings to Resist Progressive Collapse UFC 4-023-03", expanding the 2001 document for the US civilian design community (Stevens et al., 2012). Even though the GSA's "Progressive Collapse Guidelines developed by the General Services Administration" (2009) and DOD's "Design of Buildings to Resist

Progressive Collapse developed by the Department of Defense" (2013b) are considered the "most comprehensive PC mitigation and modelling guidelines"(Byfield et al., 2014), both provide indirect design methods only. In the DOD's United Facilities Criteria (UFC) 4-023, derived from UK provisions, indirect methods prescribe minimum inter-member connectivity, thereby eliminating requirements of abnormal loading. Similarly, Federal Emergency Management Agency published "Reference Manual to Mitigate Potential Terrorist Attacks against Buildings" (FEMA 426), which was part of the Risk Management Series (FEMA, 2003a).

Unfortunately even less prescriptive and of less value to practicing engineers, ACI 318 has no explicit mention of redundancy or alternate load path and hence no threat specificity (2004). Similarly, ASCE 7 suggests an unspecified degree of redundancy and alternate load paths, both threat independent (2002; 2005). In 2005, NIST's recommendations were, "a call for redundancy in all buildings, independent of the nature of level of threat to the building. The report also calls for the development of methods for the rational analysis and design of buildings for specific threats (which would, presumably, supersede the absolute redundancy requirement)" (Nair, 2004). However, there are no requirements, only conceptual suggestions, thereby lacking the specificity required for practicable design. Furthermore, research has found codes would have been ineffectual even if the provisional methods were employed prior to the abnormal loading event (Table 2-1).

An additional example of such shortcomings is load sensitivity—forces just above the maximum design loads should not produce significantly different failure responses. Although "It is recommended that the good practice requirement is introduced that the design of a building should be insensitive to the design assumptions by examining the performance of the building

under higher-than-normal design requirements" explicit criteria does not exist (Arup, 2011). Similar to the suggestive wording in design codes, with no explicit prescriptive provisions, this load sensitivity issue remains unimproved. Design codes are deficient in defining performance-based criteria for loads beyond the traditional loads, and thus need further development for PC. Understanding so many shortcomings are abundant throughout PC design provisions and the ever-increasing popularity of mid- and high-rise buildings, the need for improved understanding and mitigation of PC is an urgent need, and will continue to be increasingly imperative.

2.2 The Alternate Path Method in Regulatory Design Provisions

The Alternate Path method is a direct design measure, ensuring only minimal redundancy in the vertical load-bearing system of a multi-story structure. Procedurally, the Alternate Path method entails removing a column at various prescribed locations. For US-based guidelines, the Alternate Path method has origins in ASCE 7-88, which includes illustrations of structural systems. These illustrated Alternate Path method provisions were included in the subsequent '93 edition, removed in the '95 edition, and returned for all post-95 editions. Although ASCE 7-10 discusses the Alternate Path method in the commentary, "no quantifiable or enforceable requirements for progressive collapse prevention are provided" (Ghosh, 2014). The Alternate Path method is more of a suggestion, not a requirement, in ASCE 7-10, and, due to the nature of this specification, considers loading related information only. As intended, ASCE 7-10 is referenced in all three of the bulleted codes listed below for prescribing (the required) combinations of traditional loads.

The Alternate Path method is included in the provisions of several design specifications. For the sake of clarity, the specifics of the Alternate Path method discussed herein are per the following UFC specification:

- Design of Buildings to Resist Progressive Collapse UFC 4-023-03

    - Includes 14 July 2009 and 1 June 2013 (Change 2) updates/revisions
    - Located in § 3-2 p. 33

Two additional US regulatory provisions commensurate with the unofficial authority, the DOD's UFC 4-023-03, include the following:

- Alternate Path Analysis & Design Guidelines for Progressive Collapse Resistance
    - Includes 24 October 2013
    - Located in § 3.2, pp. 7 – 16
- Blast Protection of Buildings ASCE/SEI 59-11

There are also a large number of additional domestic (local, regional, and national) and international design codes that include the Alternate Path method, many of which reference ASCE, UFC, GSA, or others. Comprehensive presentations of such provisions are available, e.g. Dusenberry, 2003.

In contrast, the UFC and GSA design guidelines are required for qualifying buildings. Qualification, or exclusion, of these guidelines is determined per the occupancy categories. More obvious are the specification designations, UFC 4-023-03 including change 2 evolved from the initial, and equally titled, 2003 edition. The 2013 GSA document listed above evolved from the 2003 GSA document, "Progressive Collapse Analysis and Design Guidelines for New Federal Office Buildings and Major Modernization Projects"—essentially a subsequent and expanded version of the 2000 GSA PBS Facilities Criteria.

For purposes of performing a comprehensive review, the ten-story office building is classified occupancy category III. This designation is most appropriate given this structure would be designed to accommodate over 500 occupants, as nearly 12,150 m^2 of office space is provided; UFC 4-023-03 § 2-1 ref. UFC 3-310-01 § 1-6.1. In addition, the Alternate Path method requires single column removals at three external and four internal locations on predetermined floors. The exterior columns are: 1) near the middle of the long edge, 2) middle of the short edge, and 3) at a corner (UFC § 3-2.9.2.2). Although removal is prescribed for

multiple stories (UFC § 3-2.9.2.3), only columns at ground level are considered. As per the leading US guidelines (ASCE 59-11, GSA, and UFC), three different analytical methods, with associated acceptance criteria for each, are allowed when performing the Alternate Path method. These three methods include linear static (LS) § 3-2.11, Nonlinear Static (NS) § 3-2.12, and Nonlinear Dynamic (ND) § 3-2.13, all of UFC 4-023-03. Each analysis method includes unique modeling stipulations such as loading combinations, procedural methods, and increase factors. Force and displacement criteria are also associated with each of these analytical methods, as well as a fourth: nonlinear dynamic per 4-023-03 (UFC 2013).

Moving forward, ASCE 7-16 will have a significant expansion of performance-based design criteria for extreme loadings, e.g. an entire chapter will devoted to mitigation from Tsunami loading events. As the reader may have surmised, this is again a reactive measure—in response to the tragic events at the Fukashima Daiichi Nuclear facility on March 11, 2011.

For the reasons discussed above and in the following section below, the Alternate Path method is not an effective approach for mitigating PC. Fortunately, several PC experts have published their findings in an effort to minimize use of the Alternate Path method; e.g. "analytical approaches such as the alternate path method and specific local resistance should not be used as the primary preventive measures for resistance to progressive collapse" (Dusenberry and Juneja, 2003; Ellingwood and Dusenberry, 2005; Ellingwood, 2007; Ellingwood et al., 2007).

2.3 Structural Damage Incurred from Known Explosive Terrorist Threats

The Alternate Path method correlates to a single column failure. However, blast-induced damage from known explosions have resulted in destruction of the impacted building well in excess of a single column—regardless of a building's response with respect to PC. For example, the Alfred P. Murrah Building was highly susceptible to PC, as evidenced by the rapid PC (recall

Figure 2-2) following the loss of three columns supported by the non-redundant transfer beam (FEMA/ASCE, 1996). In contrast, the Kansallis House (Figure 2-3) exhibited robustness—enduring the destruction of 1367 ft^2 (127 m^2) of the first floor, and 785.8 ft^2 (73 m^2) of both the second and third floors, in addition to three columns (Crowder, 2005). PC events have often had charge weights in the thousands of pounds, deliverable only by very large transport vehicles. Although the four explosive events discussed thus far (Ronan Point, Alfred P. Murrah Federal Building, World Trade Center Towers 1 and 2, and Kansallis House) may not be considered representative of the majority of blast threats, the overwhelming majority of explosive threats have resulted in damage well beyond destruction of a single column.

The disparity between a single notional column removal and the damage incurred from actual blast loading events is contrasted further when considering the level of threat, i.e. explosive energy, required to initiate collapse. Typically, the charge weight commensurate with initiating PC of a multi-story steel frame building is at least several hundred, if not thousands of pounds. Thus, a heavy transport vehicle (capable of such a payload) is required, e.g. the 1983 Beirut barracks bombings. Hence, a vehicle-transported explosion such as a car bomb is a likely threat, assuming a number of other factors. The diagrams below illustrate an extreme (explosive) loading event and charge weights as a function of vehicle size. Figure 2-4A illustrates an airblast delivered by large van, or small truck, with the primary event parameters illustrated. Figure 2-4B defines damage levels as a function of standoff distance and weapon yield. For example, a 500 kg (1,102 lb.) charge of TNT, which can be delivered by van, detonated 4.0 m from the building exterior yields a scaled distance of 0.6348 $m/kg^{1/3}$, which is in the industry standard distance to target-cube root weight of charge ($dist./wt.^{1/3}$) format. Additional information regarding blast events are available (FEMA 2003a; FEMA 2003b).

Although a myriad of viable threats exist, especially in more densely populated urban environments (with multiple forms of mass transportation adjacent, if not internal, to occupied buildings), the threats discussed are indicative of a vehicle-transported threat, or car bombing. Specifics of the threats considered may be highly critical when designing and/or analyzing a structure, given any number of potential building characteristics and threat conditions. However, such specificities are of no import in this study as threats capable of initiating PC are assumed. The methods used to simulate the air blasts considered are discussed (§ 2.4).

Regardless of the severity of blast loading, accurately predicting threat-specific damage levels requires use of sophisticated numerical tools. The state-of-the-art numerical modelling approaches typically employed are either Computational Fluid Dynamics, Finite Element Analysis, or a combination of both, e.g. Multi-Material Arbitrary Lagrangian Eulerian (MM-ALE) simulations. Unfortunately, all of these methods are technically rigorous, time-intensive, and computationally expensive, thus rendering this approach impractical for most practicing design engineers. In lieu of utilizing such technically rigorous software, several simplified programs have been developed to serve the protective design community. For example, several programs calculate the pressure and impulse to be applied to a structure in a significantly more efficient manner than explicitly modeling an explosion, e.g. ConWep (Hyde, 1988). However, such programs calculate the applied loading, i.e. pressure, time histories only. In compliment to such software, there are also simplified programs available to calculate damage once the impulsive loading curve has been characterized. Thus, a software package capable of using the detonation parameters to not only calculate the applied loads, but also determine the resulting structural damage was used: Dynamic Structural Analysis Suite (DSAS) (Astarlioglu and Krauthammer, 2012).

2.4 DSAS: Simulating Explosions

The following introduction to the Dynamic Structural Analysis Suite (DSAS) software program (version 4.2.0.26229) is included to aid in explaining the role of DSAS within this research study. DSAS is a multifunctional structural analysis program for modeling the response of a given structural component to static and dynamic loads (Astarlioglu and Krauthammer, 2012). This program was developed to analyze severe dynamic loads by simplifying a structural member's resistance into a single degree-of-freedom function, thereby expediting the analysis. Reinforced concrete, steel, and masonry materials are available.

DSAS's Air Blast Loading module (Figure 2-5) generates the pressure impulse loading applied to a given structural member within the blast area. Using the pressure-time history generated by the Air Blast Loading module (Figure 2-6), DSAS performs a time-history analysis for the structural member under consideration. In addition, moment-curvature, resistance functions, and failure determination are also generated. DSAS has been validated for assessing structural performance, most notably for identifying threat levels capable of causing structural damage.

2.5 Ten-Story Moment-Resisting Steel Frame Building

2.5.1 Historical Reference and Relevant Antecedent Research

The structure of interest is a ten-story steel frame—a hypothetical building designed to code as part of a large multi-entity collaboration of engineers, researchers, and investigators—a result of seismic mitigation efforts in response to the Northridge earthquake on January 17, 1994. The Structural Engineers Association of California (**S**EAOC), Applied Technology Council (**A**TC), and California Universities for Research in Earthquake Engineering (**C**UREe) (SAC) joint venture (JV) commissioned the design of three buildings in seismically active US cities (FEMA, 2000). The structure in this study is the mid-rise building located in Boston,

MA—a designated Seismic Zone 2A. The primary interest was the pre-Northridge (WUF-B) moment connections, due to the failures during the Northridge earthquake (Gupta and Krawinkler, 2000).

Although initially for purposes related to seismic events, these buildings were later studied for addressing blast-loading events, in part due to the plethora of published data developed from the seismic research. Several blast studies (Lim and Krauthammer, 2006; Krauthammer, 2007a; 2007b) focused on various building characteristics, including the WUF-B connections. Multiple deficiencies were identified, thus requiring retrofits for preventing PC (Krauthammer et al., 2004b). Most relevant to the present study, the ten-story building designed for Boston was used in an earlier CIPPS study, where simplified models of the WUF-B connections were developed for determining the effects of the connections on PC (Yim and Krauthammer, 2009).

2.5.2 Structural System

The 10-story, or 9-story with a basement, building has 29,000 ksi steel throughout, with 50 ksi yield columns, and 36 ksi yield beams and girders. All slabs are comprised of 3,500 ksi concrete with a 4-ksi yield, are 100 mm thick with 1.5% 36 ksi yield mild steel reinforcing in both directions. The framing plan is shown—illustrating all column orientations, connection type (moment or shear), and the associated perimeter beams tabulated per floor (Figure 2-7).

An additional illustration provides all column cross-sections with splice locations and elevations. For simplicity, the dissimilar column layout supporting the penthouse (not depicted) is not included in the numerical models. Thus, columns C-3, C-4, D-3, D-4, E-3, and E-4 are modified to match the same cross sections and splice elevations of the remaining interior columns (Figure 2-8). Further details are available (Appendix B).

2.5.3 Reductionist Modelling of Connections by Yim and Krauthammer

As mentioned above (§2.5.1), an antecedent CIPPS study examined the effects of connections on PC (Yim, 2007). This prior study, of primary import to the work presented here, incorporated the moment and shear connections of the mid-rise steel frame discussed above—concluding connection strength is a significant contributor PC, thus requiring numerical representation assessments of susceptibility. In this prior study, connections were modeled using a reductionist approach. Simulating PC of a structural frame that accounts for the behavior of all connections with highly discretized continuum elements is too computationally expensive. Thus, a significantly more (computationally) efficient approach was taken, but with minimal loss in accuracy. Most succinctly, rotational springs were used to represent the connections, resultant beam elements represented the columns and girders, and shell elements represented the slabs.

Initially, models with highly discretized resolutions of continuum (brick) elements represented all structural components in and around the connections. With rotations defined as the relative motions between the beam and column, quasi-static simulations were performed for both moment and shear connections. The moment- and rotation-time histories from these simulations were extracted to develop nonlinear moment-rotation (M-ϕ) curves. The numerical results were validated with experimental data obtained from the AISC Northridge Test program (Engelhardt and Sabol, 1994).

Yim's simplified connection models used Abaqus-specific Join and Cardan features. The Join feature constrained, or prevented, translation between the girder and column. Rotation was defined with a Cardan-angle parameterization of finite rotations, also known as a 1-2-3 parameterization or yaw-pitch-roll parameterization. These Cardan-angle parameterizations

were defined using the nonlinear moment-phi (M-ϕ) curves from the computationally expensive continuum models.

Additional quasi-static simulations were performed, verifying the simplified connection method, i.e. Join + Cardan. Using equivalent boundary conditions, loads were applied to the resultant beam elements representing the girders, in both the vertical and horizontal planes. The resulting nonlinear M-ϕ curves from these simplified connection models were then compared to the resultant curves from the continuum models. The simplified models described the connection behavior with acceptable accuracy and with significant reductions in computation expense. Thus, the Join + Cardan approach was used throughout Yim's simplified building models.

This preceding study, antecedent in nature to the proposed, verified using the nonlinear M-ϕ curves from the quasi-static simulations is, "computationally efficient and reliable not only in PC rate quasi-static analyses but in the blast-rate dynamic analyses considering high velocity nonlinear and failure behaviors. The simplified frame models considering connector element properties were capable of maintaining good accuracy in the quasi-static and blast-rate loading simulations while effectively reducing simulation time. It was concluded that frame analyses could be carried out readily and accurately using simplified beam and connector elements instead of modeling detailed and complicated combinations of the beam, column, and connection members" (Yim and Krauthammer, 2009). Consequently, the nonlinear moment-rotation curves developed by Yim are used in the LS-DYNA models in the work presented here. These curves and all related support information are available (Yim, 2007).

2.6 Review of Energy and Traditional Approaches to Structural Behavior

2.6.1 Energy and Power Flow Analyses for Mechanical Engineering Applications

Mechanical engineers have been studying energy flow, referred to as energy- or power-flow in the mechanical engineering field, in structural components for several decades. In fact, finite element analyses became the preferred power flow approach to vibration problems nearly thirty years ago (Hambric, 1988). While this research is related to the proposed work, with respect to energy conservation and solid mechanics, such work has focused on vibrational and acoustical behavior under steady state conditions. In addition to the inherent disparity between steady state and failure, there a number of additional fundamental differences. Figure 2-9 illustrates differences between the frequency and amplitude domains of vibration and acoustics, seismic, blast, and wind. An additional region illustrating PC response was added to illustrate the relative period and amplitude of PC to the specified hazards, i.e. extreme event loadings. It is also understood structural materials are rate dependent, not to mention the differences in linear and nonlinear behavior. Due to these disparities between the fundamentals of failure, and vibrational and acoustic phenomena, these prior energy- and power-flow studies are related to PC applications only from the broadest perspective framed with respect to energy principles.

2.6.2 Traditional Force-Based Approaches to Progressive Collapse

Multitudes of studies have analyzed PC from a perspective of either local (single member) or global (total structural system) failure. To illustrate the localized approach, Nassr et al. developed a single degree-of-freedom model to represent a steel beam-column experiencing blast loading (2013). Others have taken global approaches to PC, developing FE models of moment-resisting steel buildings, then evaluating and analyzing the model's response to blast loading and as well as its resistance to PC. Although such studies have made strides in improving modeling capabilities of blast-induced PC loading events, such work is not relevant to

the energy *flow* approach presented here. Thus, an extensive list of traditional force-based PC work is not discussed.

2.7 Literature Review of Energy Approaches to Structural Phenomena

In contrast to such a plethora of research by mechanical engineers focused on vibrational and acoustical behavior and structural engineers using traditional force-based methods, only four known studies have taken an energy-based approach to structural collapse phenomena.

2.7.1 Energy Approaches Prior to CIPPS Research

The first known study of relative significance incorporated energy capacity for single columns as an additional design parameter (Smythe and Gjelsvik, 2006). Hence, that study dealt with collapse of a single structural element only, not PC. However, Smythe and Gjelsvik's research is conceptually very similar to the preceding CIPPS energy-based approach (Szyniszewski and Krauthammer, 2012), as both studies addressed structural failure with respect to an energy threshold. Although similar in concept, Smythe and Gjelsvik's study was significantly more simplified compared to Szyniszewski and Krauthammer's work. For example, elastic-perfectly plastic material was assumed, the scope was limited to pin-pin supports, one material, one cross-section, and pseudo-static analyses only.

Although methodologically distinct, a second study similarly advanced the effort of quantifying a structure's resistance to PC with an energy balance approach (Dusenberry and Hamburger, 2006). The approach methods used in this prior work included push down analysis and flexural/catenary energy absorption. The approaches in both of these non-CIPPS studies assumed a sequential formation of hinges to determine if PC occurs, and are founded upon the energy-based principle that if the change in potential energy exceeds the energy absorbed by the structure, then PC occurs. Of significant contribution, this work better defined the global energy fundamentals for an energy-based approach to structural systems. "… if the energy absorbed by

the structure exceeds the change in potential energy, the structure has come to rest and has potential to survive" (Dusenberry and Hamburger, 2006). In other words, if internal strain energy does not fully absorb the total energy flowing into the member of interest, failure extends to adjacent members. Although this study has conceptual similarity on a global level, the analytical methods chosen by Dusenberry and Hamburger are not contributory to the study presented herein—given the narrow and simplified methods of push down analysis and flexural/catenary energy absorption.

The third study incorporating energy capacity (for individual structural elements) as an additional design parameter was the first to demonstrate an energy-based approach for addressing system-wide failure in structural frames as a viable method (Surahman, 2007). Although for the purposes of protecting against earthquake-induced damage, Surahman showed an energy-based approach could be used to develop a design method based on the distribution of energy throughout the structural frame, using energy-time histories to determine the energy distribution, and confirming energy distribution is a function of member strength. More specifically, finding "Stronger or more flexible components suffer less damage," and "… member energy absorption capacity is determined by the member ductility, strain hardening, strength degradation effects, and imperfections" (Surahman, 2007). These findings contributed to all subsequent energy-based approach work to collapse mitigation. Although highly analogous to the preceding CIPPS study by Szyniszewski, a number of fundamental differences exist. The two most significant are the impulsive domain versus the dynamic domain and the application of damage in relation to the event loading. In addition, the building was subjected to earthquake loads prior to incurring structural damage. In the antecedent research (Szyniszewski, 2009), as well as the work presented herein, analysis begins after damage is applied by means of

member removal. Thus, the damage considered in Surahman's study occurred in the same time domain as the loading event, as opposed to analyzing behavior after load application. This is a highly significant disparity, especially for large mass structures, as inertia can govern the response of structures experiencing dynamic loading. Additional discussion of these differences is included (§ 2.1).

One of the antecedent studies at CIPPS entailed the development of an energy-based approach for PC (Szyniszewski and Krauthammer, 2012). Using a typical moment resisting steel frame for a low-rise building, this prior work showed an energy-based approach could assess PC susceptibility successfully—supported by analysis of the energy flow throughout the structure. However, this work *did not consider the rate of energy flow* transmitted throughout the structure, the connections, or a building of sufficient height to warrant concern for PC. As a structure's susceptibility to PC is a function of its capacity to redistribute energy, the efficacy of an analytical approach based on energy flow (magnitude and rate) was investigated. Since the work presented herein extends this preceding CIPPS study, with the items listed above, a cursory review of the antecedent research is offered.

2.7.2 Energy-Based Approach by Szyniszewski and Krauthammer

Given the antecedent nature of Szyniszewski and Krauthammer's work (2012) to the research presented herein, this prior study is discussed in further detail to compare and contrast these two research studies. Finite element models of this mid-rise building were developed and nonlinear transient dynamic finite element simulations were performed with varying levels of structural damage imposed by removing structural elements. Simulated damage ranged from the removal of a single column, per the Alternate Path method, to the removal of the minimum number of structural elements initiating PC. A unique nonlinear transient dynamic finite element

simulation was performed with the removal of each additional structural member. Energy-time histories were recorded and analyzed, resulting in using column energy to indicate collapse.

Being the origins of this preceding energy-based approach, this approach begins with the principle of conservation of mechanical energy, Equation 2-1, expressed in terms of the Energy Balance Equation:

$$W = \Delta E \tag{2-1}$$

, where W is work done on the system and ΔE is energy transferred into the system. Considering the system under consideration (building frame, applied loading, boundary conditions, and various prescribed damage levels) is isolated, the global mechanical energy remains constant. Energetic effects from frictional and other non-conservative forces are negligible. Consequently, conservation of mechanical energy is an acceptably comprehensive accounting of the system. Thus, energy is transferred between various forms, neither created nor destroyed, per the conservation principle.

Using nonlinear transient dynamic finite element simulations, this antecedent study began with characterizing the response of structural members in both force and energy domains for numerous loading conditions. The energy forms considered included internal with Equation 2-2, kinetic with Equation 2-3, and potential, or gravitational with Equation 2-5. The potential energy associated with the gravitation field, or gravitational energy, is an energy source in this energy-based approach that is released with the failure (by means of removal) of a load-supporting structural member. Internal energy, the sum of elastic and inelastic strain energies, is:

$$E_{\text{int}} = \int\left(\int \sigma d\varepsilon^{e}\right)dV + \int\left(\int \sigma d\varepsilon^{p}\right)dV \tag{2-2}$$

, where E_{int} is internal energy, $\int(\int\sigma d\varepsilon^e)dV$ is elastic strain energy, σ is stress, $d\varepsilon^e$ is elastic strain increment, $\int(\int\sigma d\varepsilon^p)dV$ is permanent deformation work, and $d\varepsilon^p$ is plastic strain increment. Kinetic energy is:

$$E_{\text{kin}} = \int \frac{1}{2}\rho v^2 dV \tag{2-3}$$

, where E_{kin} and $\int\frac{1}{2}\rho v^2 dV$ is kinetic energy, ρ is mass density, and v is particle velocity. Work done on the system is the summation of the change in both kinetic and internal energies. Internal energy is the sum of elastic strain energy and plastic strain energy, or work done through permanent deformation. Referencing above formulations, the consequent definition of work is:

$$W = E_{\text{int}} + E_{\text{kin}} = \int\left(\int\sigma d\varepsilon^e\right)dV + \int\left(\int\sigma d\varepsilon^p\right)dV + \int\frac{1}{2}\rho v^2 dV \tag{2-4}$$

Extending the energy work from the prior CIPPS' study (Szyniszewski, 2009), potential energy associated with the gravitational field, or gravitational energy, is

$$U_{grv} = \int -mgdy \tag{2-5}$$

, where U_{grv} is the gravitational energy, m is mass of all parts of the structure supported by the removed member(s), g is gravity, and y is vertical distance. Energy transfer with member removal is known to be proportional to the recoverable elastic strains in the removed member(s) as well as the mass supported by the removed element, which is a transfer from potential to kinetic energy. Thus, the elastic strain energy portion of Equation 2-2 can also be used to define the strain energy portion of the (internal) potential energy released upon the removal of (a) structural member(s).

To translate the energy principle on which the antecedent and current work is based, in terms of the selected finite element code, recall the simplified form of energy equilibrium with Equation 2-1. This Conservation of Energy Equation is redefined with energy forms relevant to

finite element software in Equation 2-6. To elucidate, using the energy forms recorded by the nonlinear transient dynamic finite element code LS-DYNA, the conservation of mechanical energy expressed in total energy equilibrium terms is defined as:

$$E_{total} = E_{kin} + E_{int} + E_{si} + E_{rw} + E_{damp} + E_{hg} = E^{0}{}_{kin} + E^{0}{}_{int} + W_{ext} \quad (2\text{-}6)$$

, where E_{total} = total energy, E_{kin} = current kinetic energy, E_{int} = current internal energy, E_{si} = current sliding interface energy (including friction), E_{rw} = current rigid wall energy, E_{damp} = current damping energy, E_{hg} = current hourglass energy, $E^{0}{}_{kin}$ = initial kinetic energy, $E^{0}{}_{int}$ = initial internal energy, and W_{ext} = external work. All energy forms listed were reviewed. Sliding interface, rigid wall, and hourglass energies were checked for quality control. Damping energy was employed to filter non-relevant high frequency content, and reviewed to confirm the damping energy is negligible with respect to total system energy levels. The energy equation above illustrates equilibrium principles are embedded in nonlinear transient dynamic finite element codes. Thus, the energy flow, magnitude and rate, – failure relationship is understood to exist, even though this relationship has not been demonstrated for either failure or PC.

The infused mechanical energy is equivalent to the potential energy released by all parts of the structure supported by the column removal (through gravitational forces). In other words, the strain energy in the column prior to removal is transferred to the remaining structure. This mechanical energy flows throughout the structure along multiple pathways concurrently. Energy flows through a structure until it is fully transferred into structural displacements and material deformations, whether failure is arrested, or continues until collapse occurs. Hence, PC is known to be a function of a structure's ability to accommodate energy flowing through its components, which is a function of constitutive material definitions, cross-sectional properties, and structural parameters. Energy-time histories of each mechanical form considered (total, potential, and

kinetic) were analyzed to determine correlation between energy capacity and collapse. In result, column failure energy was a more effective indicator of collapse than traditional methods.

However, Szyniszewski's study did not consider a building of sufficient height to warrant concern for PC, connections, or the rate of energy flow. As discussed (§ 2.5.3), prior research has shown connections affect PC (Yim and Krauthammer, 2009). Although energy flow rate can affect failure, its role in PC has been unknown—until the research presented here was conducted.

However, the above plot shows failure begins to be affected by loading rates above 3000 kip/s. A more recent CIPPS study showed structural failure, as well as the mode of failure, is a function of both energy flow as well as the rate of energy flow (Tsai and Krauthammer, 2015). In accord with both findings, PC is affected by columns experiencing sufficiently high-energy flow rates, i.e. above 3000 kip/s. This antecedent study analyzed two similar low-rise frames only—structures that neither exemplify PC susceptibility nor are of primary import to PC mitigation. Thus, the research presented herein applies the energy – energy-rate relationship with failure Learned from Tsai and Krauthammer's work (2015) to a mid-rise frame susceptible to PC.

2.8 Summary

Over two decades after formative advances following WWII, PC garnered international focus, primarily in response to the Ronan Point apartments collapse. Nearly fifty years after the Ronan Point tragedy—a seminal event for the field of PC—comprehensive understanding of PC phenomenon remains outside the technical scope of the overwhelming majority of structural engineers practicing today. Given the state of practice lacks sufficient understanding of PC, an effective approach to PC mitigation is paramount—one that needs to be both rational and efficient for practicing engineers. Unfortunately, no simplified method exists. Although nonlinear transient dynamic finite element analysis software codes are available, this technique is

too technically rigorous, time-intensive, and computationally expensive to be provided by most structural engineering consultants. In addition, nonlinear transient dynamic finite element simulations yields a solution constrained to the threat and structure considered. Not surprisingly, it is understood most engineers practicing in the field of protective design rely on the Alternate Path method solely, contrary to the unreliable nature of this notional approach that has no basis in physics. Unfortunately, the Alternate Path method will continue to be used beyond preliminary design efforts until there is an efficient rational alternative.

The Alternate Path method appears to be unrealistic, proven overly conservative in certain situations (McKay et al., 2012) and possibly insufficient for others. Beyond minimal redundancy, which obviously should be well exceeded for life safety issues for any occupied building, what the Alternate Path method achieves in mitigating PC is unknown and unproven. In addition, multiple terrorist attacks in urban environments have yielded significant levels of damage, demonstrating no correlation between a single column failure and damages incurred from actual blast loading events. The Alternate Path method has not been shown to mitigate PC—*it establishes that minimal redundancy is present in the vertical load carrying system only with no correlation to the robustness needed to sustain a realistic threat*. In addition, the Alternate Path method is highly repetitive—an imposition on practicing engineers, resulting in higher costs, and extended job schedules without any corresponding improvement, accuracy, or precision. Again, a rational physics-based approach to PC assessments is of utmost importance.

To address this need, the energy-based approach for PC present in this work has been developed. The antecedent study confirmed a meaningful correlation between energy and failure, and the developed energy-based approach yielded more accurate failure predictions than traditional force-based approaches (Szyniszewski and Krauthammer, 2012). Although

successful in using pre-calculated energy thresholds to determine failure, neither the structural connections nor the rates of energy flows were considered. In addition, low-rise buildings are immaterial to PC—a phenomenon proportional in relevance to the height of a building. Furthermore, there were two cases in which the energy failure threshold was exceeded with *no* corresponding member failure—offering an opportunity for improvement with the demand over capacity (D/C) ratios presented. Hence, connections, the evaluation of energy flow rate on failure, and a mid-rise structural relevant to PC is considered in the EFA presented here. In addition to developing a novel EFA for PC, the current study presents the limits of the effects, or energy redistribution, extending from a single column removal, larger blast-damaged zones, and consequently a determination as to the suitability of the DOD's Alternate Path method procedures for assessing PC.

Table 2-1. Efficacy of US-based codes in mitigating the three most influential PC events (Source: reproduced from Nair, 2006 – Figure 4).

	Redundancy	Local Resistance	Inter-connection	Threat-dependent analysis	Ronan Point	Murrah Bldg.	World Trade Center 1 & 2	World Trade Center 7
ASCE 7(-05)	•				?	N	N	N
ACI 318(-02)			•		Y	?	N	N
GSA PBS, 2000	•				?	N	N	--
GSA PBS, 2003				•	N	Y	N	N
GSA PC, 2003	•				N	N	N	N
NIST 2005	•			•	N	N	N	N

A B C

Figure 2-1. Ronan Point apartment tower in London in 1968 after collapse. A) Photo courtesy of Cynthia Pearson. Source: Pearson and Delatte, 2005. B) Photo courtesy of David E. Allen. Source: Allen and Schriever, 1973. C) Photo courtesy of David E. Allen. Source: Allen and Schriever, 1973.

Figure 2-2. Alfred P. Murrah building in Oklahoma City after the blast-induced collapse in 1995. Photos courtesy of Chicago Sun Times. Sources: https://s-media-cache-ak0.pinimg.com/236x/ed/2a/c5/ed2ac5c56e49b61fd37b2d08726c3451.jpg and https://s-media-cache-ak0.pinimg.com/236x/a7/36/ae/a736ae79aeb7799562446468ae758713.jpg.

A B

Figure 2-3. Damage to the Kansallis House in Bishopsgate area after 1993 bombing in London. A) Photo courtesy of Daily Mail Pictures, 2011. Source: https://po4ep.s3.amazonaws.com/785/l/19064000.jpg http://mailpictures.newsprints.co.uk/view/19064000/elib_assc-mmglpict000005171717_jpg. B) Photo courtesy of Dick Polman. Source: Polman, 2013.

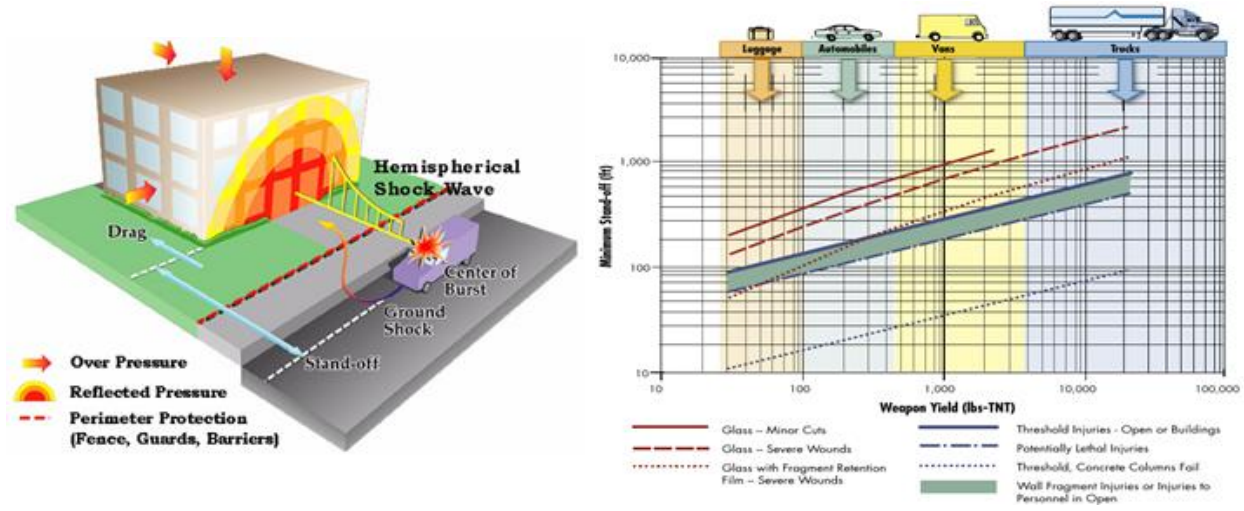

A B

Figure 2-4. Detonation parameters and yield weights per transport vehicle. A) Offset explosive threat delivered by van with pressures to building exterior visualized. Image source: FEMA 427. B) Weapon yield as function of standoff, or offset, distance and mode of vehicle transport. Image source: FEMA 426.

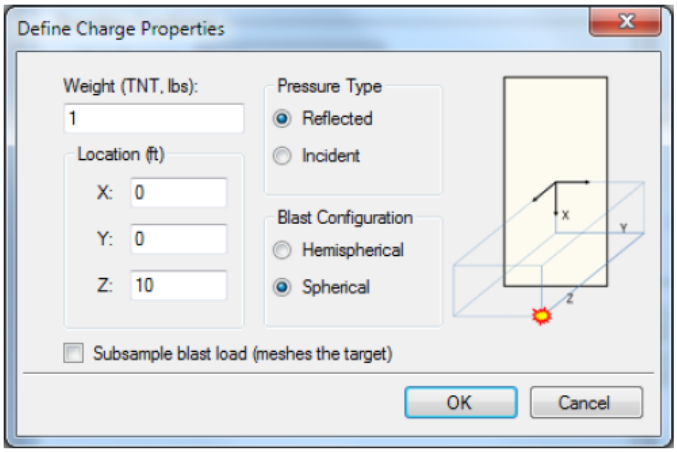

Figure 2-5. DSAS's air blast loading module.

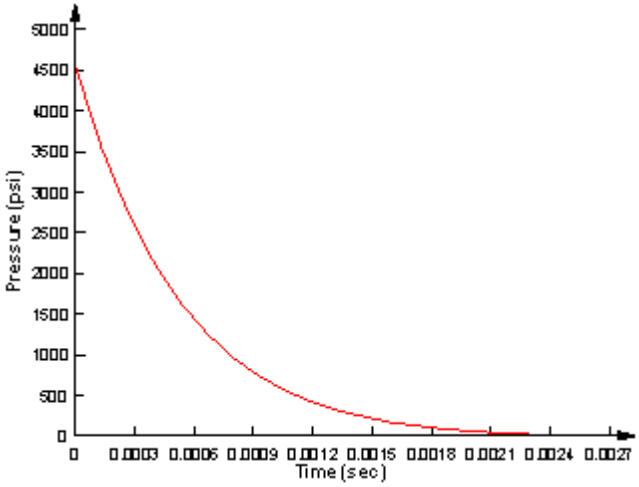

Figure 2-6. Pressure-time history (for 0.504 m/kg$^{1/3}$) output from DSAS.

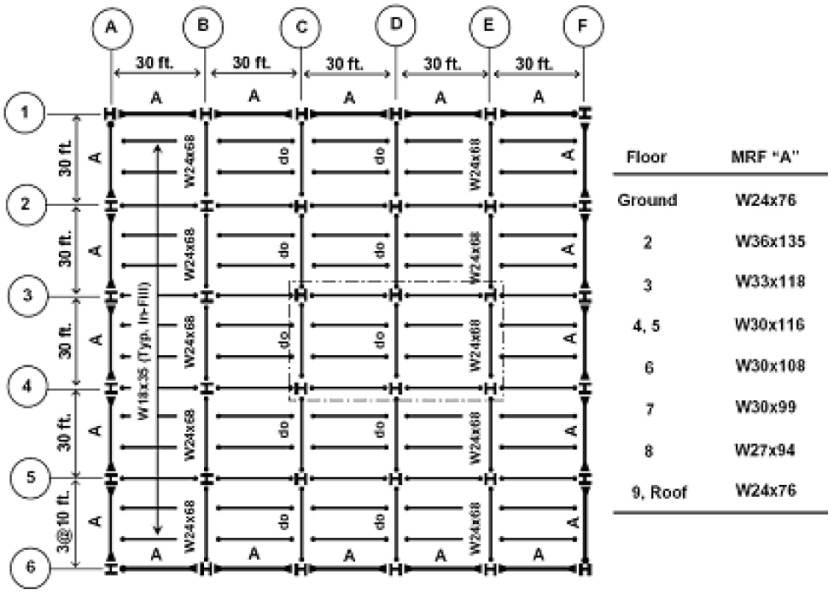

Floor	MRF "A"
Ground	W24x76
2	W36x135
3	W33x118
4, 5	W30x116
6	W30x108
7	W30x99
8	W27x94
9, Roof	W24x76

Figure 2-7. Plan layout of beams with WUF-B connected "A" beams tabulated per floor.

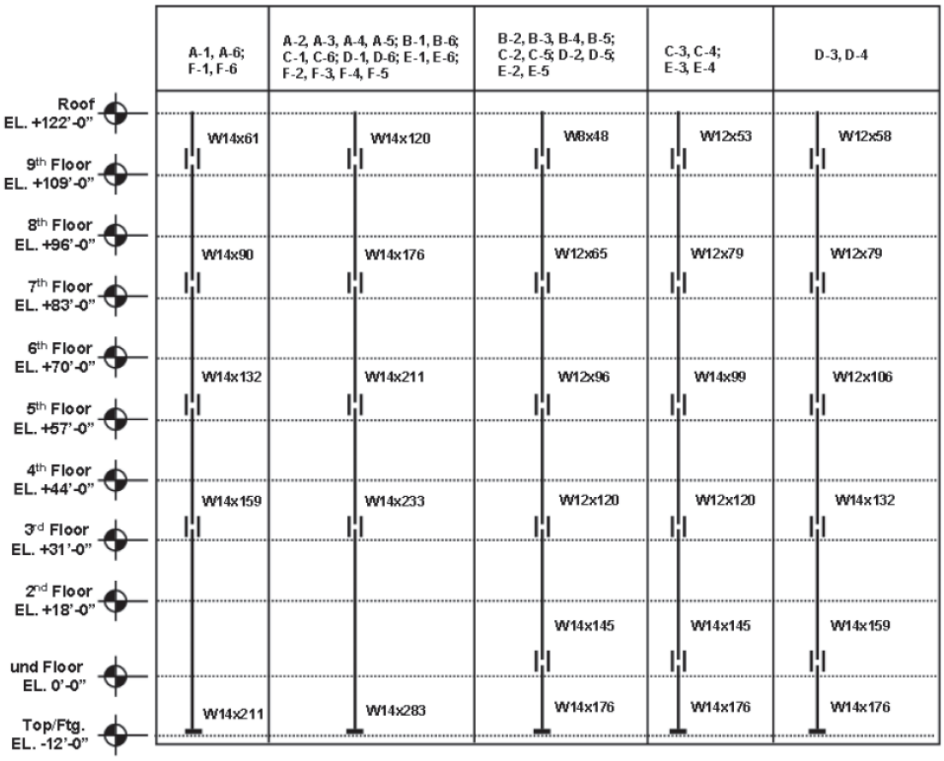

Figure 2-8. Elevation of steel columns cross-sections with splice locations.

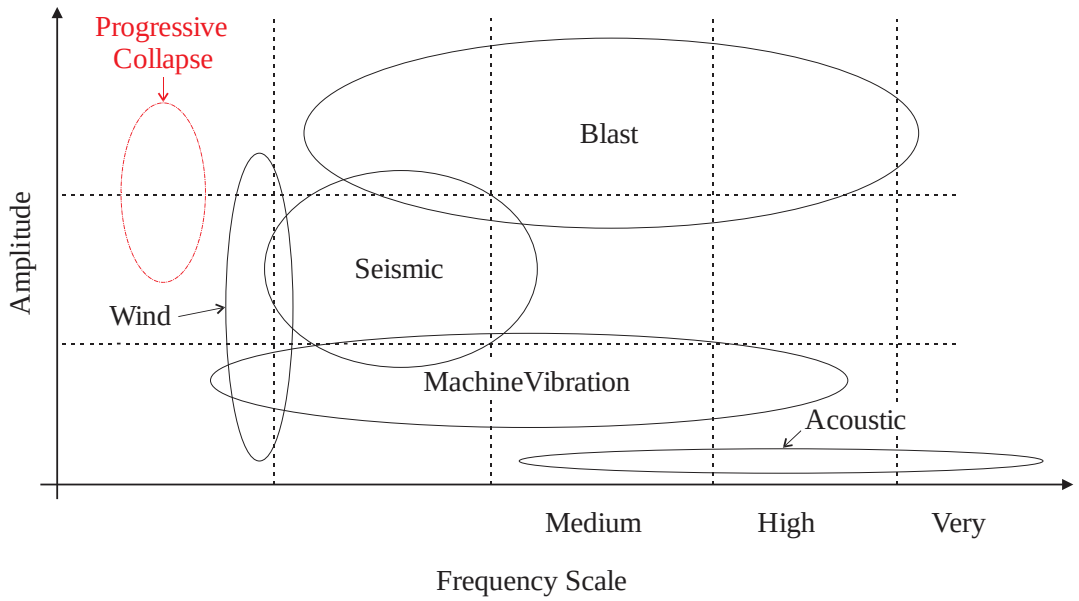

Figure 2-9. Qualitative Frequency-Amplitude Distribution for Different Hazards. After source with inclusion of PC region: Ettouney, 2003.

CHAPTER 3
ENERGY FLOW APPROACH (EFA) TO PROGRESSIVE COLLAPSE (PC)

This study is based upon the thesis that member failure, and consequently (Progressive Collapse) PC, correlates with energy flow—both magnitude (E) and rate ($\dot{E}$)—more closely than any other measure of state, e.g. force as is currently done in traditional approaches. Thus, measuring these two parameters provides the most accurate and precise indicators of failure. This hypothesis was initially examined for a single structural element (Tsai and Krauthammer, 2015), for a single story single bay frame in the proposal to this study, subsequently for a two story two bay by two bay frame for collapse (Appendix A), and then ultimately for two ten-story mid-rise buildings.

The energy flow approach (EFA) presented here is an amalgamated successor of three dissertations performed at CIPPS. The first study demonstrated the significant effects of connections in moment resisting steel frames on PC (Yim, 2007; Yim and Krauthammer, 2009; Yim and Krauthammer, 2010; Yim and Krauthammer, 2012). Therefore, in both this prior and current studies, the strength of all frame connections was considered using nonlinear strength curves developed from quasi-static simulations with discretely modeled high-resolution continuum models. The second study developed an energy-based approach to PC, yielding a more accurate and more reliable failure assessment approach than traditional force-based approaches (Szyniszewski, 2009; Szyniszewski and Krauthammer, 2012). Failure was defined using an energy threshold value, whereas this work defines failure as a function of the magnitude and the rate of energy flow, herein referred to simply as energy flow. The third study demonstrated the use of an energy-energy rate failure threshold (Figure 3-1) for an individual structural element (Tsai and Krauthammer, 2015). Combining this antecedent CIPPS research—numerically representing structural connections, the use of energy parameter for determining

collapse susceptibility, and using the combined energy flow and rate of energy flow as failure-indicating parameter—the work presented here considers the PC of a mid-rise steel building and the demonstrates the efficacy of using energy flow for assessing PC susceptibility. In short, the EFA discussed here provides an unprecedented level of accuracy and reliability for assessing PC susceptibility within the most comprehensive physics-based framework. A flowchart of the process employed (Figure 3-2) Procedures for development of this novel EFA are presented.

3.1 Mid-Rise Office Buildings

The structural steel building of interest was part of a national seismic research project in response to the 1994 Northridge earthquake (FEMA, 2000). Additional details regarding the historical relevance and incorporation into prior studies was discussed (§ 2.5). This mid-rise moment-resisting frame is ten-stories. Hypothetically located in Boston, this design served as a cautionary example for consulting engineers in reference to seismic loading; i.e. although designed to code, the frame was known to be highly susceptible to collapse. Additional structure-related information, extracted directly from the FEMA document, is included for reference (Appendix B).

3.1.1 Development of Finite Element Model of Ten-Story Moment Resisting Steel Frame

A significant portion of the numerical methods employed in developing finite element models of the ten-story building (Figure 3-3) were presented (§ 2.5). For example, the LS-DYNA features selected for representing the steel connections in this study were analogous, if not equivalent, to the Abaqus features employed in the antecedent research on connections (Yim and Krauthammer, 2009). A comprehensive discussion of the modeling techniques used in both the antecedent and present study is available (Yim, 2007). Given the high level of similitude in the finite element models of both studies, the methods for the proposed finite element model are presented in cursory fashion. All finite element techniques have either been verified with high

resolution models comprised of continuum elements fully and/or validated with structural experiments.

With respect to all steel connections throughout the building, the finite element models used here are computationally efficient numerical representations of the mid-rise building. In short, resultant beam elements represented beams, girders, and columns, with shell elements for the reinforced slabs. Connections were represented with springs—nonlinear curves developed from prior efforts verified with continuum models (§ 2.5.3).

3.1.1.1 Boundary conditions

Fixed supports are applied at the base of all columns (Figure 3-4). Given this simplification of rigidity for the foundation, the slab on grade is not considered. For visual clarity, the fixed supports are shown with a two bay x two bay x two-story frame. For additional information regarding the fixed based assumption, see Appendix B in Report 355C (FEMA, 2000).

3.1.1.2 Columns, girders, beams, and slabs

A 'fully descriptive' continuum model, i.e. a fully discretized representation consisting of a high-resolution of solid 'brick' elements, of a ten-story steel frame is beyond available computing resources, and thus time-prohibitive, especially if nonlinearities are considered. To circumvent such expense, a computationally efficient numerical representation of the building was developed (Figure 3-5). Fortunately, there are well-established modeling methods capable of characterizing a building's structural elements with acceptable accuracy.

As modeled, there are sixteen different (16) column cross-sections and ten (10) beam profiles, or cross-sections—one (1) in-fill beam, one (1) interior beam, one (1) interior girder, and eight (8) exterior girders in the ten-story structure. All structural element types were defined with unique profiles, represented with Hughes-Liu beam elements with cross-section integration

(Hallquist, 2014). The material model was elasto-plastic with a nonlinear constitutive definition using effective true stress and effective true strain, including strain rate dependency, and failure. The Cowper-Symonds strain-rate material model was employed with material-dependent C and Q factors of 40.5 sec^{-1} and 5, respectively (Jones, 1997). Failure was strain-based, occurring in the highly plasticized region at 0.2 in./in.—executed with LS-DYNA's element deletion feature (LS-DYNA, 2014).

Slabs were modeled with fully integrated, selectively reduced 4-node shell elements. The material definition was an elasto-visco-plastic material with a prescribed stress-strain curve and strain rate dependency. In addition, damage was considered before rupture/failure occurs, which was defined by tensile strength-based strain. The LS-DYNA material model selected (MAT_PLASTICITY_WITH_DAMAGE) most closely parallels the Abaqus-specified CONCRETE DAMAGE PLASTICITY (CDP) material definition used by Koh (2011). Further discussion regarding the material properties used, e.g. the selected uniaxial compressive stress-strain curve, the post-failure tension stiffening stress-strain curve, and a number of plasticity parameters, are available (Koh et al., 2011). Cross-sectional properties were calculated by the finite element code subsequent providing dimensional input.

3.1.1.3 Connections

Reductionist modeling approaches are necessary due to the computational expense of discretely representing all of the structural components contributing to the connections in steel frame with continuum elements, e.g. bolts, welds, shear tabs, coped flanges, etc. A series of antecedent CIPPS studies entailed the development of simplified models capable of mimicking continuum element-only models with satisfactory precision and accuracy across all relevant time loading domains—from impulsive to quasi-static. Highly nonlinear finite element analyses with

high-resolution continuum models of steel connections were developed to verify the simplified connection models.

These simplified models, comprised of nonlinear spring elements, were subjected to an array loading scenarios to examine the efficacy of representing such complicated structural componentry. Degree-of-freedom-specific connecting elements proved to be significantly more economical, computationally, without any meaningful loss in fidelity. An illustration depicting the incorporation of six degree-of-freedom bema elements at the connections is included (Figure 3-6). As shown in multiple prior studies (Yim & Krauthammer, 2007, 2009, 2010, 2012), resultant elements with rotational springs can represent complicated connections with accuracy, i.e. (nearly) numerically equivalent to the full continuum models. In lieu of the Abaqus-specific Join + Cardan approach used in the antecedent CIPPS' studies, a similar method—capable of accounting for all of the energy within the system—was employed using LS-DYNA. Six (6) degree-of-freedom discrete beam elements, often referred to as springs, represented the connections (Figure 3-7). In addition, it is important to note this connection model was used for *all* connections in the mid-rise steel building, as in-fill beams are present throughout the entire structure (Figure 3-7C), which connects the in-fill beams to girders, not columns.

In a more recent study from this series of connection-related research, Yim and Krauthammer quantified the significant contributions of the connections in a structural steel frame to PC (Yim and Krauthammer 2012). Thus, the research presented here accounts for *all* connections throughout the framing system—an additional step beyond any known research toward a more accurate assessment of collapse susceptibility. All curves used in this research were derived, either directly or with equivalent methodology, from prior CIPPS research (Yim and Krauthammer, 2009). This reductionist approach was taken by using results from separate,

more numerically sophisticated continuum models. In antecedent studies, computationally expensive models comprised solely of high-resolution continuum elements were developed and loaded in quasi-static simulations. The resulting nonlinear strength, or M-ϕ, curves were installed at all (moment and shear) connections in the ten-story steel building. As presented in detail above (§ 2.5.3), the nonlinear curves developed in the antecedent work were used (Yim, 2007). A more extensive discussion of the methods used to represent the connections is available (Yim, 2007).

Performing highly nonlinear quasi-static analyses using high-resolution continuum models of small portions of the structure affords representation of complicated structural componentry with simplified spring elements. Although employing nonlinear curves to represent connections with degree-of-freedom -specific springs, a vastly more economical computational effort is yielded without any meaningful loss in fidelity. As shown in multiple prior studies (Yim & Krauthammer, 2007, 2009, 2010, 2012), resultant elements with rotational springs can represent complicated connections with accuracy, i.e. (nearly) numerically equivalent to the full continuum models. The primary structural members (columns, girders, and beams) are represented with resultant beam elements, the secondary structural members (slabs) are modeled with shell elements, and the connections are modeled with degree-of-freedom -specific beam, or spring, elements. In addition to using the aforementioned springs for capturing the effects of connection strength, employing the material model discussed above allows the connection to not only transfer energy but also absorb and dissipate energy as well. In addition, a material definition incorporating nonlinear strain hardening and strain-rate properties was used. The selected element type and material definition have proven effective in prior studies, e.g. Wilkes, 2002.

Multiple approaches to represent the behavior of the connections were performed. Although multitudes of alternatives were considered, they were found to be (theoretically) flawed. More specifically, none of the constraint techniques could be used as it was revealed (during analyses of all types considered, e.g. *CONSTRAINED_JOINT_SPHERICAL,) energy is dissipated during employment of the constraint itself. If this energy was of significantly small (relative) value, it could have possibly been overlooked. However, the output used to report the energy-time history of the connections was the spring and damper energy, which includes this energy associated with the joint constraints. This energy type was selected due to the use of translational and rotational springs installed at the connections.

In short, the energy dissipation from the constraint could not be parsed from the energy dissipated from the joint through motion, without an additional sensitivity study. Thus, the energy associated with application of a constraint relationship could not be quantified independent of the connection energy, and hence not allowing for a quantification of the contribution of the constraint to the overall energetic behavior of the connection.

3.1.1.4 Non-structural

The effects of non-structural members (on the propagation of stress waves through a structure) in response to blast loads are not considered. Additional information regarding the mid-rise building and finite element modeling methods is available per Yim (2007) and Yim and Krauthammer (2009), respectively. Given the importance of connections, proven by prior studies, this additional improvement in finite element modeling methods increased the likelihood the EFA would yield improved assessments of PC susceptibility, as well as the mechanics of PC once initiated. Although non-structural building components were neglected for this study, the extent of the numerical representation of all structural components for a mid-rise building is

novel, and the consequent correlation between member failure, the magnitude, *and* rate of energy flow, and the collapse susceptibility is unprecedented.

3.1.1.5 Gravitational loads

Gravity loads, superimposed dead and live, were determined using ASCE 7 specified live load reduction factors for columns. Given the exorbitant nature of applying conservative loadings for all stories of a mid-rise building intended for typical office utilization, reductions for the application of live loads were appropriate and necessary. Furthermore, it is important to note these building designs for the SAC commission were developed to highlight the inadequacy of the building codes at the time. Thus, these frames would likely collapse under the governing load combinations for extreme/abnormal events without the code-permitted reduction factors. However, it should also be noted that the live load reductions for beams supporting large floor areas were not utilized incorporated into the applied loading calculations. For reference, results from a multitude of in-depth studies to determine the effective live loads in buildings for typical office environments are available, e.g. Mitchell and Woodgate (1971), McGuire and Cormell (1974), Culver (1976), and Ellingwood and Culver (1977).

To elaborate on the methods employed for this study, gravitational loads were applied using two different combinations of dead (D) and live (L) load. The Finite element building models followed the Alternate Path method provision in UFC 4-023-03. This method entails notionally removing a single column (§ 3-2.13.4.1) from a building that is subjected to 1.2·D+0.5·L per the Equation 3-19 load combination (UFC, 2014). Finite element models of building classified as 'PC', or analysis models, include multiple levels of damage, up to levels capable of initiating PC. This entailed subjecting the structure to a load combination of 1.0·D + 1.0·L.

Per ASCE-7 (2002; 2005), both load combinations used particular dead loading constituents, e.g. ceilings and partitions, with the prescribed pressures, and 50 psf for live loading (Robertson and Naka, 1980). The global application of gravity activates the self-weight dead loads of the structural members modeled, calculated from the prescribed material density and volume (via the defined cross-sections and element lengths for columns and beams). Although the Alternate Path method specified single column level of damage may be insufficient to initiate PC, it is understood conservatism is included with the Alternate Path method by using factored load combinations and strength reduction factors. For all simulations, gravity loads were superimposed and applied as pressure to the slab shell elements in a pseudo-static manner. Lateral loads, which are 0.2% times the unfactored sum of the (D and L) gravity loads to be applied per floor one side at a time in combination with the gravity loads, as prescribed by the UFC 4-023-03 specification, Equation 3-20, may not be included, if possible. This potential exclusion of lateral loading is appropriate given the intent behind the loading requirement is satisfied indirectly with asymmetry being an inherent result from with the application of damage to the structure in an asymmetric manner.

3.1.1.6 Air blast loads: damage yields per DSAS

Simulations with increasing damage levels were performed, in an incremental fashion. Fundamental to the tertiary objective of determining the efficacy of the Alternate Path method, the structural response to notional removal of a single column must be determined. Thus, the minimum level of damage considered was a failed single column only, commensurate with the Alternate Path method. Essential to the primary objective of assessing PC, the minimum damage level capable of initiating PC must be determined. Consequently, applied damage began with single column removal under both factored and unfactored load combinations; continue with

incremental increases, and ending with the *minimum* number of structural elements necessary to trigger PC. The specific sequence of failed structural members was determined by DSAS.

The specific sequence of structural element failed, or removals, is critical for modeling realistic damage levels, capturing the response of a structure to realistic threats, and determining the minimum damage necessary to initiate PC. DSAS was used to determine the incremental levels of damage (Figure 3-8) to be considered for the nonlinear transient dynamic finite element simulations—from single column destruction to multiple member failure capable of initiating PC. Specifically, the time of failure of all members in the blast vicinity was calculated—determined by simulating explosions adjacent the column of interest using DSAS (§ 2.4). DSAS determines the time of failure with respect to the detonation mark for all structural elements necessary to initiate PC. Using the consequent array of time-of-failure data, the damage was applied to the LS-DYNA building model in the form of incremental element removal, with one element removed per simulation. As damage levels increase, any type of structural element may fail, include connections, girders, beams, and/or slabs. In effect, this iterative process entails performing analyses in a specific sequence, in accord with the results calculated by DSAS. A description of the process employed to estimate damage using DSAS was presented (§ 2.4). Additional information regarding DSAS is also available (Astarlioglu and Krauthammer, 2012).

Using the two model types as defined within the gravitational loading discussion (§ 3.1.1.5), the first simulation was performed with the Alternate Path method design model. This initial simulation includes factored loads, whereas all subsequent simulations (with the analysis model) had non-factored loads. All Alternate Path method procedures are followed per the UFC specification for the stated ten-story building of interest, i.e. the nine-story building with a single-story basement. Additional details regarding the Alternate Path method were provided (§

2.2). The first simulation with the PC analysis model included removal of the same column in the Alternate Path method design model, but with the unfactored gravitational load combination, as discussed (§ 3.1.1.5).

To maintain consistency between the Alternate Path method design model and the PC analysis model, comparative analyses was performed under analogous conditions. In other words, the detonation was adjacent the notionally removed column from the design model when performing the DSAS analysis. For example, an exterior column near the middle of the long side of the building was removed in the design model per the Alternate Path method (Figure 3-9A), and so this same column was subjected to an offset (hemi-spherical) air blast loading in DSAS for the analysis model (Figure 3-9B). All at ground level, air blasts were detonated at a corner column, the edge column near middle of the long side (as illustrated), and an interior column: comprising three unique air-blast threat locations, or column removal, scenarios. For the corner and interior columns, the explosion was diagonally offset, at grade, perpendicular to column centerline, also resulting in a hemispherical shock wave. These locations are chosen to maximize damage to the affected column while minimizing damage to adjoining structural members. Additional details regarding the processes employed for applying blast-induced damage are available (Wilkes and Smith, 2015).

Although a significant number of various blast events were considered, it is important that many threat scenarios were not simulated. For example, blast events above the bottom floor level were not considered. Although nefarious attacks (like those becoming increasing common in unstable regions) are typically LVBIEDs, the tragedy at the Ronan Point apartments occurred on the eighteenth floor due to a gas leak. Although such threats are anomalous, these types of potential loading scenarios would need to be considered prior to incorporation of energies

approaches into design provisions. Detonation locations near the corner of the building and interior to the building were also exempt from this study. Such additional threats should be incorporated in future numerical research. Consideration of some of these additional threat scenarios is available (Wilkes and Krauthammer, 2016). In addition, partially damaged structural elements, i.e. not experiencing complete failure, were not represented numerically. Although inherently conservative for the damage assessments for columns, partially damaged depiction of various horizontally oriented structural elements is not necessary conservative. Such considerations are suggested for future numerical research.

3.1.2 Modified Version of the SAC-Commissioned Mid-Rise Building

The ten-story, or nine-story with basement, building was designed to expose the shortcomings of the design provisions current at the time of the Northridge earthquake. Thus, a code-compliant soft story was incorporated into design. This soft, or weak, story was achieved by created floor two to be eighteen feet (18') in height, as opposed the thirteen-foot (13') stories for all remaining stories above ground level. In addition, the W-shape cross-section for the interior column locations was for the second floor was chosen to be the same as for the shorter first, third, and fourth floors. Furthermore, the top of the basement level was considered to be laterally braced. Thus, the SAC-commissioned designs were intentionally made to be susceptible to failure of the second floor for earthquake loading events.

Although useful for illustrating the efficacy of the EFA methodology, modifications were made to this design in order to develop a second numerical model of a mid-rise building frame. This modified building model is a better representative of typical mid-rise office buildings, and with moment connections included for the N-S column – girder connections, allows for additional insights into the energy flow behavior during a PC event. All SAC-commissioned

buildings were designed to expose the shortcomings of the design provisions current at the time of the Northridge earthquake.

Thus, these building designs were not necessarily intended to be representative of typical mid-rise buildings, more so to highlight the inadequacy of the design codes for protecting against seismic loading events. Due to this atypical soft-story nature of the SAC-commissioned building, a second version of this same building was analyzed. In short, this modified version is equivalent in all respects with the exception of the second story being reduced from eighteen feet to thirteen feet in height (Figure 3-10) and the inclusion of moment-resisting behavior for the girder – column connections in the interior of the building, as was done in the preceding moment connection modeling research (Yim, 2007).

3.2 Energy Principles

3.2.1 Energy Flow Analyses using LS-DYNA

Energy principles used in the antecedent study, namely conservation of mechanical energy and Newton's Second Law, also form the basis of the proposed EFA. Similarly, both studies consider mechanical energy forms only. By removing extraneous terms and including the energy released with member failure, LS-DYNA's total equilibrium, Equation 2-6, can be redefined as:

$$E_{total} = E_{kin} + E_{int} = E^{0}_{kin} + E^{0}_{int} + W_{ext} \propto \Delta\sum(I_{str} + U_{grv}) \tag{3.1}$$

, where I_{str} is the internal strain energy, U_{grv} is the potential gravitational energy, and $\Delta\sum(I_{str} + U_{grv})$ is the total energy released from the removed, or failed, structural member(s). The additional energy summation term is included to represent the energy from removing a structural element, known to be proportional to the released strain and gravitational energies. Removing failed structural members from a structure causes the transfer of potential energy to kinetic energy and recovery of elastic strains. In other words, every nonlinear transient dynamic finite

element simulations is a numerical investigation of a structure's response to the creation of an imbalance in the internal energy distribution, continuing until a new state of equilibrium, including collapse, is achieved.

3.2.2 Incorporating the Rate of Energy Flow

There are multiple reasons in which the rate of energy flow should be considered when determining failure, and consequently studying PC. In the interest of brevity, only material behavior is discussed. Material behavior is substantively rate dependent, as briefly mentioned in relation to the mechanical engineering research on vibrational and acoustical behaviors. Dusenberry points out in § 15.2.2 Connection Ductility (pg. 386) and references in Chapter Seventeen (pg. 450) of *Handbook for Blast Resistant Design of Buildings* (2010), prior studies have clearly shown the differences in material behavior between dynamic and impulsive loading events can be highly dissimilar (Malvar, 1998; Malvar and Ross, 1998; Crawford et al., 2001a; Crawford, 2001b). Other researchers have delved more deeply into material science to determine behavior as a function of loading rate (Ožbolt et al., 2011; Adhikary et al., 2013). Although such research is beyond the scope of this proposal, it is widely known loading rates cause changes in the observed behavior of structural materials. Material evolves from behaving elastically to plastically to fracture based, as the applied loads change from the static to plastic to impulsive domains. Therefore, material behavior is flow rate dependent. Thus, the proposed work incorporates the rate of energy flow as an additional parameter for determining failure—constituting a novel component of the proposed research.

In addition, it is important to note that the effects of rate on failure were investigated more extensively in the antecedent CIPPS study by Tsai and Krauthammer (2015). This prior study developed failure thresholds for not only an individual behavioral mode, but also for multi-mode behavior (Figure 3-11). More details regarding this effort are detailed below.

3.3 Fluid-Energy Flow Analogy of the EFA

Strictly speaking, energy is not visually observable. So, to communicate the proposed EFA in a visual manner, a conceptually analogous system comprised of physically representable parameters is offered. Two fluid – energy analogy illustrations are provided. The first was developed in the antecedent study by Tsai and Krauthammer, and best explains the energy flow behavior into, within, and out of a single structural element (Figure 3-12). The second was developed uniquely for this study and although it illustrates energy flow through a single structural element (Figure 3-13), it adds a dimension of magnitude to convey the relative energy form contributions. Each energy form present within a structural element is represented with a tank. The fluid volume inside a given tank corresponds to the magnitude of energy flow (E) for a given form of energy, e.g. E_K is the kinetic energy. Thus, volumetric flow rate per tank represents energy flow rate ($\dot{E}$) for each energy form considered; e.g., $\dot{E}_{PS}$ is the internal plastic strain energy rate.

In accord with the cumulative nature of energy flow, the rate of energy flow within a given structural element ($\dot{E}$) is the summation of all (three) energy forms considered—elastic strain ($\dot{E}_{ES}$), plastic strain ($\dot{E}_{PS}$), and kinetic energy flows ($\dot{E}_{KS}$), per Equation 3-7. Consequently, energy flow (E) is the summation of elastic strain energy (E_{ES}), plastic strain energy (E_{PS}), and kinetic energy (E_K).

The rate of energy flow into a structural element ($\dot{E}_{IN}$) is the sum of energy absorption rates of all forms per Equation 3-5. More accurately, the rate of input energy is initially absorbed internally as elastic strain ($\dot{E}_{ESIN}$). If loading continues beyond the onset of yielding, input energy is absorbed internally as plastic strain ($\dot{E}_{PSIN}$). This transition from elastic to plastic strain corresponds to the transition in material behavior from the linear-elastic region to the non-

recoverable nonlinear inelastic region, as the element begins deforming plastically. In addition, the rate of input energy is also transferred into the rate change of kinetic energy ($\dot{E}_{KIN}$) through movement of the structural element.

In compliment to the influx of energy, the rate of energy flowing out of a structural element ($\dot{E}_{OUT}$) is the summation of energy flow rates transferring to adjoining components through elastic strain ($\dot{E}_{ESOUT}$), plastic strain ($\dot{E}_{PSOUT}$), and kinetic energy ($\dot{E}_{KOUT}$) per Equation 3-6. Using these definitions, the rate of energy flow absorbed into the element, the rate of energy transferred to connecting element(s), the rate of energy flowing through the element, and the energy flow in the element is defined by the following, respectively:

$$E_{IN} = E_{ES_{IN}} + E_{PS_{IN}} + E_{K_{IN}} \tag{3-2}$$

$$E_{OUT} = E_{ES_{OUT}} + E_{PS_{OUT}} + E_{K_{OUT}} \tag{3-3}$$

$$E = E_{ES} + E_{PS} + E_{K} \tag{3-4}$$

$$\dot{E}_{IN} = \dot{E}_{ES_{IN}} + \dot{E}_{ES_{IN}} + \dot{E}_{K_{IN}} \tag{3-5}$$

$$\dot{E}_{OUT} = \dot{E}_{ES_{OUT}} + \dot{E}_{PS_{OUT}} + \dot{E}_{K_{OUT}} \tag{3-6}$$

$$\dot{E} = \dot{E}_{ES} + \dot{E}_{PS} + \dot{E}_{K} = \dot{E}_{IN} - \dot{E}_{OUT} \tag{3-7}$$

The sum total tank capacity depicts the magnitude of energy flow threshold, $E_{FAILURE}$, the point at which failure occurs given the magnitude, or level, of energy flowing through the member at a given point in time. Although located above the plastic strain 'tank' only, this threshold is the sum total of internal (elastic and plastic strain) and kinetic energy flows, but indicates failure occurs by means of excessive plastic deformation of the element material. Similarly, the change in the sum total volume per unit time of all three energy types is also limited with a rate of flow threshold, $\dot{E}_{FAILURE}$, which unfortunately is not depicted in the fluid analogy diagram. However, a non-mechanical visual of the rate of energy flow parameters is

shown with positive (+) and negative (–) arrows for the plastic strain energy tank. An analogous non-mechanical visual for the elastic strain and kinetic energy tanks is not included for clarity. Analogous to $E_{FAILURE}$, $\dot{E}_{FAILURE}$ is the point in time at which failure occurs given the rate of energy flowing through the member. The magnitude and rate of energy flow thresholds, are not only temporal and dynamic, they are interactive and interdependent.

In the context of the fluid-energy analogy, the proposed approach entails recording the E time-history for all structural components. This data was then be post-processed to calculate the $\dot{E}_{IN}$, $\dot{E}$, and $\dot{E}_{OUT}$. The resulting time-histories were analyzed to determine if, and when, a structural element fails. Extending the fluid-energy analogy from energy forms to behavioral modes, failure can be depicted for a given model of failure (Figure 3-14). This is significantly different, as this tank represents a behavioral mode (of failure) and the prior illustration represented energy modes, recall Figure 3-13. An extended version of this fluid-energy analogy in terms of mode of behavior (Figure 3-14), a diagram analogous in breadth to the fluid-energy analogy in terms of energy forms, recall Figure 3-13.

Although illustrating the energetic behavior of a single element inside a larger structural system with the fluid flow diagram is instructive, recall Figure 3-13, this diagram does include multiple unintended inaccuracies and over-simplifications. First, energy flow and energy flow rate are not only interactive, which is not visually represented, but the interdependency between these parameters is dynamic. Prior research (Tsai and Krauthammer, 2015) revealed the strength of a structural member is a function of energy flow—magnitude and rate, illustrating the member's behavior is markedly different in in different time domains.

Second, these two energy parameters also interact with the energies in connecting elements. Although there is visual reference to adjoining members with one input and four

output pipes, there is no physical representation of the adjoining members, much less interaction with the energy in the illustrated member. Although not represented, it is known the cross-section, material properties, and structural parameters of adjoining members have the utmost effect on energy flow in and out of any connected structural element.

A third significant over-simplification is flow directionality. Energy flow is not bi-directional, much less unidirectional. The energy in any given structural element flows in 3-D, thus a 4-D problem when considering time. Analyzing, and hence describing, such phenomena becomes significantly more complicated due to the additional complexities from accounting for the energies in adjoining structural members *and* the energetic interactions between members. Subsequent the first energy pulse, which travels from the failed member to, and through, all adjoining members, energy flow is highly complicated. Ensuing pulses flow in all directions, with varying wavelengths, frequencies, and magnitudes, yielding additive, subtractive, and other complicated energy flows. As shown, energy is transferred in many directions, many times. For example, even the simplest 3-D frame, examined in the following section, exhibited complicated energy flows in response to the removal of a corner column. For a structural system that is neither significantly overdesigned nor highly susceptible to PC, i.e. essentially non-redundant, the structure *must* transfer energy in order to regain stability. Thus, arresting PC requires accommodating highly complicated energy flows not only within a structural component but also between structural components and throughout the entire structural system.

The following is provided in addition to the energy-form based fluid-energy analogy. Due to the incomplete nature of the energy form-based analogy, recall Figure 3-13, a structural mode of behavior-based analogy is below (Figure 3-15). For example, Behavioral Mode A could refer to a crushing failure response, Behavioral Mode B could refer to a localized shear response,

and Behavioral Mode C could refer to a global flexural response. Thus, the following illustration is provided to stress the importance that the fluid-energy diagram illustrates the behavior of a structural element is limited to a single behavioral mode, and is thus inadequate to describing the energy flow behavior in a comprehensive manner.

3.4 Energy Flow Approach (EFA)

Although conceptually equivalent for all moment-resisting frames, the simple (single-bay single-story) frame was selected to present the proposed EFA in the most concise manner. Consequently, some efforts that would be present for a larger structure were excluded due to analyzing a 3-D single-bay frame. Pre-analysis calculation of energy flow thresholds for the failed beams and slab were also not included. In addition, quantifying the scaled distance yielding damage commensurate with removal of single column was not performed. These items were intentionally excluded given the ancillary goal of analyzing the efficacy of the Alternate Path method is of negligible value for a simple 3-D frame. Although not included in the proof-of-concept analysis presented above, force and stress-time histories were analyzed for the mid-rise building. The absent results and analyses from review of the simple frame simulations, to be applied when analyzing the three-story office building (§ 2.5), are discussed in the following sections to provide a more comprehensive description of the proposed work.

3.4.1 Determination of Energy Flow (Magnitude and Rate) Failure Thresholds

The EFA presented with the single-bay frame included several simplifications. For example, vertical propagation of failure is impossible in a one-story structure. In reality, continuing failure through the vertical-load bearing system is most catastrophic, and thus it is the principal focus for progressive collapse mitigation. To aid in identifying failure in the vertical load-bearing system, and provide a measure of quality assurance, two series of nonlinear transient dynamic finite element simulations with single columns represented with both resultant

beam elements and continuum elements was performed prior to analyzing the mid-rise frame. In contrast to the single column model illustrated, from Szyniszewski's study (Figure 3-16), the single columns models had significantly higher mesh resolutions. All columns underwent loading simulations to a collapsed state well beyond initial (global buckling) failure, where failure is defined as the inability to carry permanent static loading. Only column failure was simulated, as all moment connections are measurably stronger than adjoining structural elements.

Failure is a function of energy flow—the combination of flow magnitude and flow rate. Given this co-variable functionality, a series of nonlinear transient dynamic finite element simulations was performed to determine failure as a function of both energy flow parameters. Although it is understood that progressive collapse occurs in the pseudo-static domain, the range is undefined, thus a series of simulations were performed to describe failure throughout a measurably wider spectrum. In the interest of prudency, the load duration in these column-collapsing nonlinear transient dynamic finite element simulations ranged from the dynamic domain ($\cong$ 0.1 seconds) well into the pseudo-static domain ($\cong$ 10 seconds). Both energy flows corresponding to failure were recorded throughout this wider time spectrum. Analysis of the building's response included comparing the energy time-histories for all (near) collapsed columns against these predetermined energy flow thresholds.

To elaborate on developing the failure threshold for the columns that experience buckling, a study was performed on a single second story-supporting column. To incorporate the time-dependent aspect of the individual structural components, energy-based failure thresholds were developed. Using a matrix of loading conditions—varying both the quasi-static and (dynamic/impulsive) rates of loading for multiple degrees of freedom, failure curves were developed as a function of load and loading rate, and consequently, energy flow and energy flow

rate. An example of one series—effectively an array of collapse simulations within a larger matrix—is shown with a curve fit of the force as a function of the loading rate (Figure 3-17). The energy flow and energy flow rate corresponding to each one of these data points was extracted to develop the failure threshold for that individual structural member.

These matrices of loading conditions provide us with a better understanding of the structural elements behavior across all potential domains. Hence, the application of an energy flow approach extends beyond impulsive loading events such as blast, throughout the dynamic region, e.g. earthquake events, and into the quasi-static regime.

3.4.2 Rational for Selection of Mid-Rise Building Structure

Prior work has shown that localized failure does not typically extend beyond five stories from the initially failed region (Kirby, 1997; British Steel plc, 1999; Lennon, 2004). Accordingly, a structure more than five stories is necessary when considering, and thus for analyzing progressive collapse. In addition, the concern for progressive collapse is proportional to the height of the structure. Low-rise structures are not typically relevant to progressive collapse phenomenon—as there are insufficient degrees of separation in the vertical load carrying system between the localized failure region and the full structure. In other words, the structure does not have sufficient vertical scale to provide opportunity for the ultimately failed region to be disproportionately larger than the initially failed region.

To expand on the selection of analyzing a mid-rise office building, the following is also considered. The ten-story, or nine-story with a single-story basement, building may also prove more useful than the three-story building analyzed in Szyniszewski's 2009 study due to a potentially higher sensitivity to energy flow rate. Significantly taller, the ten-story building has significantly higher internal energy levels in columns near the base of the building. *If* buildings collapse over a similar span of time, i.e. regardless of the total height of the structure, the

collapse of the vertical load carrying system in taller buildings are more sensitive to energy flow rate. In other words, if energy dissipates through column failure within a similar span of time, regardless of a structure's height, the influence of energy flow rate on progressive collapse would be proportional to the height of the structure. Szyniszewski revealed a narrow range of loading rates (1000 – 2000 kip/s) were observed, regardless of the loading conditions or damage applied, in both the single column and three-story-building simulations (2009). However, this narrow range of loading rates, and hence assumed energy flow rates, may apply low-rise buildings only.

The antecedent study (Szyniszewski and Krauthammer 2012) analyzed two similar low-rise structural frames only. So, multiple progressive collapse events of the ten-story frame were simulated to determine if column-loading rates exceed 3000 kip/s for a mid-rise building. In other words, energy flow rates for mid-rise structures were investigated by looking at realistic loading rates pending a wide variety of structural damage scenarios.

3.4.3 Analysis of Building Response to Incremental Damage

As shown with the simplified frame, results from the progressive collapse simulation were analyzed to reveal the energy – failure correlation. Energy flow was extracted, processed, and differentiated to yield energy flow rates. More specifically, energy-time histories of all failed members was analyzed for progressive collapse inducing simulations, focusing on the levels of both energy flow parameters at the time of collapse for each affected structural element. Analysis of these simulations focused on identifying energy – damage correlations by examining how collapse progresses through the structure—specifically, timing, location, and consequent sequence. Energy flow, both magnitude (E) and rate ($\dot{E}$), were calculated from energy input and the associated rate (E_{IN} and $\dot{E}_{IN}$), and energy output and the associated rate (E_{OUT} and $\dot{E}_{OUT}$) to identify if, and when, the structural element under consideration fails. Both energy time-

histories were compared against the pre-calculated thresholds discussed (§ 3.4.1) to determine if collapse corresponds to failure in the finite element model. In other words, failure progression through the structure was compared against the energy-time histories of individual structural members to seek correlation between the time at which failure occurs and energy flow. Comparing the location and time of each failed member with the respective member's energy flow substantiated the efficacy of the EFA presented.

3.4.4 Incorporation of Connections as Structural Elements

The simplified test frame did not consider connections. The test frame model, with members being rigidly connected as done in Szyniszewski's work, neglected the connections. For the proposed work, the strength of the connections was considered as well as the associated energetic behaviors, i.e. transmitting, absorbing, and, dissipating energy. Further details regarding the proposed modeling methods were presented (§ 2.5.3 and § 3.1.1.3). The antecedent connection reductionist modeling study concluded, "The 10-story building with full-rigid moment connections could withstand the 5-column removal case while only three column removal collapsed the building with the moment connections whose stiffness and brittleness are defined in detail" (Yim and Krauthammer, 2009).

3.4.5 Energy Flow-Based Response States for Evaluation of Alternate Path Method

To improve understanding of structural behavior as defined by energy flow, analyses of energy-time histories and resulting energy rate time-histories corresponding to three response states may serve as rational reference points allowing for a more in-depth review of the Alternate Path method. The selected response states are a) damage incurred is energetically equivalent to a single column removal, b) damage results in failure of the column with realistic damage sustained by adjoining structural members, and c) the energy flow thresholds at the onset of

progressive collapse initiation. The damage criteria for the first two response states were determined, in part, with DSAS, and the third with a combination of DSAS and LS-DYNA.

The energy flow corresponding to a single column failure was determined by means of examining permanent deformation and/or the remaining strength of the weakened structures. Additional efforts identified the scaled ranges corresponding to the other aforementioned categories. In part due to the energy flows associated with the behavioral responses being successive, with no two points being coincident, these three energy flows based on analyses with realistic damage levels yielded four (4) response categories (Figure 3-18). Graphical representation helps illustrate the correlation between the Alternate Path method and nonlinear transient dynamic finite element simulations. The illustration is also included to aid in conveying that designing a structural frame to withstand removal of a single column is providing the *absolute minimum level of redundancy* in the vertical load carrying system.

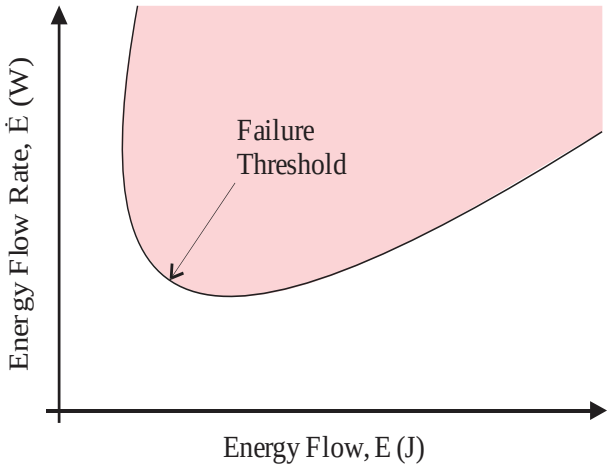

Figure 3-1. Energy based load-impulse failure threshold.

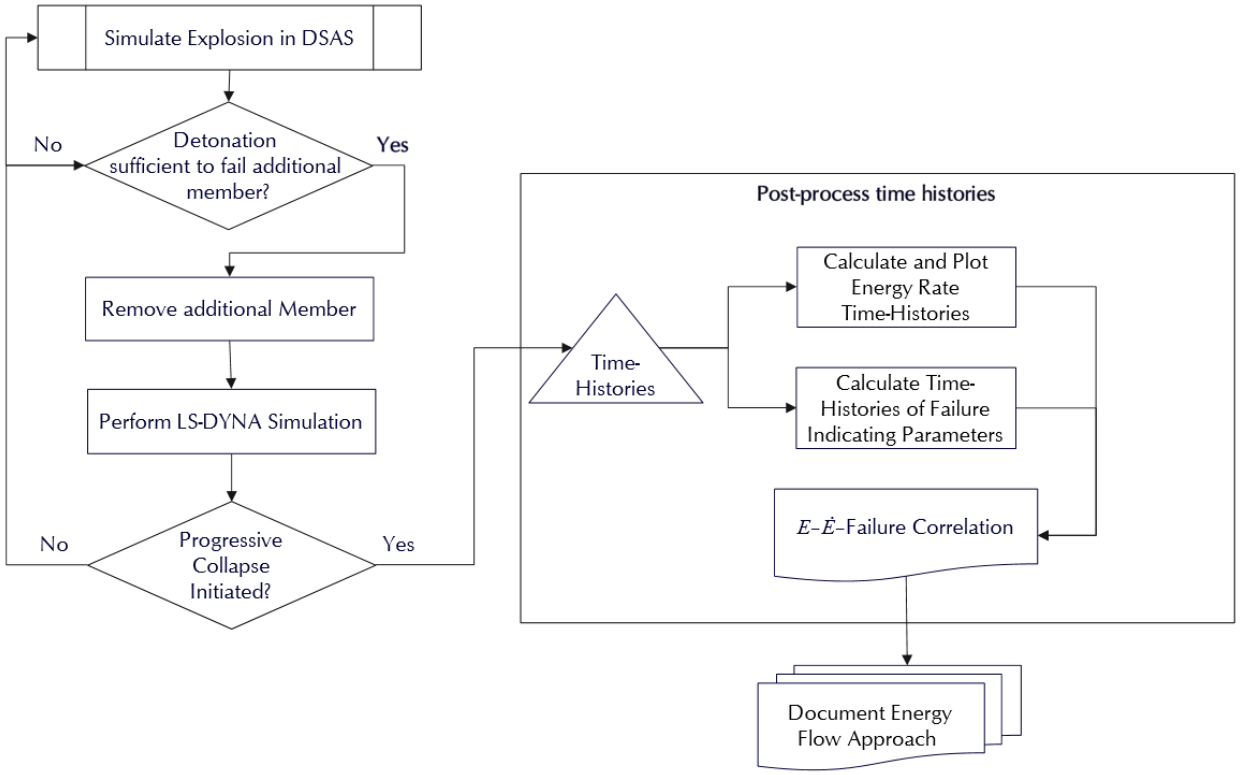

Figure 3-2. Flowchart of Analytical Process.

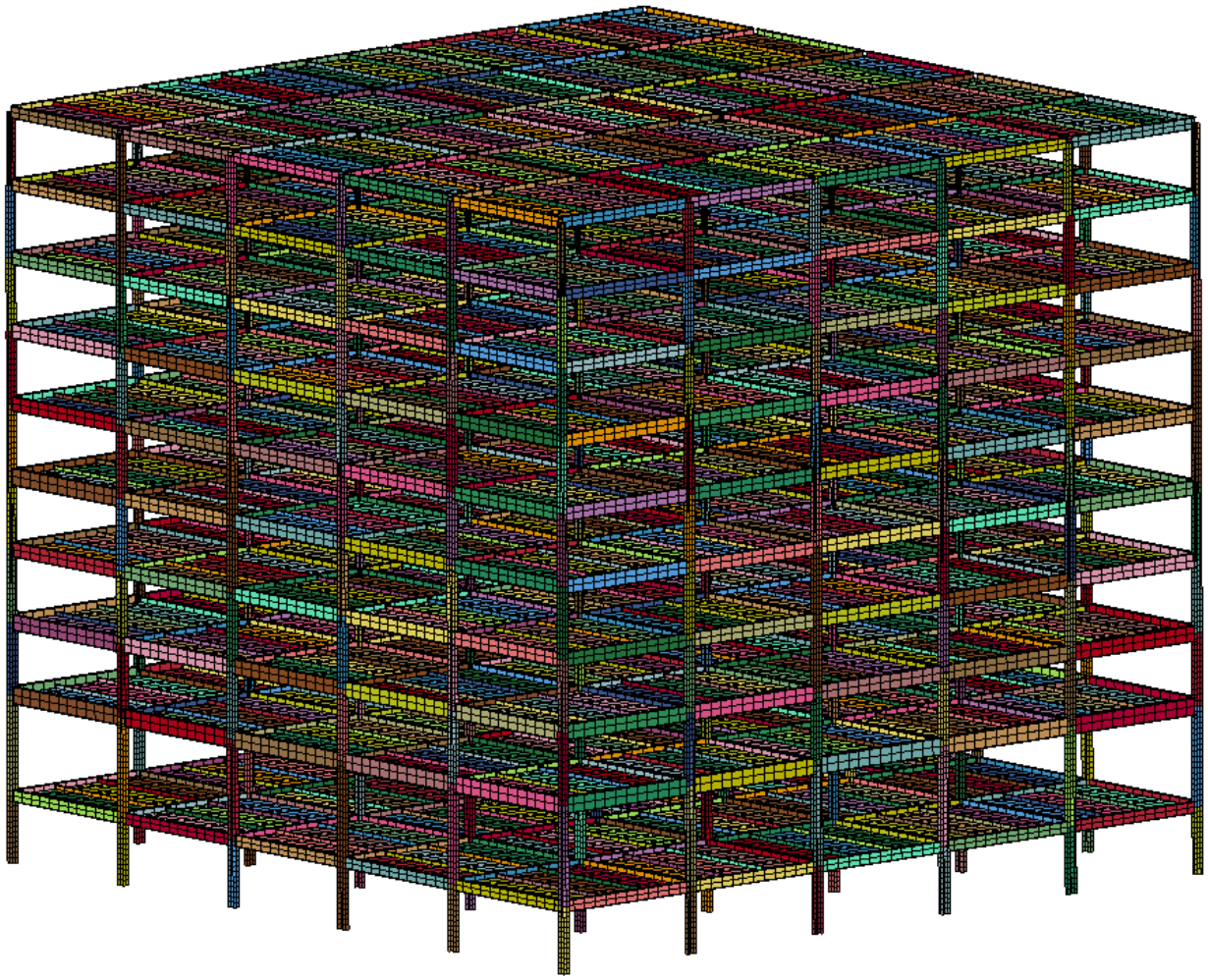

Figure 3-3. LS-DYNA Model of SAC-commissioned Mid-Rise in Boston.

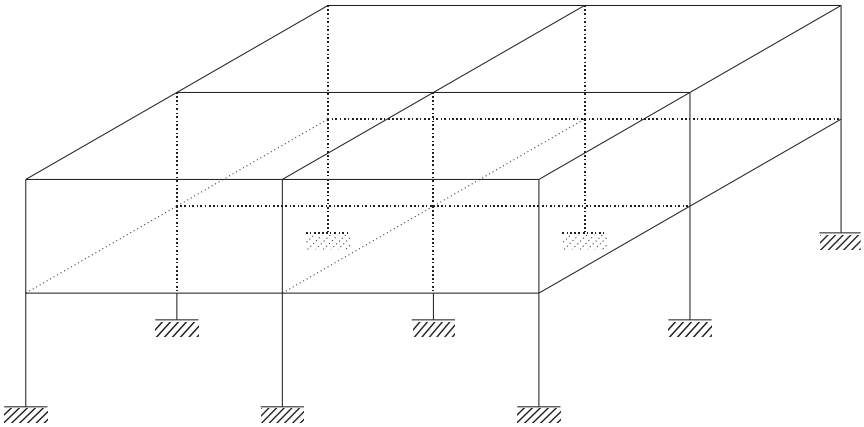

Figure 3-4. Boundary conditions: fully fixed columns bases. (Note: Two bay by two bay by two-story frame for illustration only).

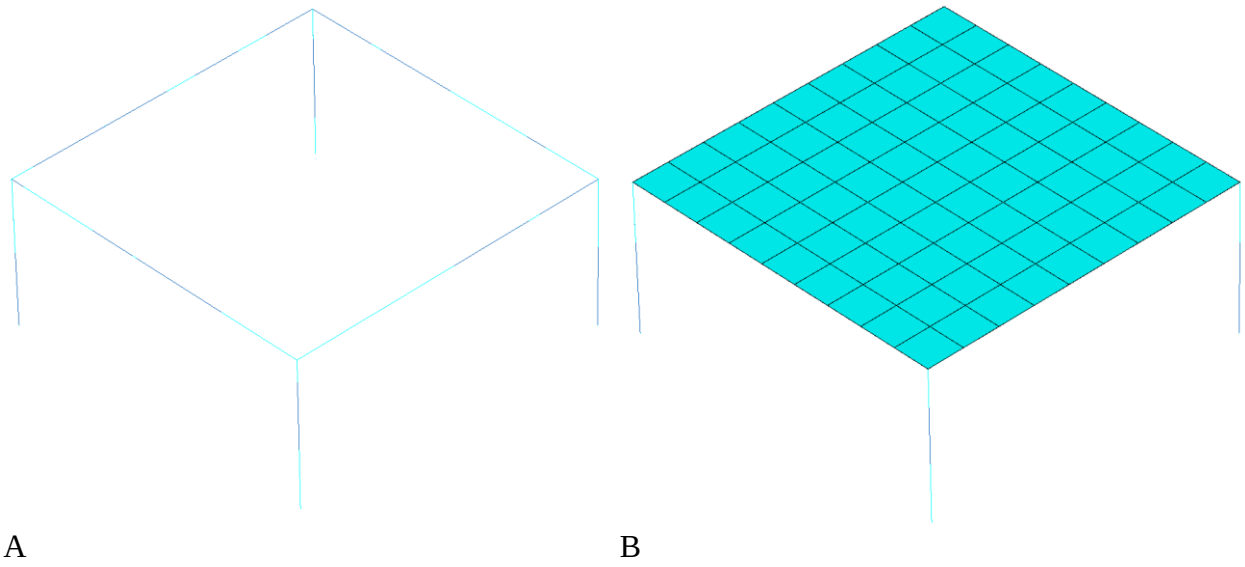

A B

Figure 3-5. Simplified model of single-bay frame using resultant elements. A) Resultant beam elements represent columns and girders (cross-section not shown for clarity). B) Column and girder resultant beam elements shown with shell elements representing slab.

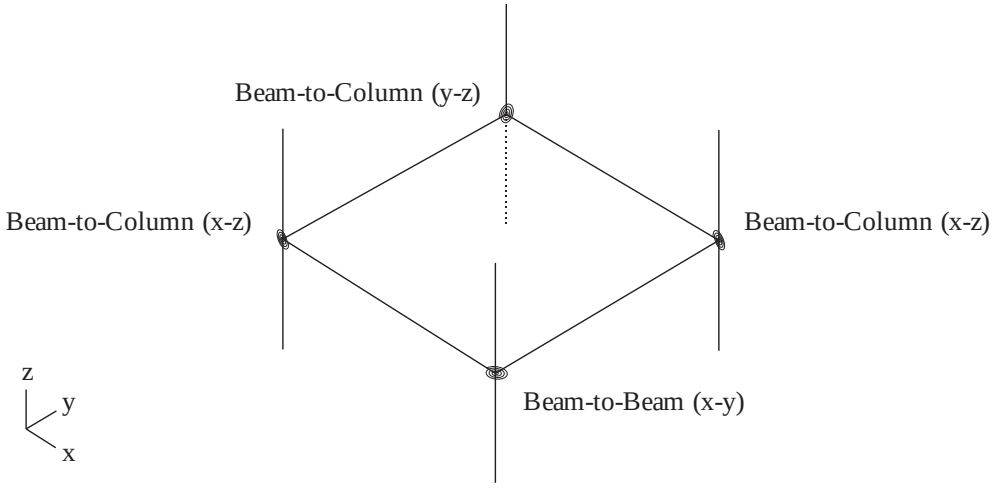

Figure 3-6. Connections modeled with springs referencing nonlinear strength curves (Illustration limited to one (1) degree-of-freedom-specific spring at four connections for clarity).

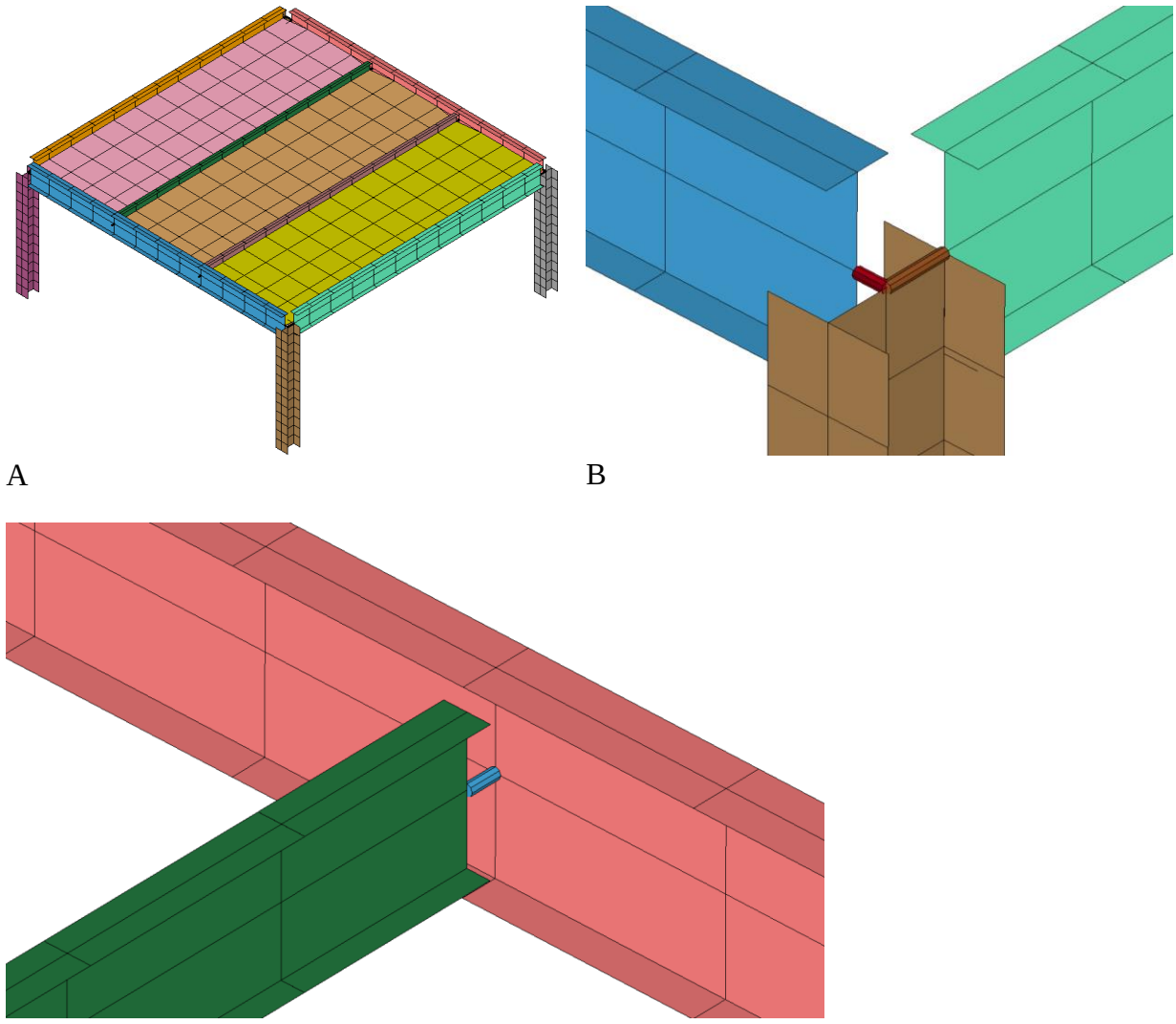

Figure 3-7. Isometric view of LS-DYNA model. A) Single bay with beams and connections rendered. B) 6 degree-of-freedom beams represent all girder – to – column connections. C) 6 degree-of-freedom beam elements represent all in-fill beam – to – girder connections.

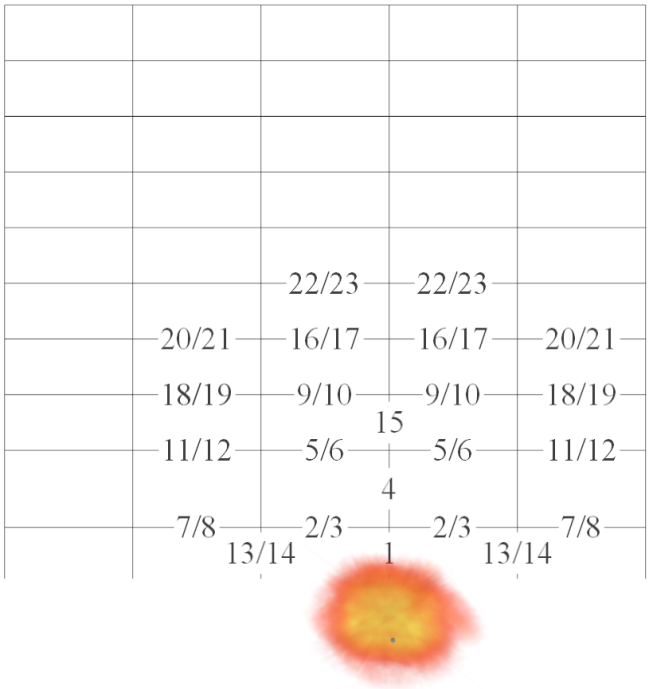

Figure 3-8. Sequence of failed members as determined with DSAS analyses.

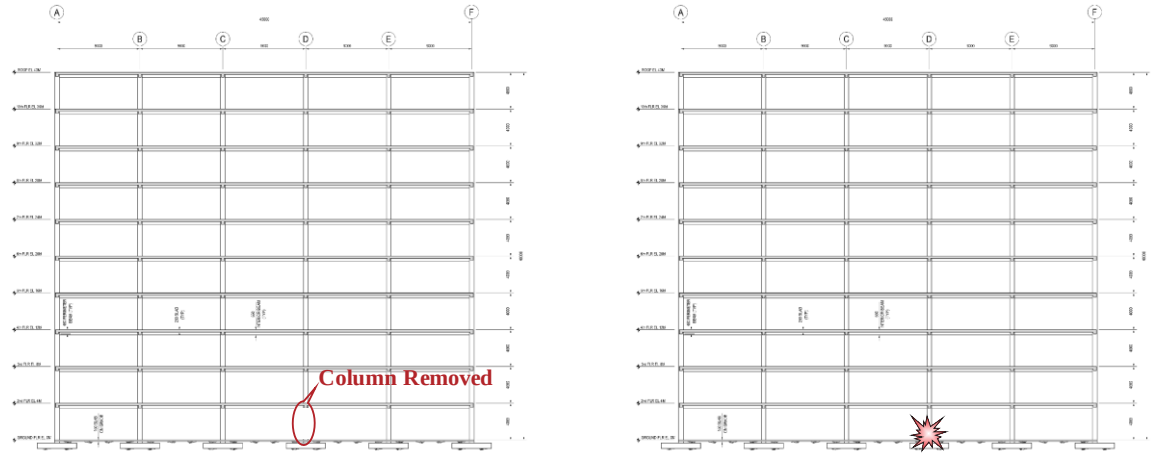

A B

Figure 3-9. Elevation of mid-rise office building. A) Location of notionally removed column. B) Location of detonation in DSAS.

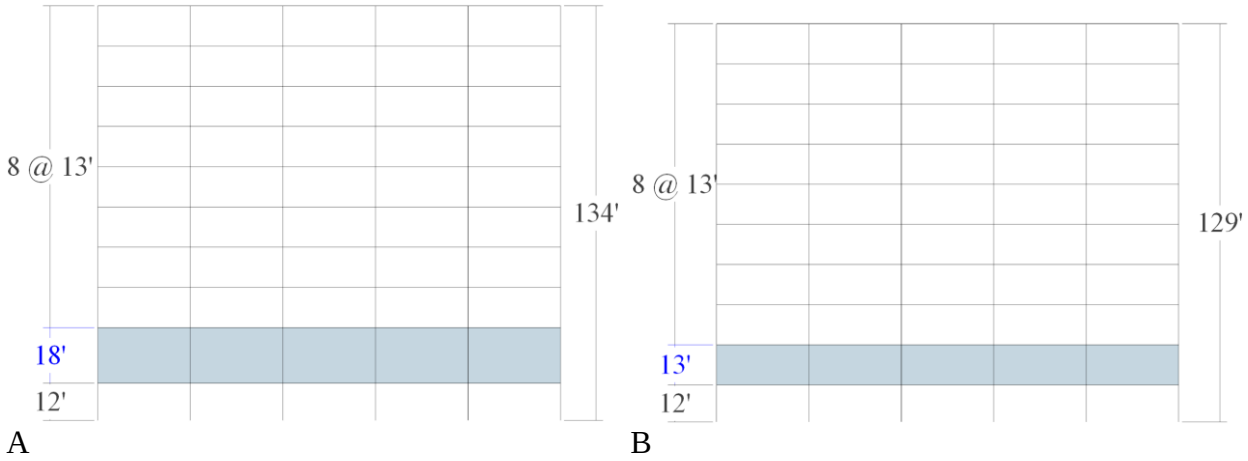

Figure 3-10. Elevation of ten-story moment resisting steel frames modeled. A) SAC-commissioned mid-rise in Boston with eighteen-foot second story. B) Modified version of same building design with second story reduced to thirteen-feet.

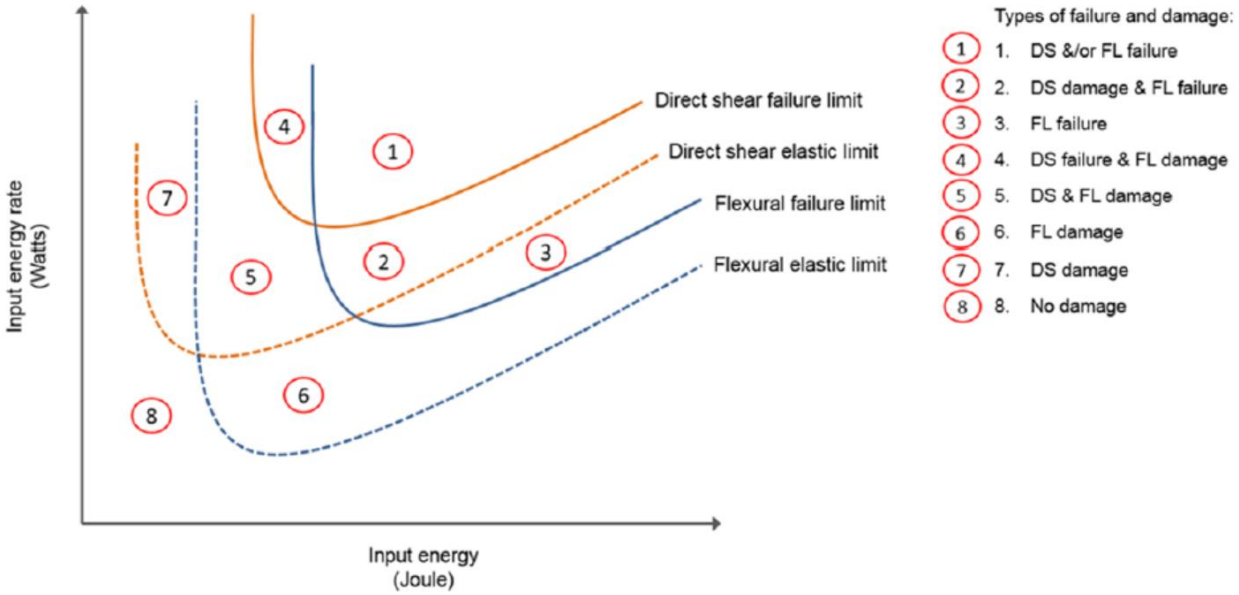

Figure 3-11. Typical energy based P-I diagrams for multi-failure modes. [Reprinted with permission from Krauthammer, Theodor. 2015. Energy Based Load-Impulse Diagrams for Structural Elements. PhD dissertation (Page 124, Figure 3-12). University of Florida, Gainesville, Florida.]

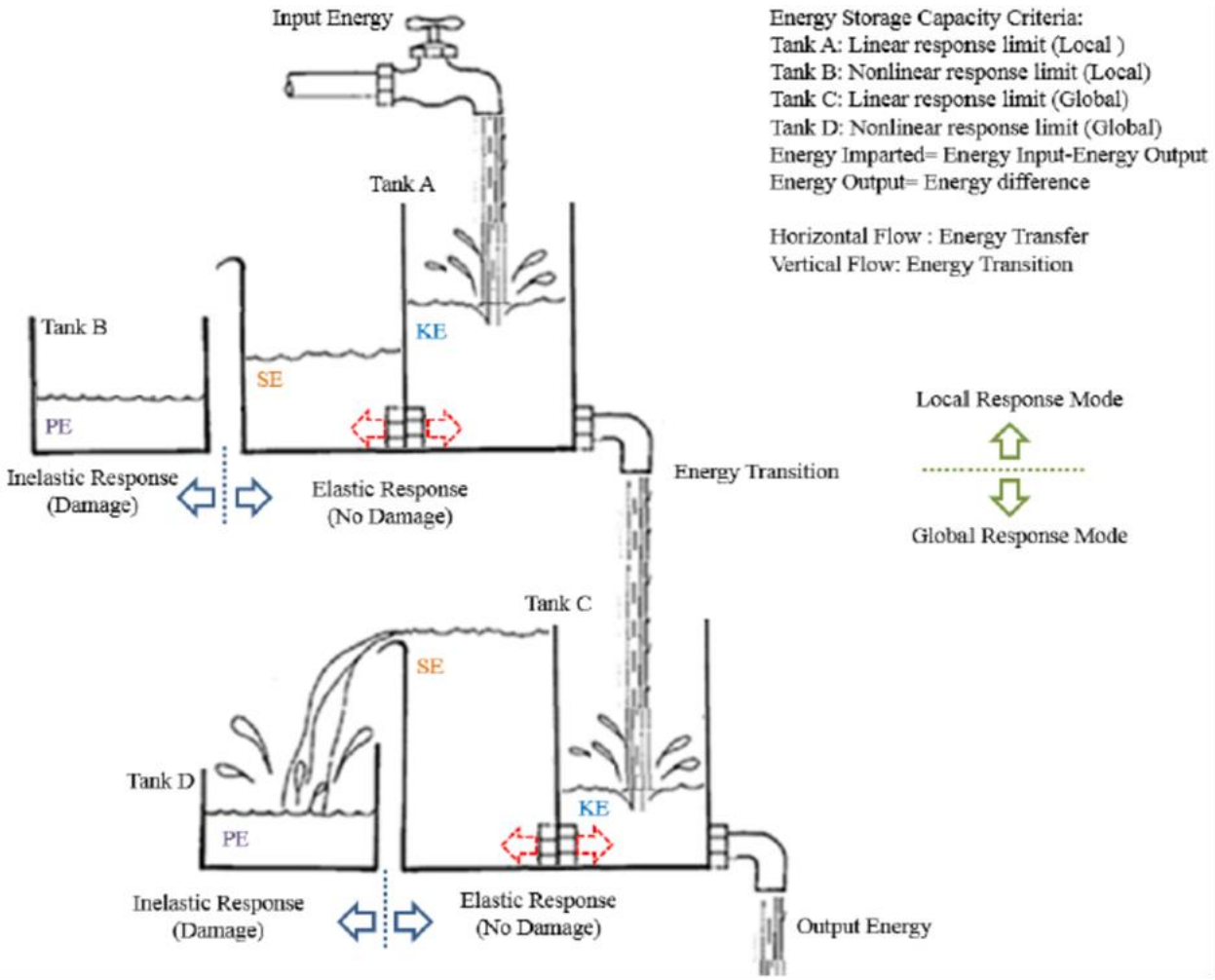

Figure 3-12. Illustration of energy tank analogy. [Reprinted with permission from Krauthammer, Theodor. 2015. Energy Based Load-Impulse Diagrams for Structural Elements. PhD dissertation (Page 123, Figure 3-10). University of Florida, Gainesville, Florida.]

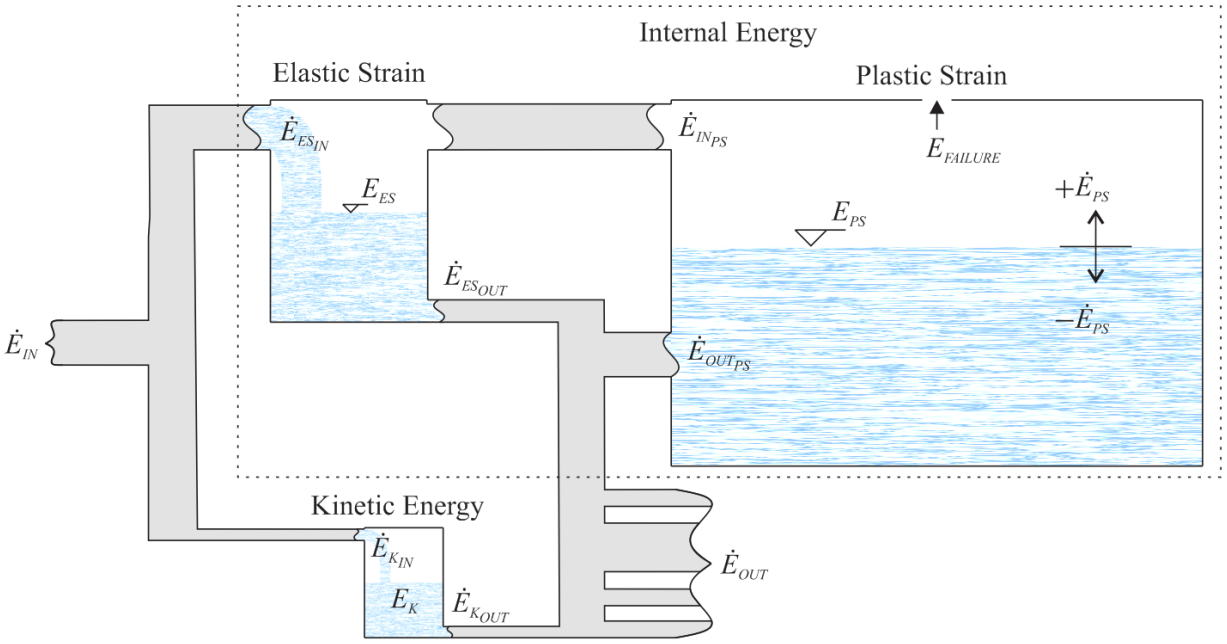

Figure 3-13. Illustration of fluid-energy conceptual analogy

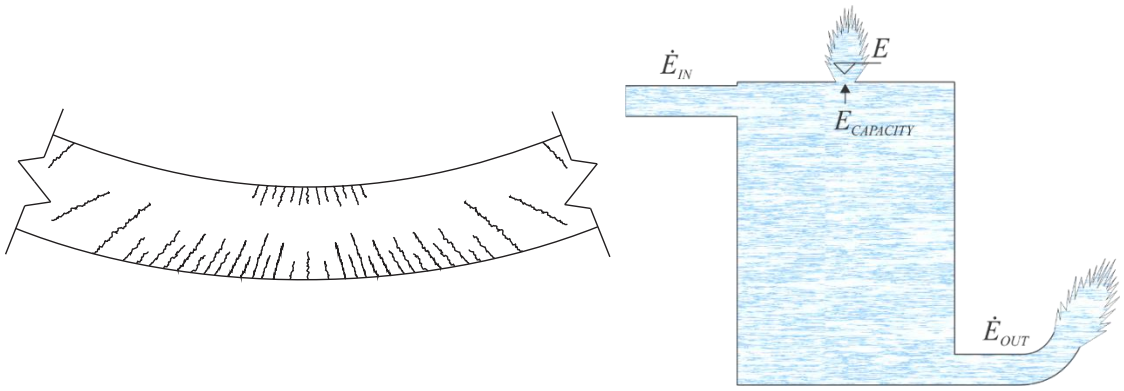

A B

Figure 3-14. Flexural failure corresponding to magnitude of energy flow threshold only ($\dot{E}$ threshold, interaction between energy modes, and adjoining members ignored for clarity). A) Bending-only behavioral response mode. B) Fluid tank corresponding to bending behavioral response mode.

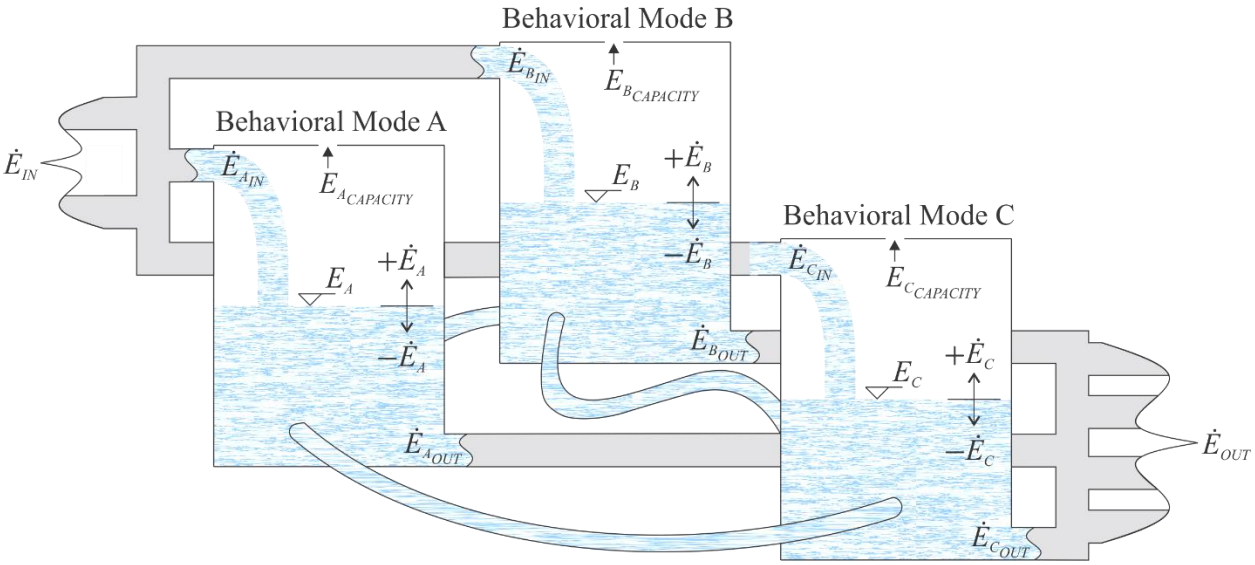

Figure 3-15. Alternative illustration of fluid-energy conceptual analogy for a single structural element in terms of structural behavioral modes.

Figure 3-16. Finite element model comprised entirely of solid ‘brick’ elements

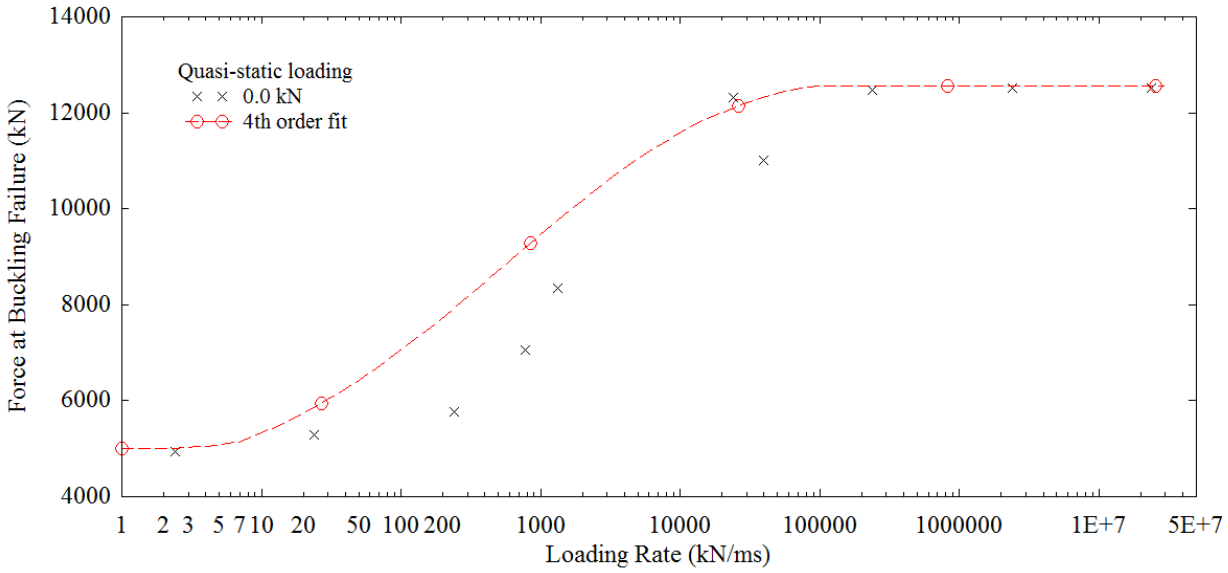

Figure 3-17. Loading rate – buckling failure of eighteen-foot columns supporting second story of the SAC-commissioned mid-rise building model.

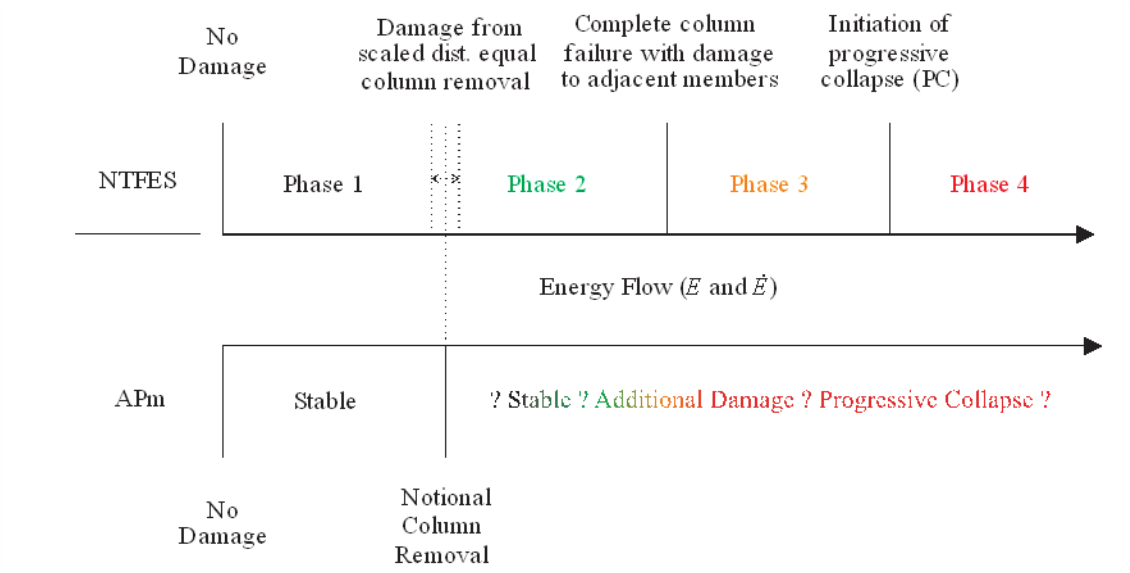

Figure 3-18. Behavioral Response Comparison between nonlinear transient dynamic finite element simulations (NTFES) and Alternate Path method

CHAPTER 4
RESULTS

The Energy Flow Approach (EFA) presented here addresses multiple research objectives with a rational and highly accurate methodology. The primary was to develop an analytical framework capable of demonstrating a successful assessment of progressive collapse susceptibility—with an accuracy and precision on par with the most rigorous state-of-the-art nonlinear transient dynamic finite element analyses. An energy flow-based presentation of energy–time histories corresponding to structural instability (§ 4.1) demonstrates the EFA detailed here satisfied this primary objective. The evidentiary support for concluding this EFA is effective is done using the results from a non-collapse building response compared against a collapse-inducing simulation.

In addition, the efficacy of the Alternate Path method for typical mid-rise moment resisting steel framed buildings was evaluated. With the Alternate Path method being a threat-independent notional approach, this method was evaluated for mitigating progressive collapse. As expected, the damage induced from realistic explosive threats was not commensurate with failure of a single column. It is important to note the results from the two initial damage states discussed in the following section illustrate the efficacy of this EFA (§ 4.1) are commensurate with viable blast loads corresponding to LVBIEDs or similar—both of which are orders of magnitude, in terms of scaled distance, from a single column removal, i.e. the Alternate Path method.

The tertiary goal entailed determining the extent of redistribution for blast loading threats that do no induce collapse, i.e. non-collapse loading events. Effective stresses and strains were analyzed to identify where the effects of a variety of initial damage conditions stopped.

Results for these three goals—the primary, secondary and tertiary—are presented accordingly, i.e. in order of importance: efficacy of the EFA (§4.1), efficacy of the Alternate Path method (§ 4.4), and the determination of the extent of redistribution is tertiary (§ 4.5).

To aid in identifying the limits, or the applicability, of the novel EFA offered, the structures considered in this research were derived from the SAC [a joint venture (JV) of the Structural Engineers Association of California (SEAOC), Applied Technology Council (ATC), and California Universities for Research in Earthquake Engineering (CUREe)] commissioned mid-rise building in Boston. This ten-story frame includes a single-story basement, moment resisting WUF-B connections, and single plate (shear tab) connections (FEMA, 2000). Although all numerical results are structure specific, the proposed EFA methodology can be to any (moment-resisting) structural frame. In fact, assuming a reliable resistance function for all potential failure modes can be calculated, *any* structural system could be analyzed for failure with the proposed EFA for any loading events—from impulsive to quasi-static.

4.1 Non-Collapse vs Collapse of SAC-Commissioned Building Model

The thesis of this research is that energy flow (E and $\dot{E}$) determines failure. The energy – failure correlation is inherent in physical systems, and exists in nonlinear transient dynamic finite element software because the development of these numerical codes is based on energy equilibrium principles. Hence, progressive collapse is known to be a function of a structure's ability to accommodate energy flowing through its components, which is a function of constitutive material definitions, cross-sectional properties, and structural parameters. Given these understandings, energy-time history, quantifiable with nonlinear transient dynamic finite element simulations, was extracted, post-processed, and compared to the behavior of the finite element model to determine the efficacy of using energy flow to predict progressive collapse susceptibility.

Initially, the energy – failure relationship was described using the results of analyses with a FEM of a simple 3-D frame (Figure A). Execution of the proposed methodology on a simplified structure provided data that helped serve as a guide for best potential approaches when subsequently analyzing the larger mid-rise building frame. Following success with the preliminary simple frame, the effects of loading rates were examined further. Specifically, the effects of loading/energy flow rates of a variety of columns within the mid-rise structure of interest were analyzed in multiple sub-studies (recall Figure 3-17).

Following these results, the EFA was applied to a two-bay-by-two-bay two-story portion of the SAC-commissioned mid-rise steel frame in Boston (Figure A-9). This larger frame was more complex not only due to more members, but also because significantly complicated techniques were employed to represent the column-to-girder connections. The connection modelling methods employed were not only theoretically consistent with the EFA—a allowing for a comprehensive account for all energy forms, but all degrees of freedom were accounted for with nonlinear curves. The moment-rotation degrees-of-freedom were derived from the curves developed from discrete models of the connections, and the translation curves from calculations incorporating the weakest connecting elements for the degree-of-freedom under consideration (Yim and Krauthammer, 2012).

Following these preliminary studies, the EFA was subsequently applied to the SAC-commissioned mid-rise steel frame building in Boston (recall Figures 2-7 and 2-8). To summarize this process, energy flow-based failure thresholds were developed from analyses of individual structural elements (recall Figures 3-16 and 3-17) per the methodology developed by Tsai and Krauthammer (2015). Utilizing these energy flow thresholds, the sequence of members (nearly) exceeding these capacities were compared against the structural response observed from

the midrise finite element models under consideration for a variety of blast-induced damage conditions (Table 4-1). A flowchart of this method was provided (Figure 3-2). Consequently, the efficacy of the proposed EFA to provide a rational means for progressive collapse was realized.

To provide some additional information regarding the challenges encountered during the development and verification of the EFA, the following is offered. Out of concern that the preferred failure indicating parameters, i.e. yielding the highest correlations, may differ between the simple frame model and the mid-rise steel framed building, multiple mini sensitivities studies were performed. For example, energy flow rate ($\dot{E}$) and displacement may yield the highest correlation for simulations with the test frame, but plastic strain and both energy flow parameters (E and $\dot{E}$) may yield the highest correlation for simulations with the mid-rise building. Regardless of the chosen parameters, the results reveal a reliable approach for damage-specific assessments of progressive collapse. After patterns suggesting correlation between energy flow and failure were identified, research efforts were focused on presenting a formalized EFA.

Upon completion, results showed the proposed EFA is more accurate and precise than traditional force-based approaches. In addition, the EFA presented yielded superior assessments of progressive collapse than the antecedent energy-based approach by Szyniszewski (2009). The energy – failure relationship being proven by the antecedent study (Szyniszewski and Krauthammer, 2012), combined with understanding the rate of energy flow affects structural behavior, the proposed work promises an accuracy and precision beyond any known approach to progressive collapse. This is expected given the additional considerations of modeling the structural connections, incorporating energy flow rates into failure prediction, and all done for a progressive collapse-relevant mid-rise steel framed building.

4.1.1 Global View: System-Wide Energy Flow

From a global perspective, information regarding the stability of the structure can be obtained from even the most superficial review of system-wide energy-time histories. If energy-time histories reach equilibrium within a scale of the energy levels measured at the onset of the simulation, i.e. initial, albeit post-blast damage, conditions, it is understood that failure of any additional structural members has been arrested (Figure 4-1A). More succinctly, progressive collapse does not occur. In contrast, when system-wide energy increase markedly beyond the initial system energy level, a catastrophic collapse event has occurred. To elaborate, the structure has become unstable, and this monumental release of energy is obvious—well before the deformations and displacement become large enough to indicate collapse is imminent (Figure 4-1B). In addition to the stress contours plots in the frame referenced above, plastic strain contours are also provided for all of the structural elements to help illustrate the differences in the progression of failure, or lack thereof, throughout the model of the mid-rise building frame. Plastic strains for all beam element types—columns, column-to-girder connections, girders, girder-to-infill beam connections, and in-fill beams are shown in Figures 4-2A and 4-2B. Plastic strains for all shell element types, i.e. slabs, are shown in Figures 4-2C and 4-2D.

4.1.2 Local View: Energy Flows of a Critical Column

To illustrate variances in the energy flow at the local level, an individual column—critical to the response of the structure—was selected (Figure 4-3). Given the detonation location, various blast-induced damage assessments considered, and origination of the failure progression observed, this second story first interior column is the most critical column for indicating a progressive collapse. In short, this column is the first to fail *if* a progressive collapse event is going to occur. For this column location, the energy flow – energy flow rate history for a damage condition on the lower spectrum of damages assessed in this study is provided (Figure

4-4). In addition, for this same column location, energy flow – energy flow rates are provided for a larger number of simulations conducted (Figure 4-54-5). As indicated, superimposing the energy flow versus energy flow rate time histories of this column on top of the energy-based load-impulse failure threshold yields and accurate and precise, i.e. repeatable, collapse prediction. In the interest of brevity, not all conditions simulated are discussed in detail here. However, a more comprehensive report with results from additional simulations is available (Wilkes and Krauthammer, 2016).

4.2 Two Collapse Scenarios with the Modified SAC-Commissioned Building Model

Despite the final states of total building collapse for both of the simulations discussed in the following sections, the energetic behavior of the building model—due to different initial blast-induced damage states—is strikingly different. The lower damage state considered consists of the removal of five columns and ten beams (Figure 4-6A). The higher damage state considers the removal of five columns and eighteen beams (Figure 4-6B). Although both simulations result in a progressive collapse event, the behavior of the damaged structural frames is markedly different, which is illustrated with differences in the energy-time histories at the global, regional, and local levels. The following investigation constitutes a novel analysis of the behavior of buildings.

4.2.1 Global View: System-Wide Energy Flow

The analogous information presented for the finite element model of the SAC-commissioned mid-rise design in Boston above (§4.1), is presented for the modified finite element model with stiffened N-S column connections and soft-story eliminated (recall 3-10). Although not apparent from observing the deformed state of the building models as far along as thirteen seconds after the application of the blast-induced damage (Figures 4-7A and Figure 4-7B), both buildings are in a state of complete structural collapse. As observed from the overall

system energies for the non-modified building model, the stability of the structure can be obtained more astutely and rather quickly from observing the energy-time histories (Figure 4-7C). To contrast the response of these two damage scenarios, the energy flow is plotted against the energy flow rate (Figure 4-8). In short, the energy flow rate of the damage severe blast-induced damage assessment with eighteen columns is severe at the onset of the numerical analysis. Although this significantly higher energy flow rate is 'short lived', the damage incurred yields a more vulnerable structure, thus failure propagates more rapidly.

4.2.2 Local View: Energy Flows of a Critical Column

Results from the same critical second floor column for the non-modified building model are provided here for the modified building model (Figure 4-9). Since both of these simulations yield a prediction of total structural collapse, the differences in the energy-time histories for this critical column is not instability vs stability, but with the differences in the rates of energy flow and thus the point at which collapse occurs (Figure 4-10). In addition, the energy-time histories for this column with the initial damage state including the removal of eighteen columns also indicates the point in time in which the element fails beyond local buckling and is partially removed by means of element deletion—a condition reached due to a plastic yielding to a strain of 0.20 mm/mm. The energy flow vs energy flow rates for this column for an array of initial blast-induced damage assessments (recall Table 4-1) are provided (Figure 4-11). Again, not all conditions simulated are discussed in detail here in the interest of brevity, but a more comprehensive report with results from additional simulations is available (Wilkes and Krauthammer, 2016).

4.2.3 Regional View: Furcating Energy Flows

Due to the soft second story of the SAC-commissioned mid-rise building, a modified (numerical model) version of this design was developed—more representative of typical mid-rise

office buildings. The modifications to the SAC-commissioned building design were reduction of the second story from eighteen feet to thirteen feet and stiffer N-S column-to-girder connections.

With this modified version of the mid-rise building, differences in the energy flow behavior were observed. Although both simulations result in catastrophic progressive collapse scenarios, the behavior of the structures between the initial blast-induced damage state and the final collapsed state are drastically different. The energy-flow based comparison could be described as an antithesis of the butterfly effect—whereby infinitesimally small differences in the initial input conditions yield drastically results. In contrast, a markedly different set of initial conditions yielded the same result—a fully collapsed structure. However, as demonstrated, the likelihood of collapse is a path-dependent process, and the two simulations in comparison here exhibit different behavior.

The two scenarios under review consist of an initial damage assessment of five columns and ten beams (Figure 4-6A) and an initial damage assessment of five columns and eighteen beams (Figure 4-6B). Specifically, with the removal of an additional eight beams along the exterior face of the building (adjacent the blast location), the structure with the initially assessed higher level of damage experiences an approach towards collapse in a more accelerated fashion. Conversely, the structure with ten removed beams approaches a structure-wide collapse in a slower fashion. This is primarily due to the a significantly lower energy flow rate at the beginning of the simulations—due to the presence of the exterior column-to-column girders on the third, fourth and fifth floors. Interestingly, neither building models succumb to collapse until more than ten seconds after the initial blast-induced damages are applied. A series of isometric views with corresponding energy-time histories, emanating from the base of the first interior column on the second floor, adjacent the detonation location, through the connections and into

the girders is provided (Figures 4-12 through 4-19). In short, this sequence of energy-time history plots illustrates the delay of energy flow for the ten-beam damage scenario in comparison to the eighteen-beam scenario. The energy-time histories for all second floor columns of both damage scenarios for the modified version of the SAC-commissioned building model are provided (Figure 4-20) to illustrate the energy behavior comparisons discussed above are representative of the entire second floor, and not a localized behavioral phenomenon. Please note the discontinuity in the energy-time histories for many of the columns in Figure 4-20B correspond to column failure by means of element deletion, as defined by a strain of 0.20 mm/mm. In addition, it is important to note the energy levels shown in the energy time histories due not necessarily correspond to damage levels or proximity to collapse.

4.3 The SAC-Commissioned vs The Modified SAC-Commissioned Building Model

The modified SAC-commissioned building model included two changes to the original SAC-commissioned building model. The first change entailed reducing the height of the second story from eighteen-feet to thirteen-feet and the second change entailed strengthening the North-South column – to – girder connections were from shear to moment-resisting.

Although a number of significant behavioral changes resulted from these two modifications, the consequential effect with respect to initiating a PC event was not markedly different. In effect, the increased robustness of the SAC-modified building model translated to the removal of one additional exterior column—for an exterior detonation offset along the side of the building. A tabulated list of the collapse results for exterior – side air blasts at ground level simulated for both mid-rise building frame models is provided (Table 4-1).

4.4 Efficacy of Notional Single Column Removal

The first ancillary portion of this work focused on determining the efficacy of the Alternate Path method for mitigating progressive collapse for mid-rise steel buildings, and

potentially setting limits for appropriate used of the Alternate Path method; e.g. quantifying an energy load limit for application the Alternate Path method. It is anticipated the UFC's Alternate Path method is unconservative once the imposed threat level causes damage in excess of failure of a single column. In addition, this energy level is expected to be less than the energy required to initiate progressive collapse. As indicated from prior research studies and course teachings at CIPPS, DSAS was utilized to develop numerical representation of damaged structural members following prescribed air blasts. The results were then be transcribed into the LS-DYNA model in the form of member removal. In short, notionally removing a column was compared with DSAS calculated damage.

To expand on this effort, localized damage was applied to a complete building frame model, improving understanding of the relationship between localized damage and progressive collapse. Again, this portion of the proposed research compares results from using the UFC prescribed Alternate Path method with a more realistic case-specific threat, both using a FEM of a ten-story moment resisting steel building. Namely, disparities between notional removal of a single column and damage resulting from realistic threats may demonstrate when the Alternate Path method becomes unconservative, and thus insufficient to prevent progressive collapse. If the Alternate Path method is determined to be of value, limitation of the Alternate Path method may be provided, e.g. a scaled range for a given structural system. Results from this ancillary portion of the research aided in describing the efficacy of the threat-independent Alternate Path method design provision for mid-rise moment resisting steel frames. In short, realizing minimum redundancy does not equate to attaining the robustness needed to sustain a realistic explosive threat.

4.5 Extent of Redistribution

An extensive series of experimental studies were performed to research the effects of severe fire loading scenarios in multi-story steel structures frames (British Steel plc, 1999). Although the loading events under consideration were a variety of fire scenarios, i.e. different from blast-induced scenarios, researchers learned about the extent of the effects throughout the entire frame resulting from a loading condition causing localized failures. The results from this work helped to answer how many stories are required to support a frame structure above a decimated story. In other words, the question of concern deals with determining how far (vertically) the effect of a removed column travels up a typical structural steel frame. In short, four to five stories above the failed members experienced increased loading.

Thus, a loading scenario in which localized damage is applied, on the order of multiple structural members—including no less than one column, requires approximately four stories of framing above the damaged area in order to supporting the hanging portion of the structure, or 'bridge' over the damage area. The results from the numerical simulations performed for this study correspond well with the prior research conducted in the UK. In effect, no less than four stories were required to support the damage story for the steel structure considered in this study.

4.6 Recommendations

Given the successful correlation shown between energy flow, energy flow rate, and failure, and thus consequently, the relationship between energy flow and the susceptibility to catastrophic collapse, the following includes a number of potential research endeavors intended to extend the aim of the present study. Such efforts could advance progressive collapse assessment methodologies for the protective structures industry.

To start, development of failure thresholds for all viable failure modes as well as mixed-mode failures is suggested. An extension of the success of the preceding work by Tsai and

Krauthammer (2015) would greatly further the potential for the inclusion of energy-based methodologies into structural engineering practice. Such a library, coupled with the efficient damage assessment capability of DSAS would provide a highly efficient approach capable of predicting more accurate susceptibility estimates for structural engineers practicing in the protective design community.

Within the framework of the UFC's current PC design guide (DOD, 2013b), an EFA could be included within a fourth analytical category—in and addition to the three current options: LS, NS, and ND. In order to improve the likelihood of extending the findings of this research into the practice of structural engineers working on protective structures, a number of additional advancements are also suggested. By considering blasts on additional floors, results may give additional information regarding the sensitivity of blast location to collapse susceptibility, which would arguably be a structure-specific investigation. In addition, evaluating the sensitivity of which structural element failures within the 'region/zone of destruction' may provide insight into the issue of the contribution of connections to stability—at the edge of the destruction zone. The methodology presented here offers opportunities in regards to quantifying collapse susceptibilities under loading conditions beyond that estimated by design provisions; i.e. determining a sensitivity to overloading. Such investigations could provide invaluable information for older structures needing to undergo retrofitting methods for modern applications and loading scenarios.

Table 4-1. Collapse result comparison between mid-rise building models.

	SAC BO Building	
Blast-Induced Damage	Original	Modified
One Column	Non-Collapse	Non-Collapse
One Column & One Girder	" "	" "
One Column & Two Girders	" "	" "
Two Columns & Two Girders	" "	" "
Two Columns & Three Girders	" "	" "
Two Columns & Four Girders	" "	" "
Two Columns & Five Girders	" "	" "
Two Columns & Six Girders	" "	" "
Two Columns & Seven Girders	" "	" "
Two Columns & Eight Girders	" "	" "
Two Columns & Nine Girders	" "	" "
Two Columns & Ten Girders	" "	" "
Three Columns & Ten Girders	Collapse	" "
Four Columns & Ten Girders	" "	Collapse
Five Columns & Ten Girders	" "	" "
Five Columns & Eleven Girders	N/A	" "
Five Columns & Twelve Girders	N/A	" "
Five Columns & Thirteen Girders	N/A	" "
Five Columns & Fourteen Girders	N/A	" "
Five Columns & Fifteen Girders	N/A	" "
Five Columns & Sixteen Girders	N/A	" "
Five Columns & Seventeen Girders	N/A	" "
Five Columns & Eighteen Girders	N/A	" "

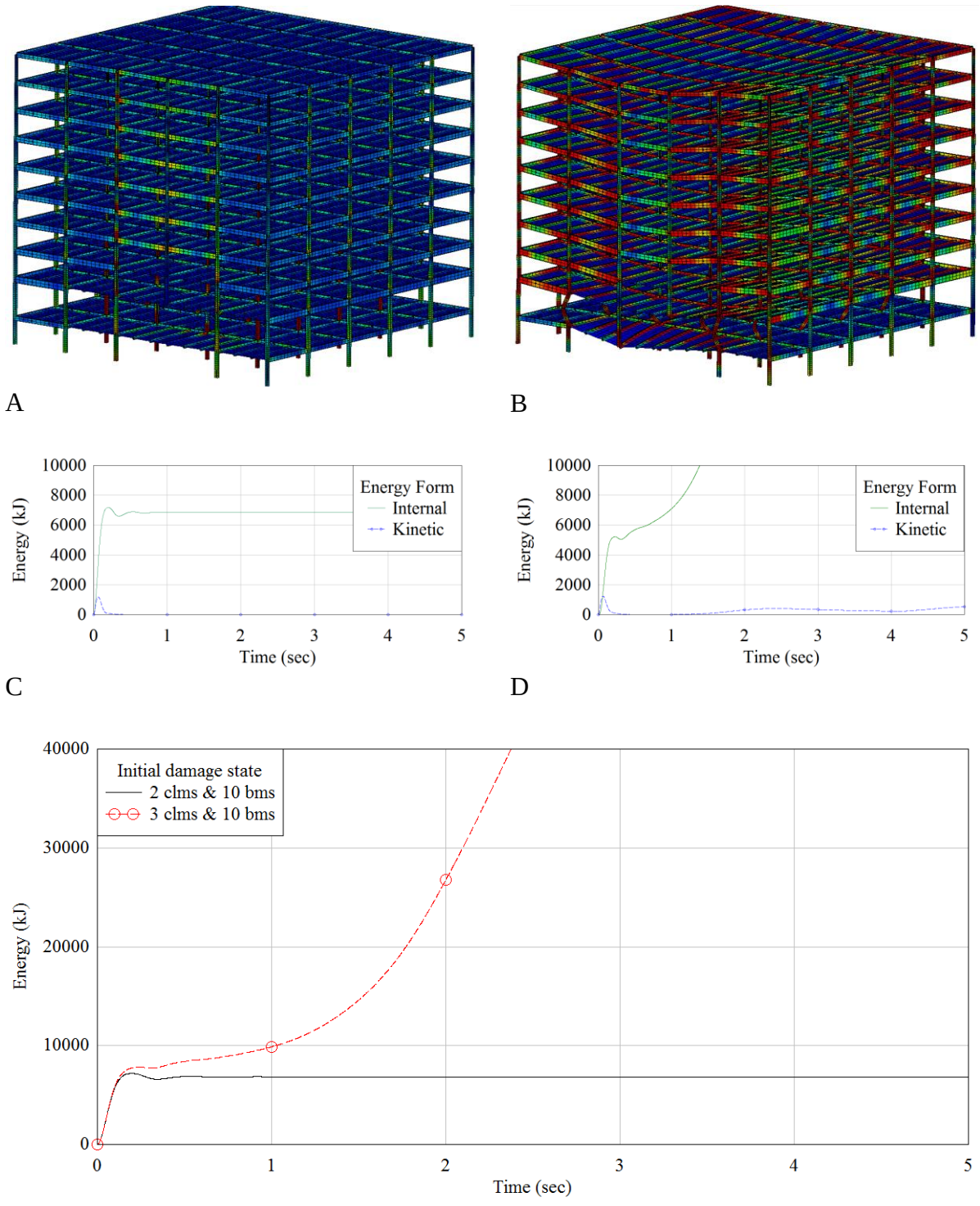

Figure 4-1. Non-collapse vs collapse. A) Beam element stresses with two columns and ten beams removed. B) Beam element stresses with three columns and ten beams removed. C) Energy with 2 columns and 10 beams removed. D) Energy with 3 columns and 10 beams removed. E) Total system energy histories.

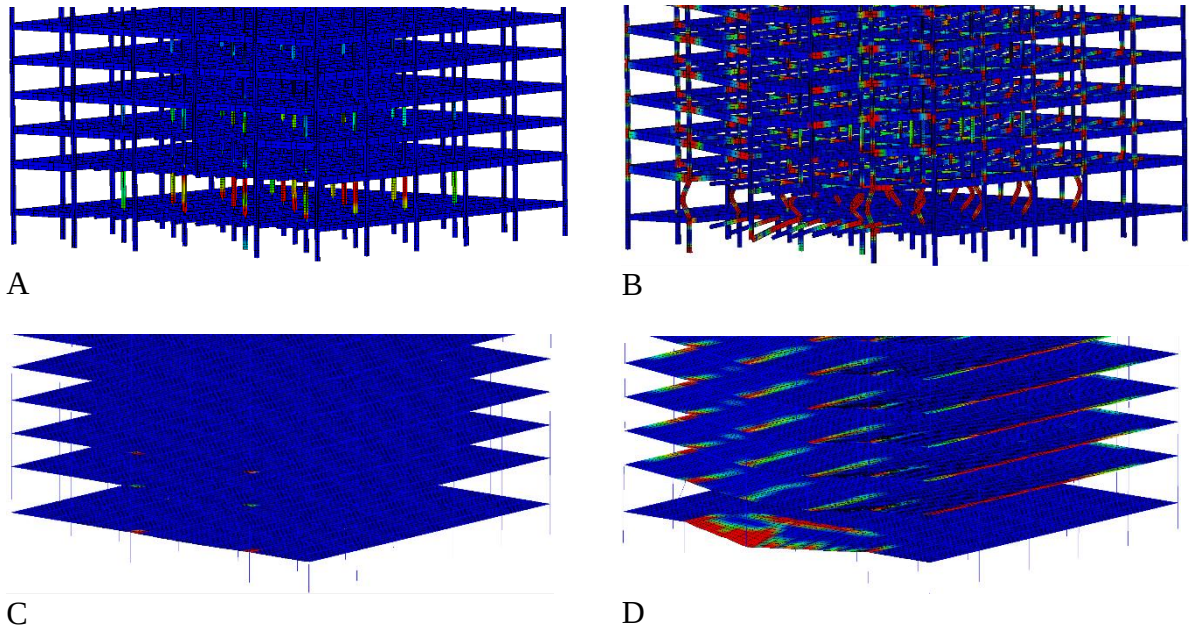

Figure 4-2. Comparative strains throughout building. A) Beam element strains with two columns and ten beams removed. B) Beam element strains with three columns and ten beams removed. C) Shell element strains with two columns and ten beams removed. D) Shell element strains with three columns and ten beams removed.

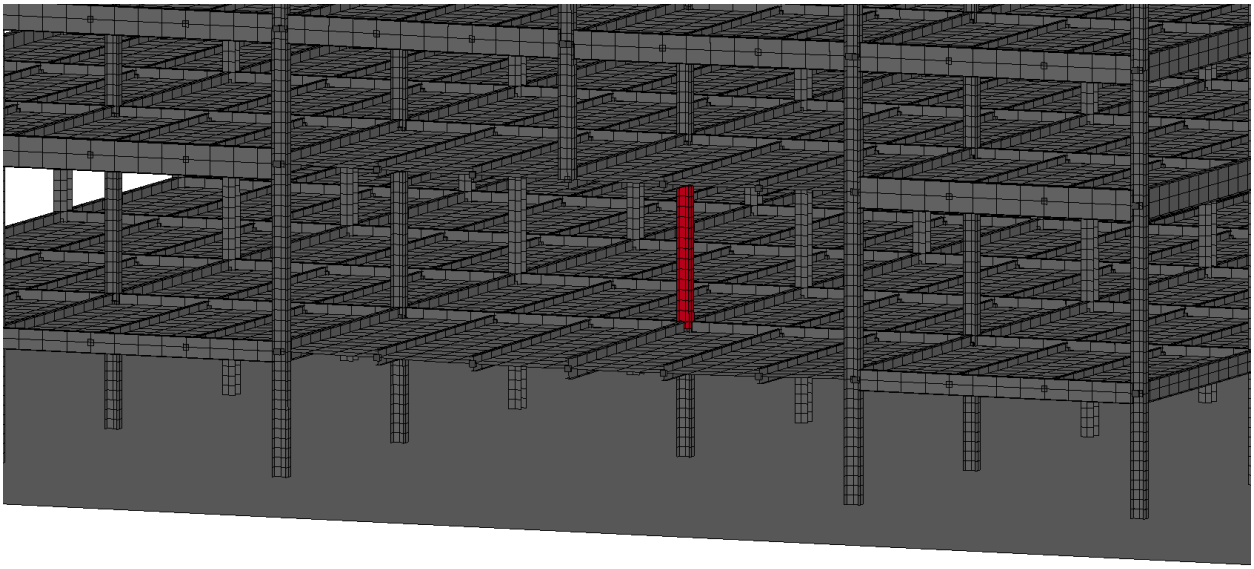

Figure 4-3. Second floor interior column closest to location of charge

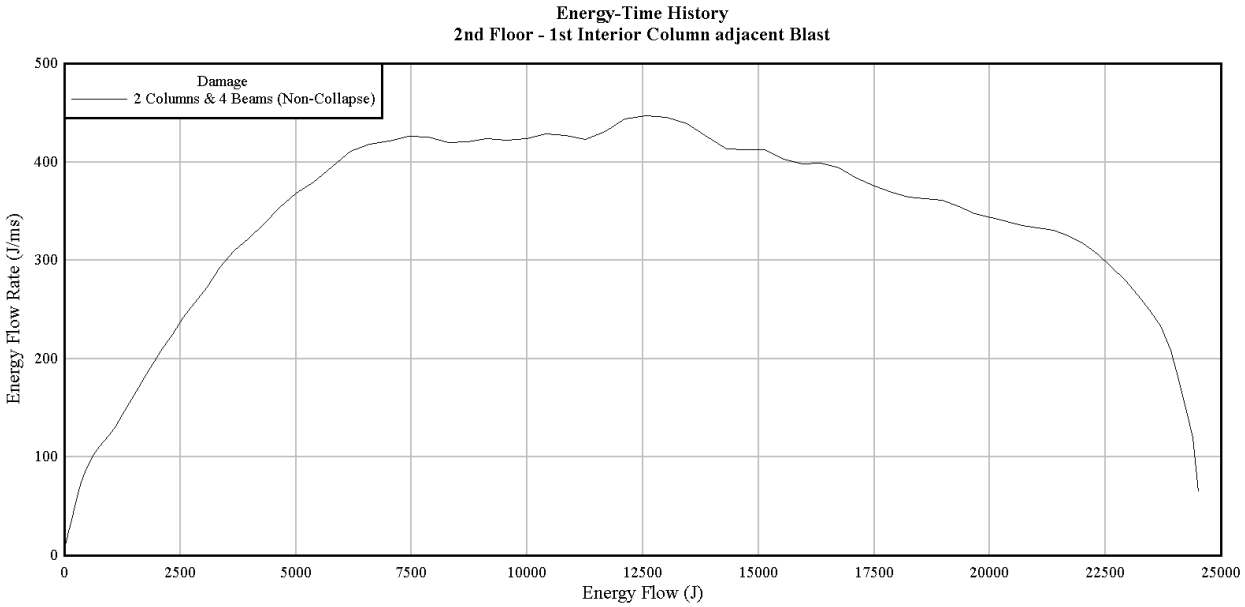

Figure 4-4. Energy-time history for referenced column (recall Figure 4-3) corresponding to a blast yielding the destruction of two columns and four beams

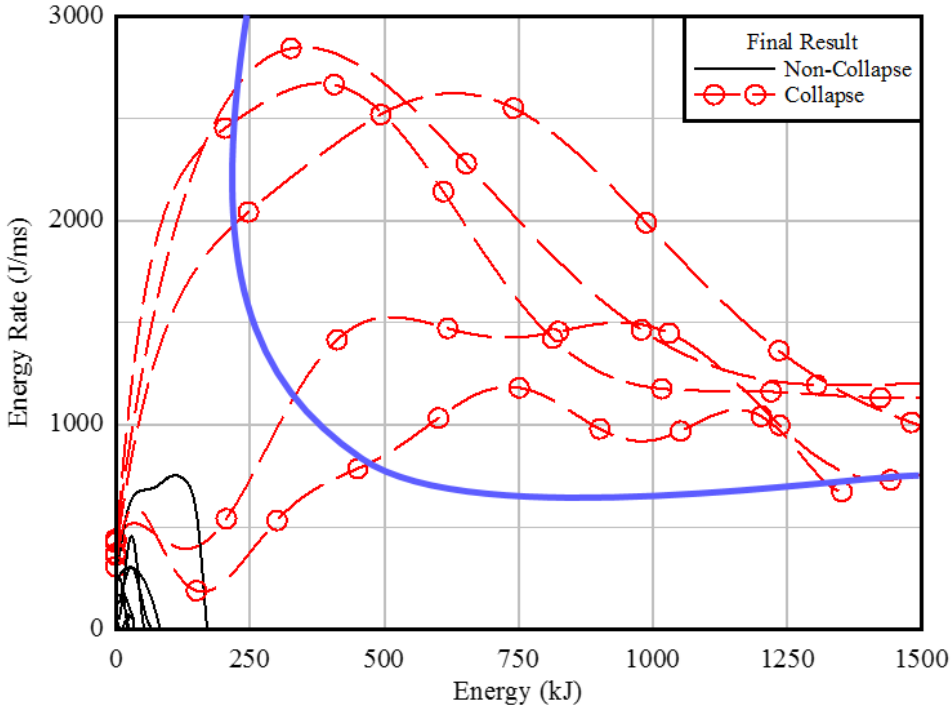

Figure 4-5. Energy flow vs energy flow rate for multiple non-collapse and collapse simulations.

A B

Figure 4-6. Isometric view of mid-rise building with soft story modified. A) Five columns and ten beams removed. B) Five columns and eighteen beams removed.

A B

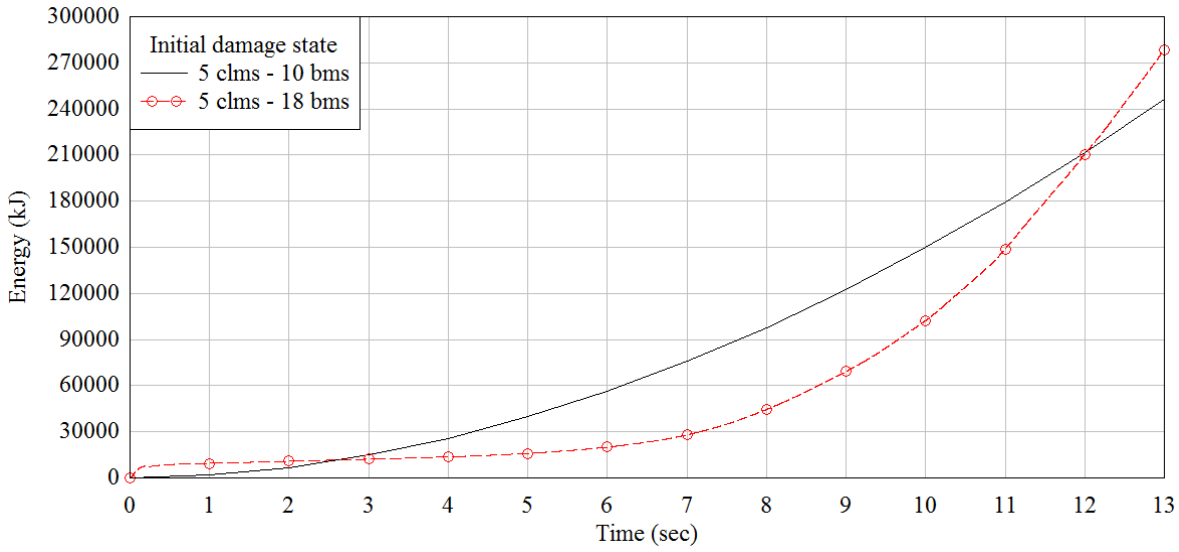

C

Figure 4-7. Comparative of different blast-induced damages with modified building model. A) Five columns and ten beams removed. b) Five columns and eighteen beams removed. c) Comparative total system energy-time histories.

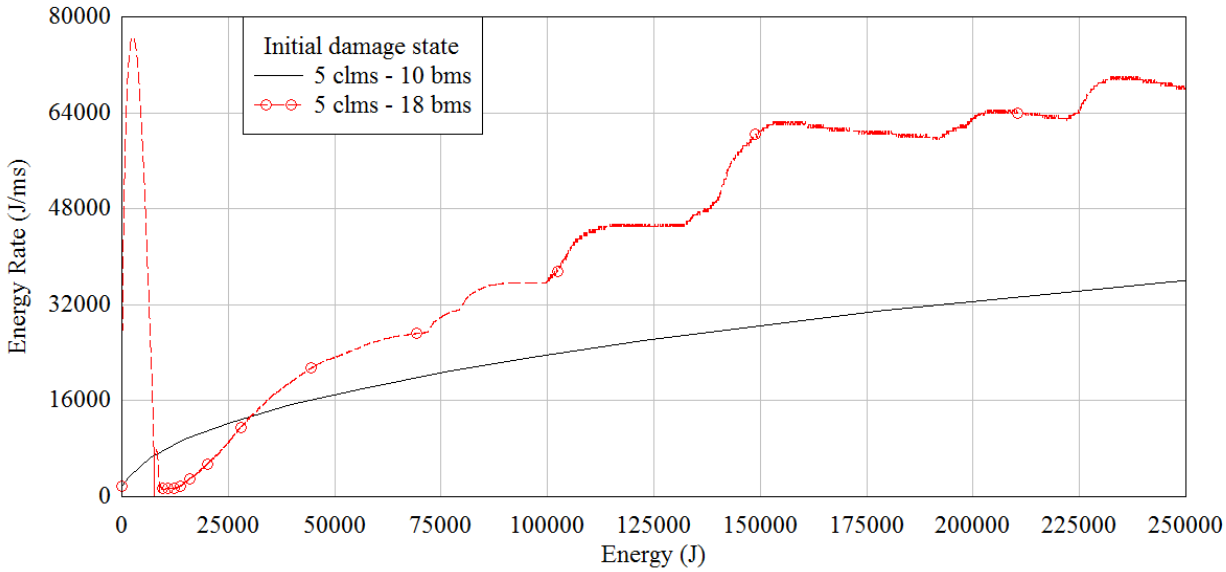

Figure 4-8. Total system energy flow vs energy flow rate with the modified SAC-commissioned mid-rise building.

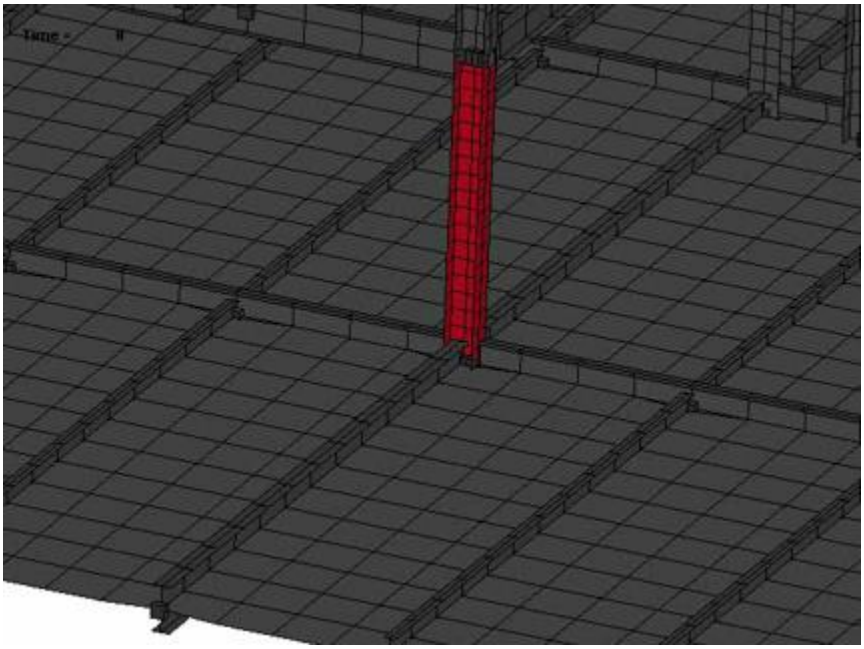

Figure 4-9. Second floor interior column closest to location of charge

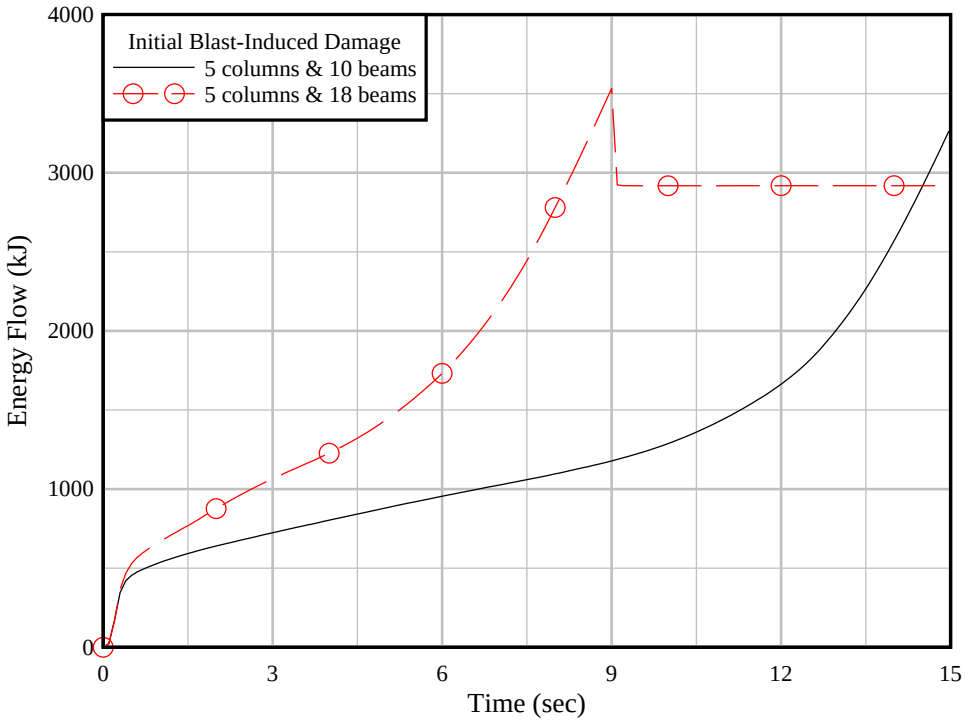

Figure 4-10. Comparative energy-time histories for second floor interior column closest to location of charge (Recall Figure 4-9).

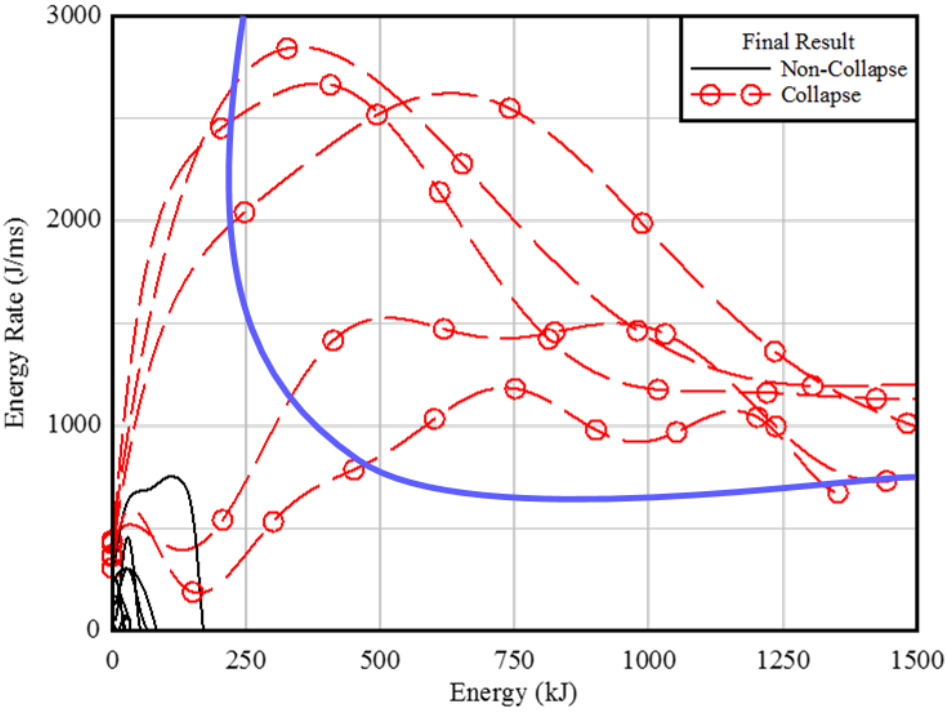

Figure 4-11. Energy histories for referenced column (Figure 4-9) from all simulations with modified version of SAC-commissioned mid-rise building model

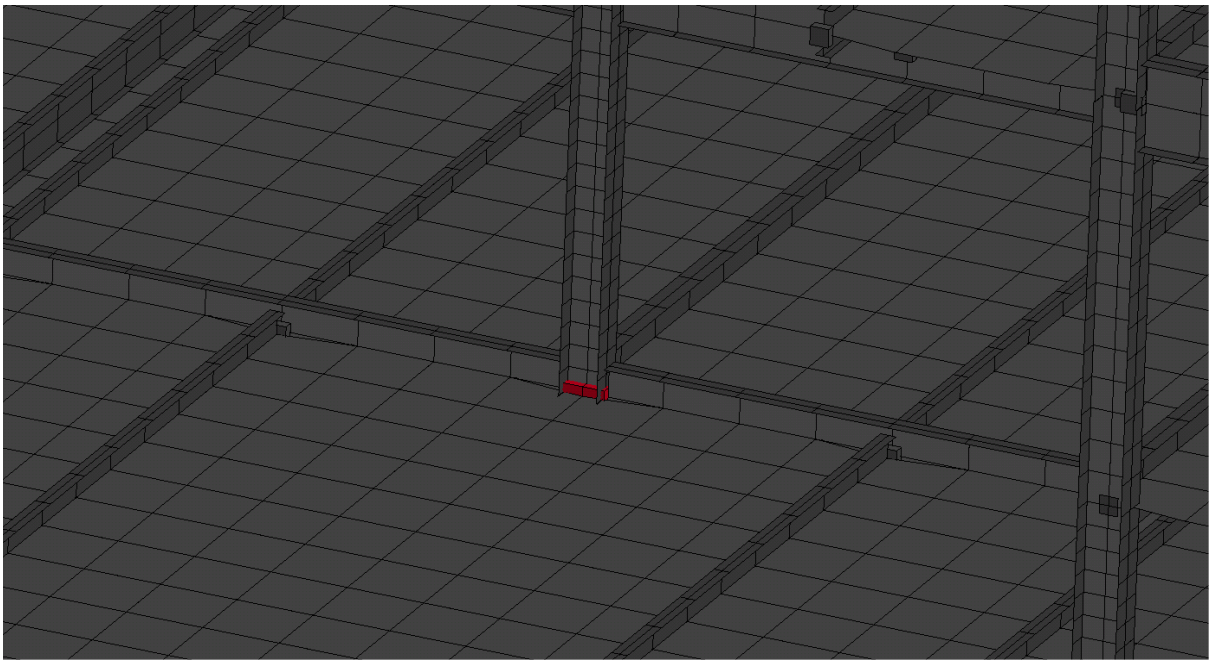

Figure 4-12. East-west connections at base of second floor interior column closest to location of charge.

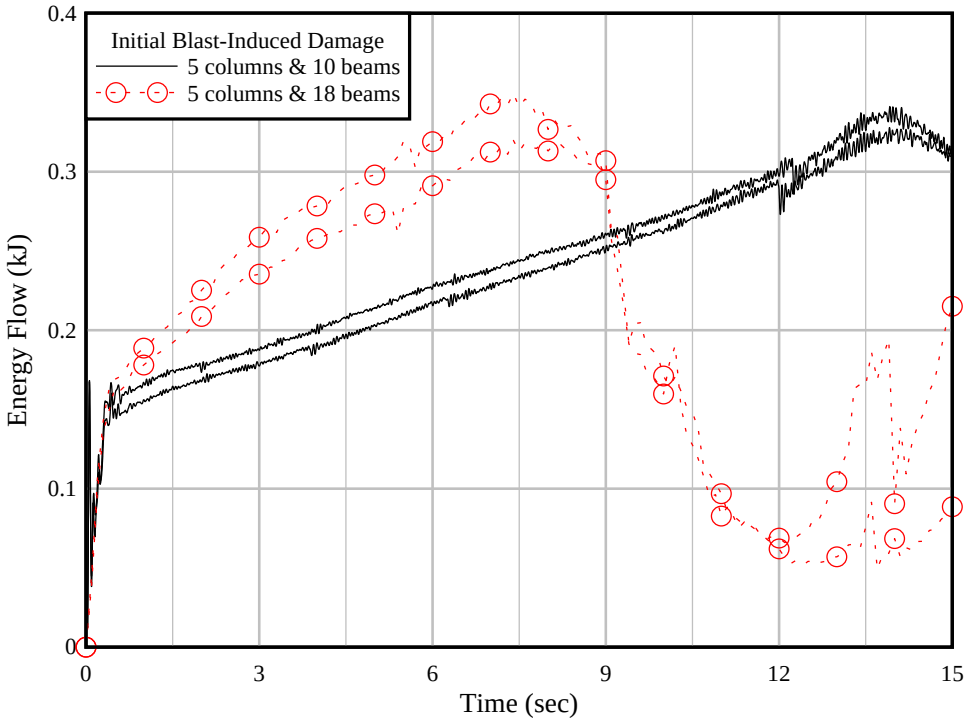

Figure 4-13. Comparative energy-time histories for east-west connections at base of second floor interior column closest to location of charge (Recall Figure 4-12).

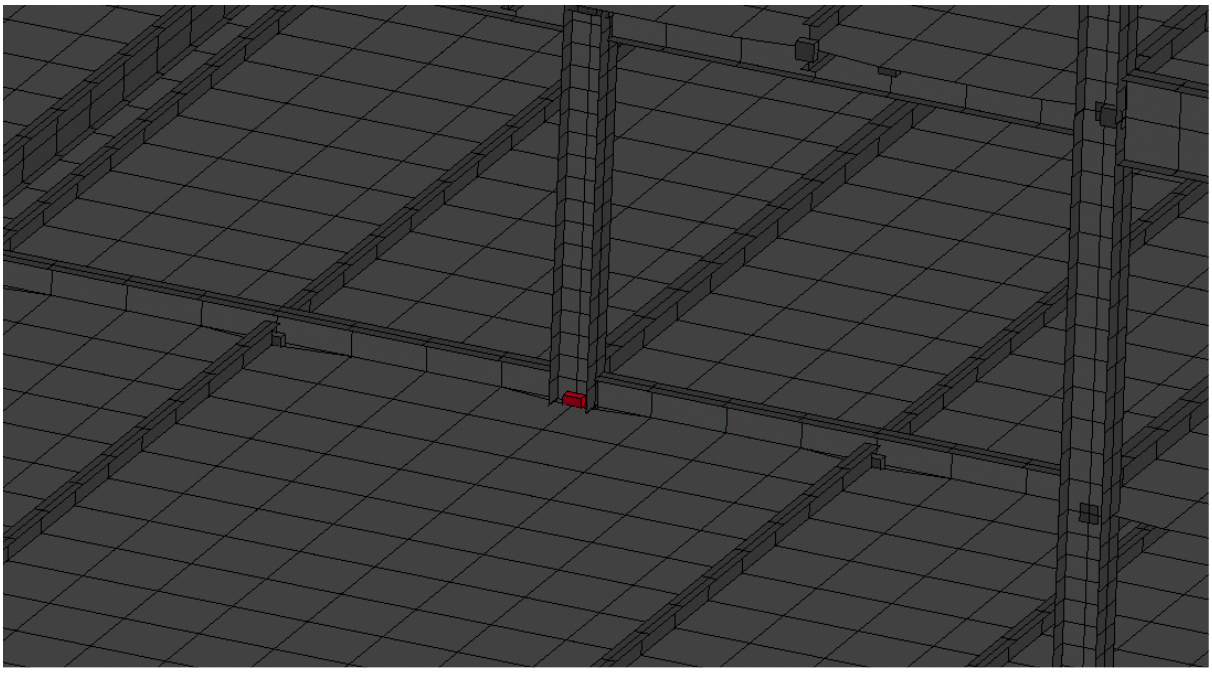

Figure 4-14. North-south connections at base of second floor interior column closest to location of charge.

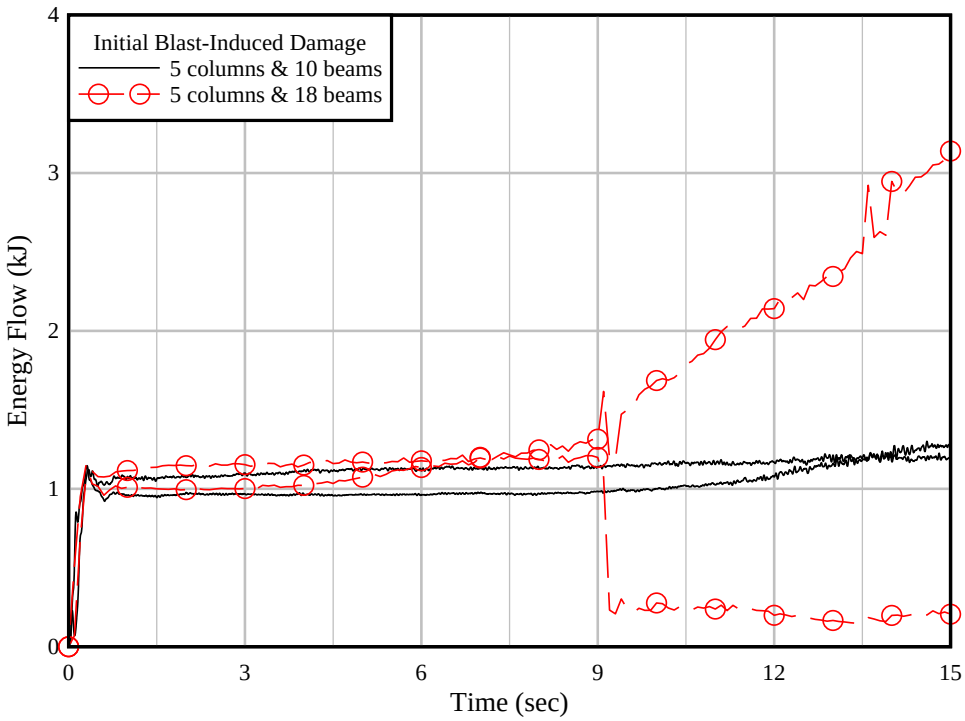

Figure 4-15. Comparative energy-time histories for north-south connections at base of second floor interior column closest to location of charge (Recall Figure 4-14).

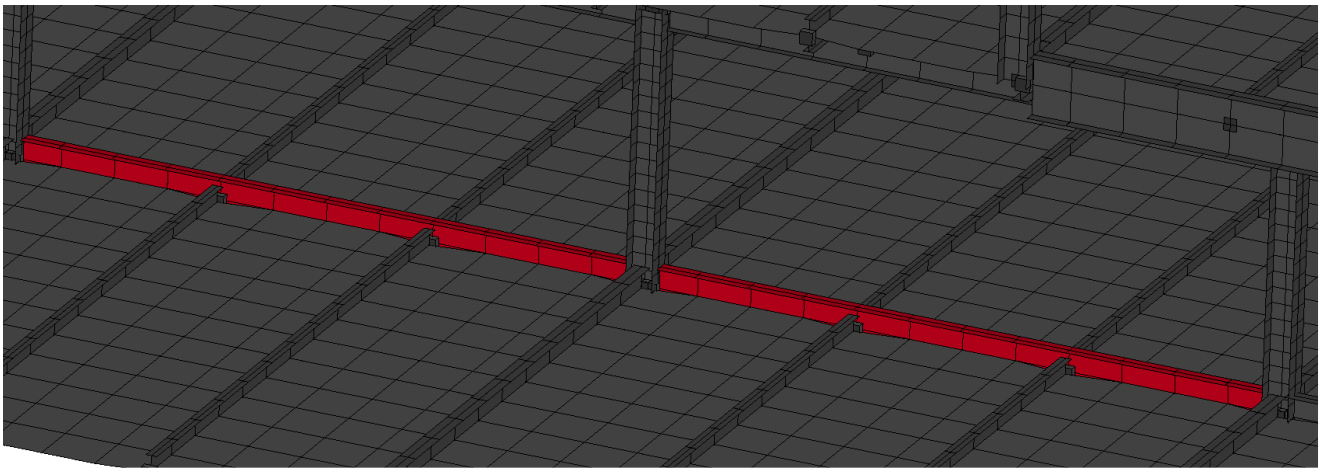

Figure 4-16. East-west girders at base of second floor interior column closest to location of charge.

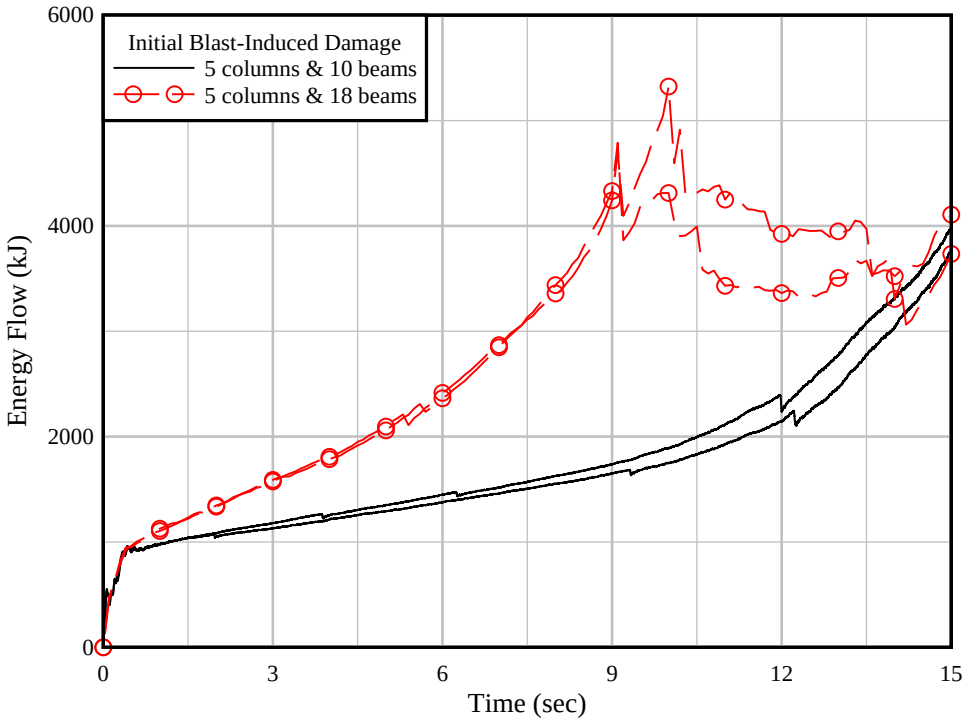

Figure 4-17. Comparative energy-time histories for east-west girders at base of second floor interior column closest to location of charge (Recall Figure 4-16).

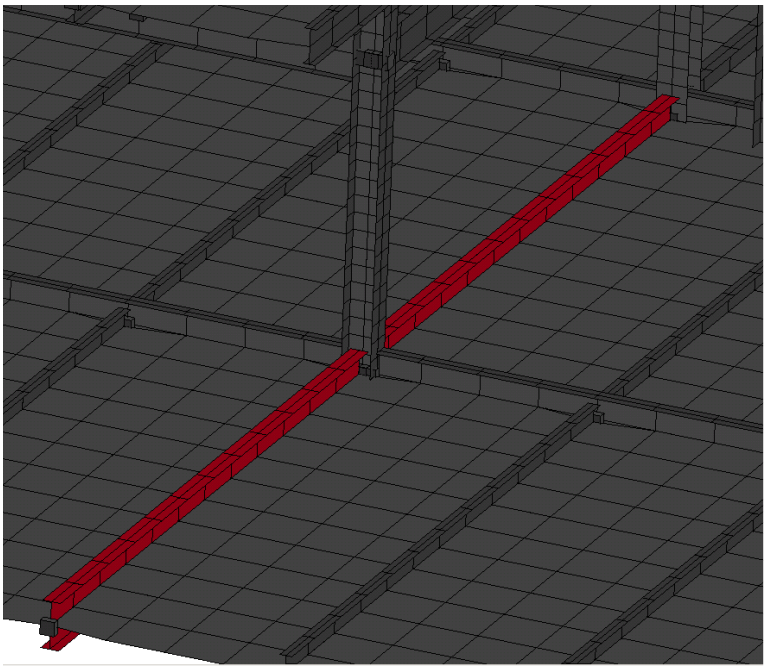

Figure 4-18. North-south girders at base of second floor interior column closest to location of charge.

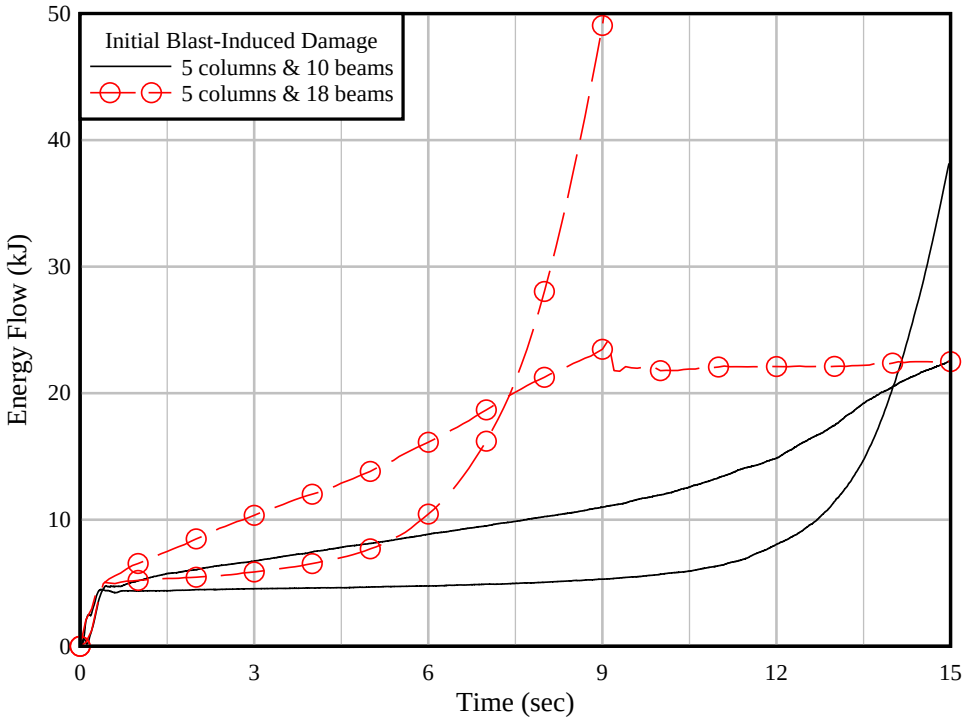

Figure 4-19. Comparative energy-time histories for north-south girders at base of second floor interior column closest to location of charge (Recall Figure 4-18).

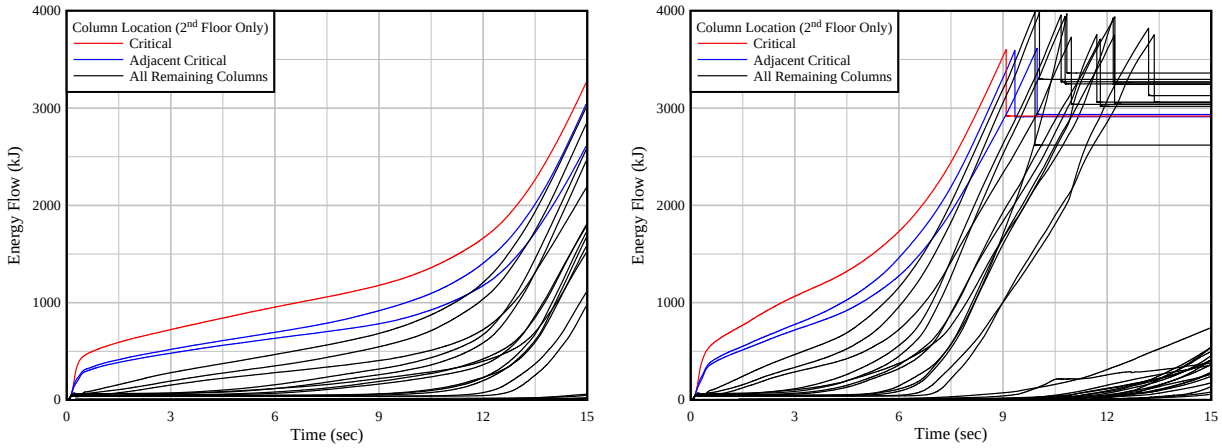

Figure 4-20. Energy-time histories for all columns on the second floor of the modified SAC-commissioned mid-rise building model. A) Blast-induced damage of five columns and ten beams. B) Blast-induced damage of five columns and eighteen girders.

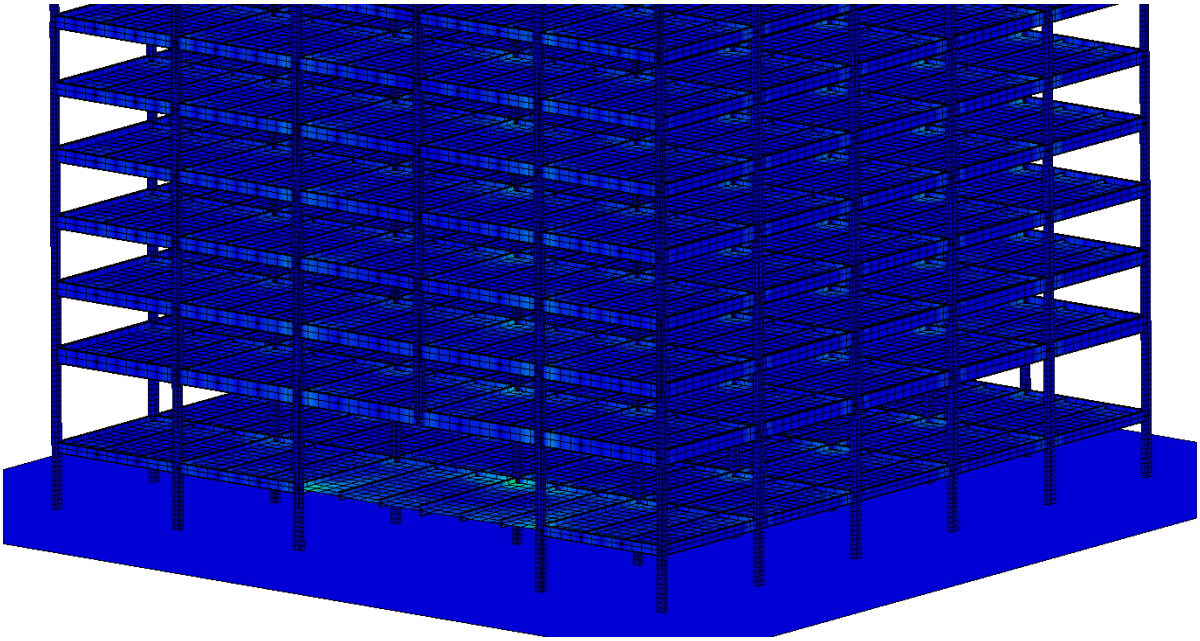

Figure 4-21. Effective (Von-Mises) beam stresses from a two columns and four beams removal

CHAPTER 5
CONCLUSIONS

This work details an energy flow approach (EFA) for progressive collapse assessment superior to current force-based methods. Redefining failure for individual structural members in terms of an energy threshold allows for a more accurate assessment of collapse susceptibility of the entire structural system. The methodology presented is a rational, highly effective approach for assessing progressive collapse susceptibility—with an accuracy and precision on par with state-of-the-art numerical modeling techniques.

This research has explicitly addressed the effects of the rates of loading and energy flow for the selected mid-rise steel frame. Analyses of the energy-time histories of a multitude of blast-induced damage simulations of the mid-rise steel frame considered in this work revealed a highly accurate and precise correlation between energy flow, energy flow rate, and structural failure. More specifically, the efficacy of using energy flow (magnitude and rate) as failure indicators was proven by analyzing the structure of interest under a multitude of extreme loading events—including both collapse arresting and progressive collapse inducing scenarios.

Beyond evidencing the efficacy of the EFA presented for assessing progressive collapse, this research demonstrates the lack of efficacy of the Alternate Path method for moment-resisting mid-rise steel buildings. In addition to the known lack of correlation between the damage induced from realistic explosive threats and a notional single column removal, this work has demonstrated the threat-independent notional Alternate Path method offers little to no mitigation against a catastrophic collapse following a blast loading event. The EFA presented here allows for a number of seminal advancements in the field of protective structures.

APPENDIX A
DEMONSTRATIONS OF THE EFA WITH SMALL STRUCTURAL FRAMES

A.1 Introduction

Although conceptually equivalent for all moment-resisting frames, the simple single-bay single-story frame was analyzed as a proof-of-concept for efficiency. Consequently, some efforts that would be present for a larger structure were excluded due to analyzing a 3-D single-bay frame. Pre-analysis calculation of energy flow thresholds for the failed beams and slab were also not included. In addition, quantifying the scaled distance yielding damage commensurate with removal of single column was not performed. These items were intentionally excluded given the ancillary goal of analyzing the efficacy of the Alternate Path method is of negligible value for a simple 3-D frame. Although not included in the proof-of-concept analysis presented above, force and stress-time histories were analyzed for the mid-rise building. The absent results and analyses from review of the simple frame simulations—applied for the analysis of the mid-rise office building are provided in the following sections to provide a more comprehensive description of the sequence of processes employed for this study.

A.2 Single-Bay Single-Story Steel Frame with Simplified Fixed Connections

For clarity and concision, the proposed EFA is presented with a single interior bay in the first floor of the ten-story building. Results from two simulations with this simple non-redundant frame are presented. The first simulation includes vertical and horizontal loads without damage. The second is equivalent in every way with the exception of the application of damage—a single failed column. Isometric views and energy-time histories of the undamaged (Figure A-1) and damaged (Figure A-2) frames are shown. Resultant data is reviewed, constituting a preliminary attempt at identifying the energy flow – failure relationship.

A.2.1 Processing Results from Collapse-Arresting Simulation

Time histories of energy flow and several failure indicators from nonlinear transient dynamic finite element simulations was processed and analyzed to identify patterns suggesting energy flow – failure correlation. Differentaion is used to calculate energy flow rates. The viability of assessing progressive collapse susceptibility was realized by comparing energy time histories with multiple failure criteria-time histories; e.g. displacement-, stress-, and strain-time histories. Force-time histories were reviewed to compare energy correlation from the EFA against those from the traditional force-based approach. More specifically, total, kinetic, and internal energies of all structural elements was recorded, extracted, differentiated, and analyzed; which includes all columns, connections, girders, beams, and slabs.

The extracted energy flow and calculated energy flow rate time-histories were superimposed against energy thresholds. Comparing this combined data with the structural response observed in LS-Prepost, the output data indicating the timing and sequence of failed members was analyzed for correlation with the superimposed time history-threshold failure data. The efficacy of this approach was revealed after performing these post-processing methods—extraction, differentiation, plotting, and potential correlation methods—for multiple loading conditions.

For the simulation with the damaged frame, half of the slab and both beams adjoining the removed column failed, collapsing fully until contacting the ground surface. Results show the majority of internal energy produced during the collapse came from the failed beams—primarily through plastic strains. The slab contributes internal energy, as do the two beams opposite the removed column. However, the energetic contribution of these three elements is small relative to the collapsed beams, ≤ 10% per Figure A-4B. The remaining three columns express negligible

internal strain energy. In reviewing the kinetic energy, we observe the expected energy transfers, with the beams playing the primary and the slab playing the secondary role. Namely, the two beams above the removed column expend the most amount of energies until hitting the ground at approximately 2400 msec (2.4 sec). As expected, the slab transfers significant kinetic energy levels due to a 4.0 m drop height and approximately half of the slab mass being in motion.

A.2.2 Processing Results from Collapse-Triggering Simulation

Reviewing the collapse inducing simulation with the damaged frame, energy-time histories of individual structural members and are differentiated to yield the rates of energy flow. Comparative plotting between both energy parameter time-histories and multiple failure indicating-time histories are performed. Due to resultant values being dissimilar in scale by three-orders of magnitude, kinetic energy-time histories are plotted on separate, independent ordinate axes.

The resultant time histories show collapse occurs over a time span of approximately 4.0 seconds, beginning at 3500 msec (3.5 sec) and ending at 7500 msec (7.5 sec). The failed beams release the most energy, in the form of internal strain—primarily plastic strain, as expected. The internal and kinetic energies from the beams and slab illustrate the deformations and displacements occurring in these members, respectively. Notably, the energy flow rate-time histories demarcate the beginning and end of the collapse event in a more pronounced fashion.

The potential and kinetic energy flows of all three failed structural elements are plotted using different scales, yielding a behavioral comparison. Nearly equivalent internal energy flow is observed. However, observable differences exist between energy flow rates at higher frequency. This content in the slab's response is present due to the absence of damping. All subsequent models had frequency-based damping, with subsequent quality controls to verify damping energy plays an insignificant role throughout the modelled event.

The observed similarities in internal energies between the slab and beams are maintained for kinetic energy, reflected in both energy flow time-histories (Figure A-5). This is expected given internal and kinetic energies are the sum total energy. To confirm, the plastic strain energy equals the summed slab and beams internal energy, which effectively equals the system's total internal energy. In effect, the equivalency of the plastic strain with the total internal energy flows confirms the absence of non-physical spurious energy forms; e.g. hourglass energy.

After reviewing all failure-indicator parameters, vertical displacement of the connection and strain at the slab center were selected. Displacement of the unsupported slab corner at the onset of the simulation is due to self-weight and superimposed dead and live loads. These two parameters indicate collapse begins at 3500 msec (3.5 sec) and ends at 7500 msec (7.5 sec). Given the primarily vertical nature of the applied loading conditions, and single story test frame, column behavior does not warrant an independent discussion. In the interest of brevity, vertical displacement and plastic strain are the only failure indicating parameters presented. However, effective stress and effective strain contours are shown for the final collapse state.

The explosive loading events under consideration occur over a time span of a few milliseconds. The structure responds over a duration of several seconds, corresponding to the pseudo-static time domain. Given approximately three-orders of magnitude separation between the time domain of the loading event and the time domain of the structure's response, applying damage in an instantaneous manner is reasonable. In other words, any disparities between the damage sustained during a blast loading and immediate removal of structural members is inconsequential because the structure responds in the quasi-static time domain. Studies examining the effect of applying damage instantaneously as opposed to over a time span of a several milliseconds have shown no observable differences result (Krauthammer et al. 2004a) in

addition to other studies that have focused solely on this approach and concluded the same (Yim and Krauthammer, 2009; and Szyniszewski and Krauthammer, 2012). All energy time histories reported by LS-DYNA were reviewed to ensure equilibrium was maintained throughout the simulation. All nonlinear transient dynamic finite element simulations are conducted with LS-DYNA 971 version (Hallquist, 2014).

A.3 Twin-Bay Two-Story Portion of Mid-Rise with Advanced Connections

The following is as an expanded proof-of-concept analysis beyond the single-bay single-story frame in the proposal, to a twin bay two-story portion of the building under consideration. In addition, a complex representation of all structural connections is also incorporated. The selected portion of the mid-rise building for this reduced model demonstration entails a corner portion of the first two levels, which includes one interior bay, two exterior bays, and one corner bay for both bottom levels (Figure A-9). In addition, the lateral restraint applied to the first elevated floor level represents the interaction of the building exterior with soil, at grade, which is symbolized by a vertical roller (Figure A-9A), is not considered in numerical representation of this reduced frame model. To demonstrate the efficacy of the proposed EFA, energy-time histories for a multitude of structural elements was processed, analyzed, and compared between two loading/damage condition states—the first arrests failure, the second progresses to collapse.

For clarity and concision, the proposed EFA is presented with two twin-bays in the first two floors of the ten-story building. Results from two simulations with this reduced frame are presented. The first simulation includes vertical loads with a single column removal. The second is equivalent in every way with the exception of the application of damage—three removed columns, two exterior and one corner—in lieu of a single corner column removal. Isometric views and energy-time histories of both damaged-simulated frames, moderate (one

column removed) and severe (three columns removed), are shown. Resultant data is reviewed to an extent that constitutes a thorough presentation of the energy flow – failure relationship.

A.3.1 Processing Results from Collapse-Arresting Simulation

A twin-bay two-story portion of the mid-rise building was analyzed following the removal of a corner column. In order to induce failure in several structural members, dead and live loads were amplified. However, these superimposed loads were maintained at a level such that a progression of collapse did not occur; i.e. a catastrophic collapse of the frame. Isometric views and energy-time histories of this moderately damaged frame are provided (Figure A-10).

Time histories of energy flow and several failure indicators from nonlinear transient dynamic finite element simulations are processed and analyzed, identifying patterns suggesting energy flow – failure correlation. Differentaion is used to calculate energy flow rates. The viability of assessing progressive collapse susceptibility was realized by comparing energy time histories with multiple failure criteria-time histories; e.g. displacement-, stress-, and strain-time histories. Force-time histories were also be reviewed to compare energy correlation from the EFA against those from the traditional force-based approach. More specifically, total, kinetic, and internal energies of all structural elements was recorded, extracted, differentiated, and analyzed; which includes all columns, connections, girders, beams, and slabs.

The extracted energy flow and calculated energy flow rate time-histories was superimposed with the energy flow thresholds. Comparing this combined data with the structural response observed in LS-Prepost, the output data indicating the timing and sequence of failed members was analyzed for correlation with the superimposed time history-threshold failure data. The efficacy of this approach was revealed after performing these post-processing methods—extraction, differentiation, plotting, and potential correlation methods—for multiple loading conditions.

For the simulation with the damaged frame, half of the slab and both beams adjoining the removed column failed, collapsing fully until contacting the ground surface. Results show the majority of internal energy produced during the collapse came from the failed beams—primarily through plastic strains. The slab contributes internal energy, as do the two beams opposite the removed column. However, the energetic contribution of these three elements is small relative to the collapsed beams, ≤ 10% per Figure A-4B. The remaining three columns express negligible internal strain energy. In reviewing the kinetic energy, we observe the expected energy transfers, with the beams playing the primary and the slab playing the secondary role. Namely, the two beams above the removed column expend the most amount of energies until hitting the ground at approximately 2400 msec (2.4 sec). As expected, the slab transfers significant kinetic energy levels due to a 4.0 m drop height and approximately half of the slab mass being in motion.

A.3.2 Processing Results from Collapse Triggering Simulation

This second simulation is analogous to the non-collapse simulation presented above, but with an additional two exterior columns removed, resulting in a collapse. Isometric views and energy-time histories of this severely damaged frame are shown (Figure A-11).

Reviewing the collapse inducing simulation with the damaged frame, energy-time histories of individual structural members are differentiated to yield the rates of energy flow. Comparative plotting between both energy parameter time-histories and multiple failure indicating-time histories are performed. Due to resultant values being dissimilar in scale by three-orders of magnitude, kinetic energy-time histories are plotted on separate, independent ordinate axes.

The resultant time histories show collapse occurs over a time span of approximately 4.0 seconds, beginning at 3500 msec (3.5 sec) and ending at 7500 msec (7.5 sec). The failed beams

release the most energy, in the form of internal strain—primarily plastic strain, as expected. The internal and kinetic energies from the beams and slab illustrate the deformations and displacements occurring in these members, respectively. Notably, the energy flow rate-time histories demarcate the beginning and end of the collapse event in a more pronounced fashion.

The potential and kinetic energy flows of all three failed structural elements are plotted using different scales, yielding a behavioral comparison. Nearly equivalent internal energy flow is observed. However, observable differences exist between energy flow rates at higher frequency. This content in the slab's response is present due to the absence of damping. All subsequent models had have frequency-based damping, with subsequent quality controls to verify damping energy plays an insignificant role throughout the modelled event.

The observed similarities in internal energies between the slab and beams are maintained for kinetic energy, reflected in both energy flow time-histories. This is expected given internal and kinetic energies are the sum total energy. To confirm, the plastic strain energy equals the summed slab and beams internal energy, which effectively equals the system's total internal energy. In effect, the equivalency of the plastic strain with the total internal energy flows confirms the absence of non-physical spurious energy forms; e.g. hourglass energy.

After reviewing all failure-indicator parameters, vertical displacement of the connection and strain at the slab center were selected. Displacement of the unsupported slab corner at the onset of the simulation is due to self-weight and superimposed dead and live loads. These two parameters indicate collapse begins at 3500 msec (3.5 sec) and ends at 7500 msec (7.5 sec). Given the primarily vertical nature of the applied loading conditions, and single story test frame, column behavior does not warrant an independent discussion. In the interest of brevity, vertical

displacement and plastic strain are the only failure indicating parameters presented. However, effective stress and effective strain contours are shown for the final collapse state.

The explosive loading events under consideration occur over a time span of a few milliseconds. The structure responds over a duration of several seconds, corresponding to the pseudo-static time domain. Given approximately three-orders of magnitude separation between the time domain of the loading event and the time domain of the structure's response, applying damage in an instantaneous manner is reasonable. In other words, any disparities between the damage sustained during a blast loading and immediate removal of structural members is inconsequential because the structure responds in the quasi-static time domain. Studies examining the effect of applying damage instantaneously as opposed to over a time span of a several milliseconds have shown no observable differences result (Krauthammer et al. 2004a) in addition to other studies that have focused solely on this approach and concluded the same (Yim and Krauthammer, 2009; and Szyniszewski and Krauthammer, 2012). All energy time histories reported by LS-DYNA were reviewed to ensure equilibrium was maintained throughout the simulation. All nonlinear transient dynamic finite element simulations are conducted with LS-DYNA 971 version (Hallquist, 2014).

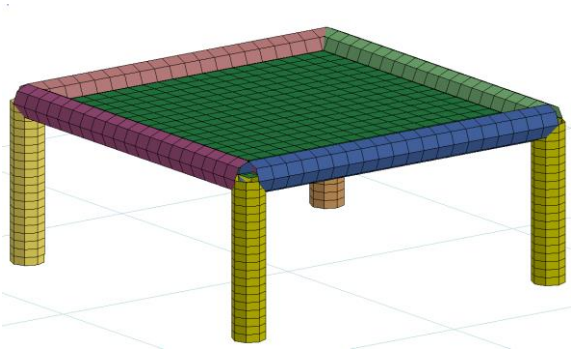

A

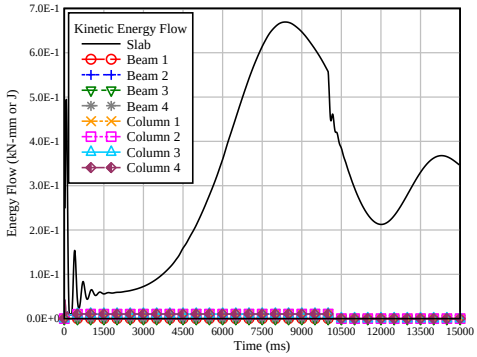

B

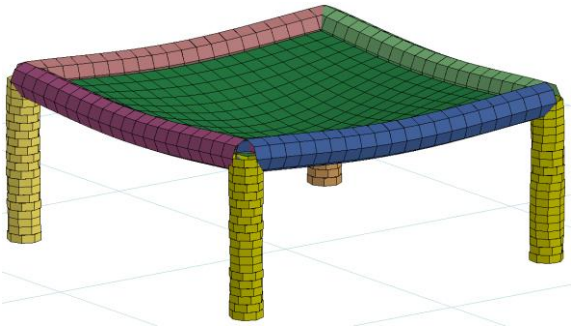

C

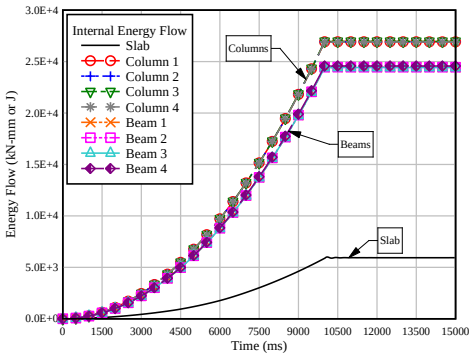

D

Figure A-1. Test Frame without damage. A) Initial state prior to loading. B) Internal energy time-history for a non-collapse. C) Final displaced state (≥≅ 10,000 msec). D) Kinetic energy time-history for a non-collapse (Note: displacement scale factor of 25 applied to subfigure c to illustrate deformations)

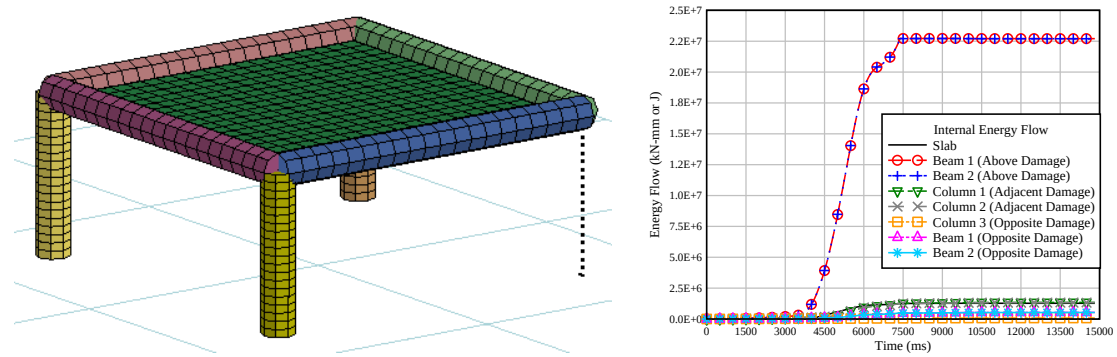

A B

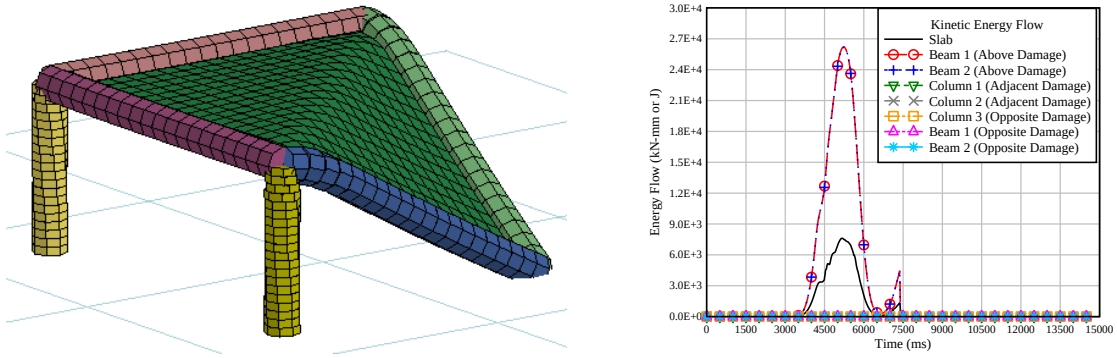

C D

Figure A-2. Test frame with damage applied – failure of a single column. A) Initial state prior to loading. B) Internal energy-time history during collapse. C) Final collapsed state (≥≅ 7500 msec). D) Kinetic energy-time history during collapse

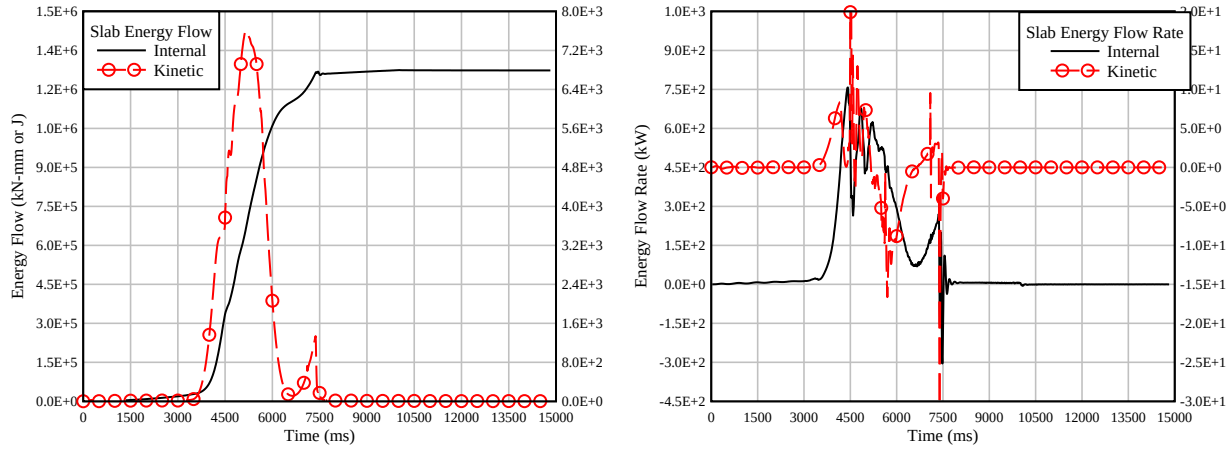

A B

Figure A-3. Energy-time histories of slab. A) Energy flow as reported. B) Energy flow rate from differentiating energy flow

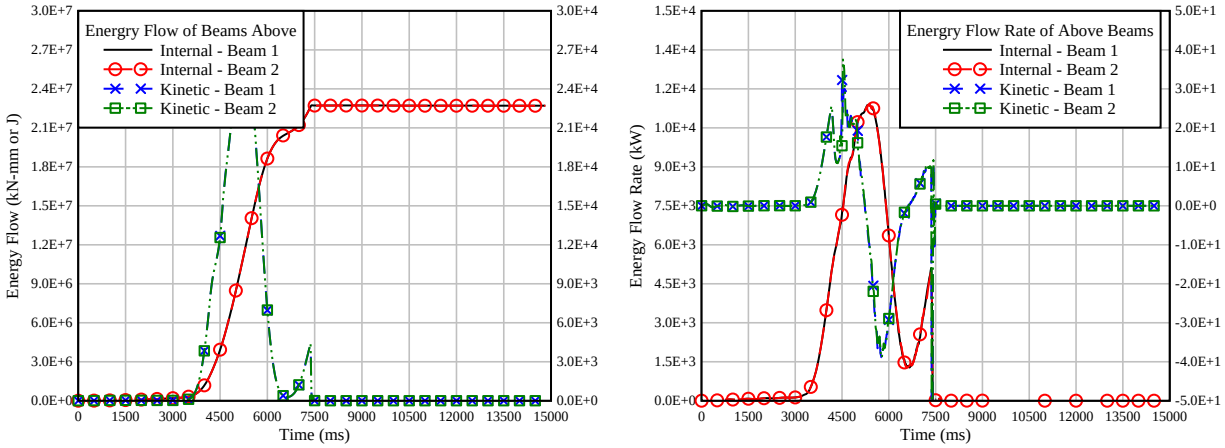

A B

Figure A-4. Energy-time histories of failed beams. A) Energy flow as reported. B) Energy flow rate from differentiation

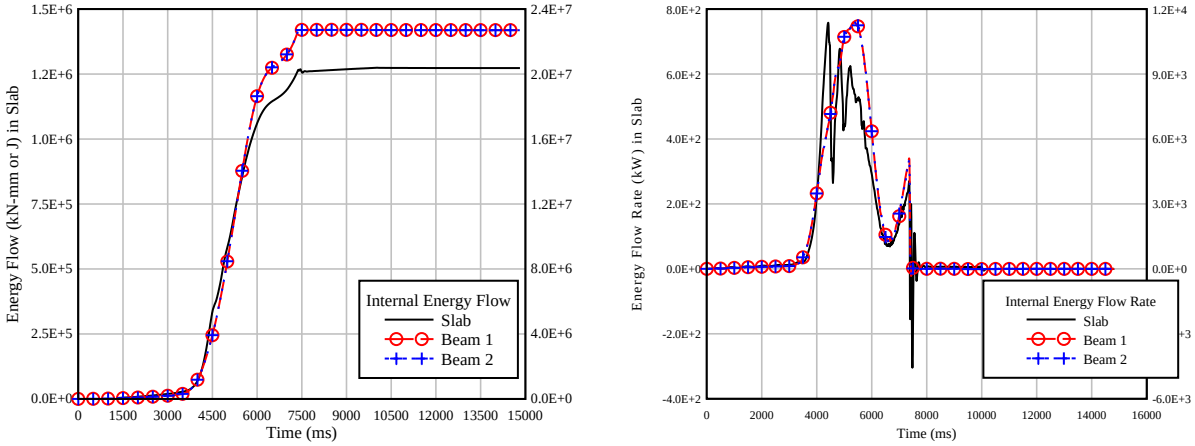

A B

Figure A-5. Internal energy-time histories of slab and failed beams. A) Energy flow as reported. B) Energy flow rate from differentiation

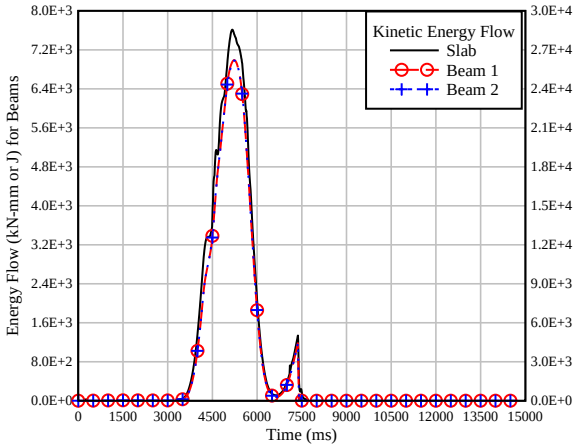

A

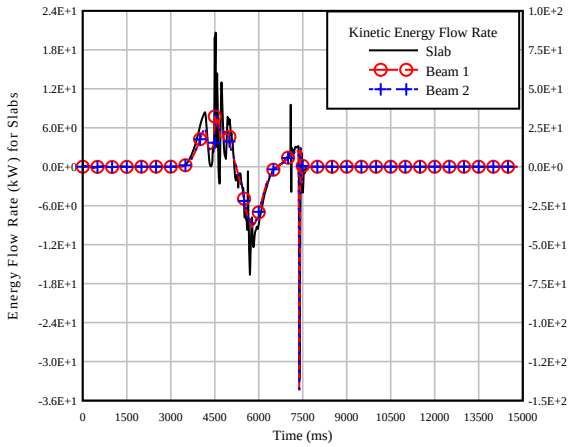

B

Figure A-6. Kinetic energy-time histories of slab and failed beams. A) Energy flow as reported. B) Energy flow rate from differentiation

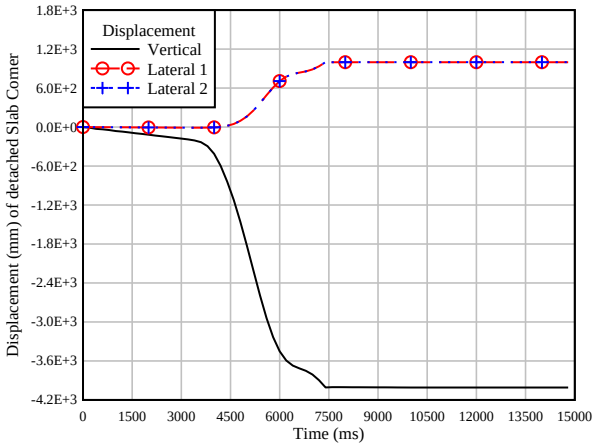

A

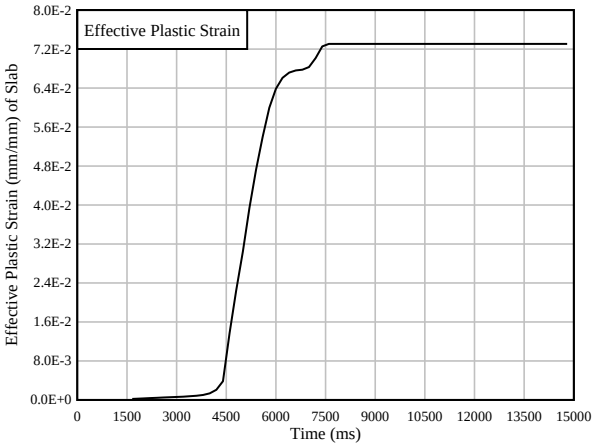

B

Figure A-7. Example failure indicating criteria-time histories. A) Vertical displacement of the connection at the top of removed column. B) Plastic-strain at the center of slab adjoining the removed column

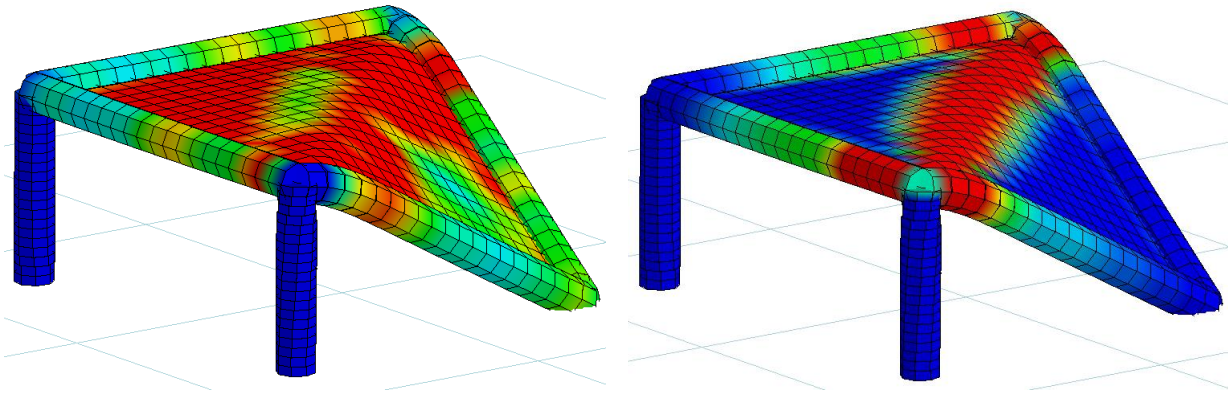

Figure A-8. Stress and strains contours at the end of collapse. A) Effective (Von-Mises) stress. B) Effective plastic strain.

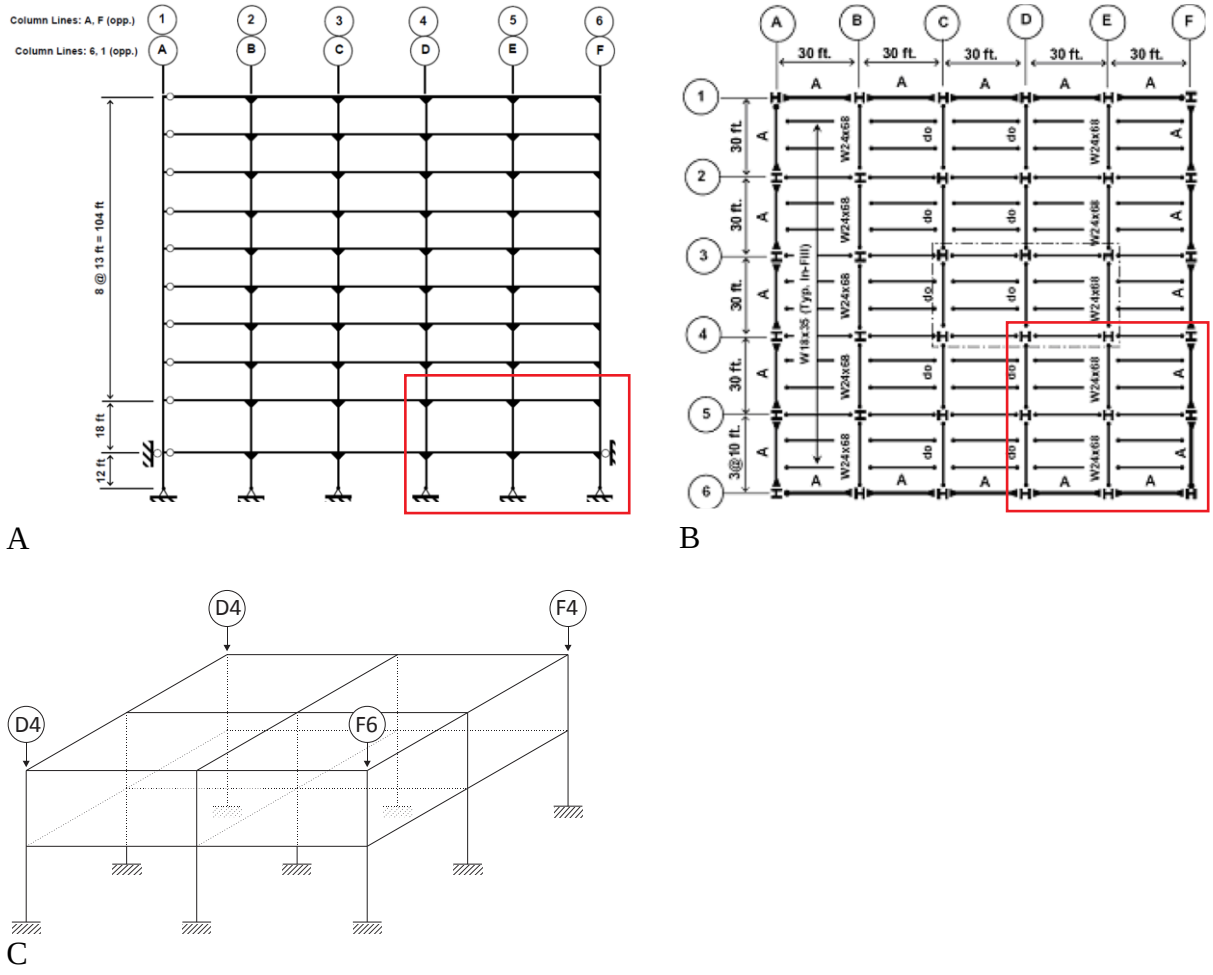

A

B

C

Figure A-9. Portion of mid-rise building analyzed for demonstrating efficacy. A) Elevation view of building. B) Plan view of building. C) Isometric view of portion modeled.

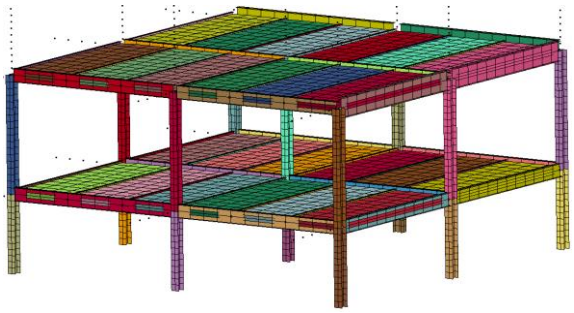

A

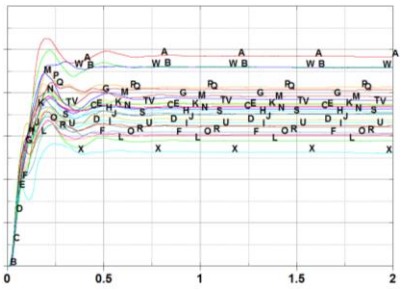

B

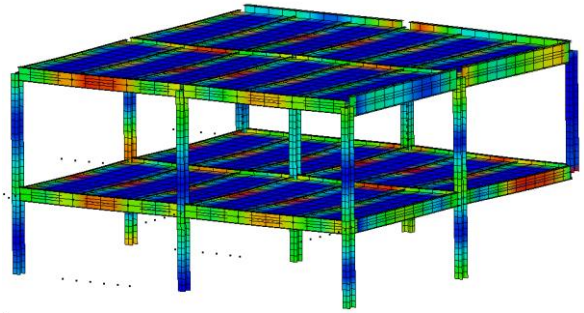

C

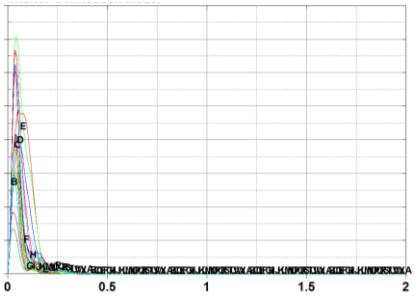

D

Figure A-10. Reduced frame with moderate damage (one column) – collapse prevented. A) Initial state prior to loading. B) Internal energy time-history for a non-collapse. C) Final displaced state. D) Kinetic energy time-history for a non-collapse

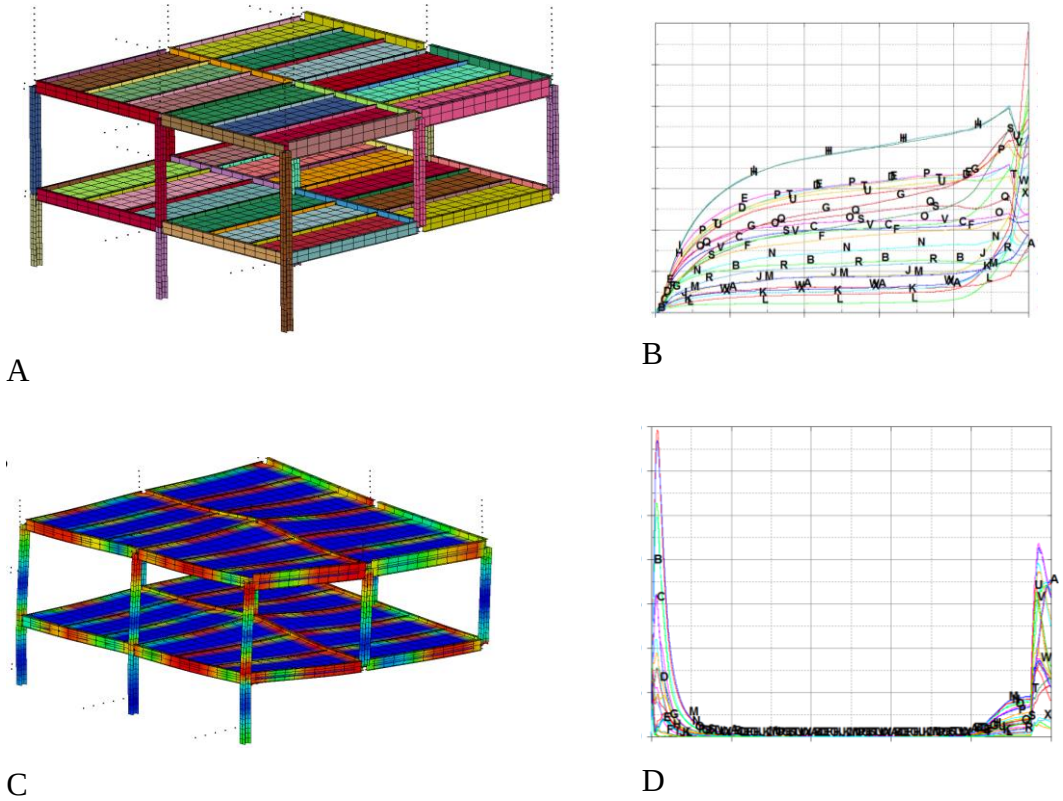

A B C D

Figure A-11. Reduced frame with severe damage (three columns) – collapse progresses. A) Initial state prior to loading. B) Internal energy-time history during collapse. C) Final collapsed state (≥≅ 7500 msec). D) Kinetic energy-time history during collapse

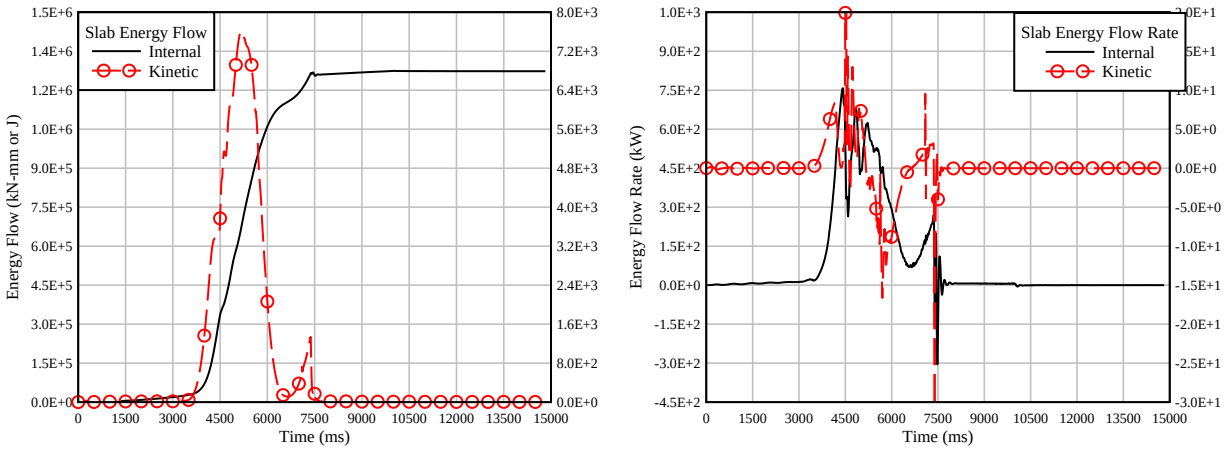

A B

Figure A-12. Energy-time histories of slab. A) Energy flow as reported. B) Energy flow rate from differentiating energy flow

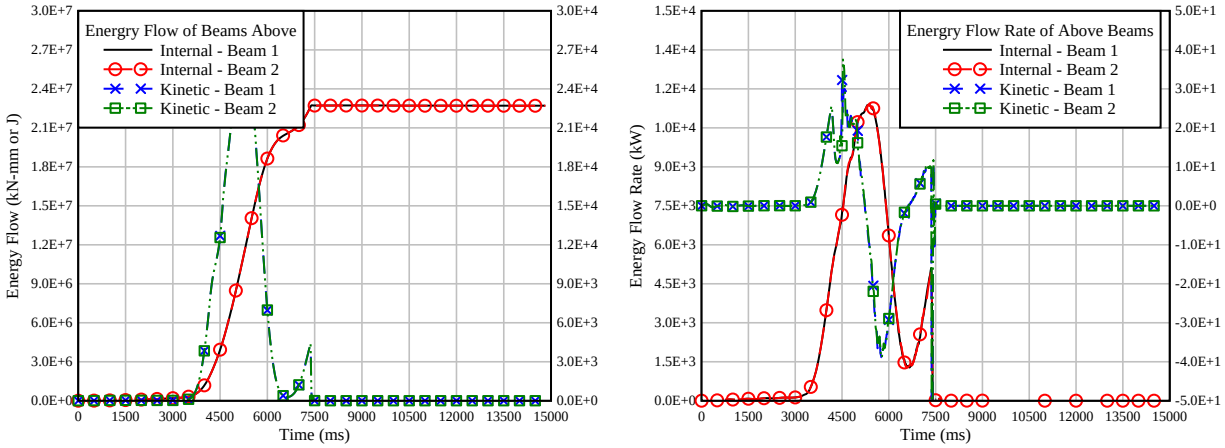

A B

Figure A-13. Energy-time histories of failed beams. A) Energy flow as reported. B) Energy Flow rate from differentiation.

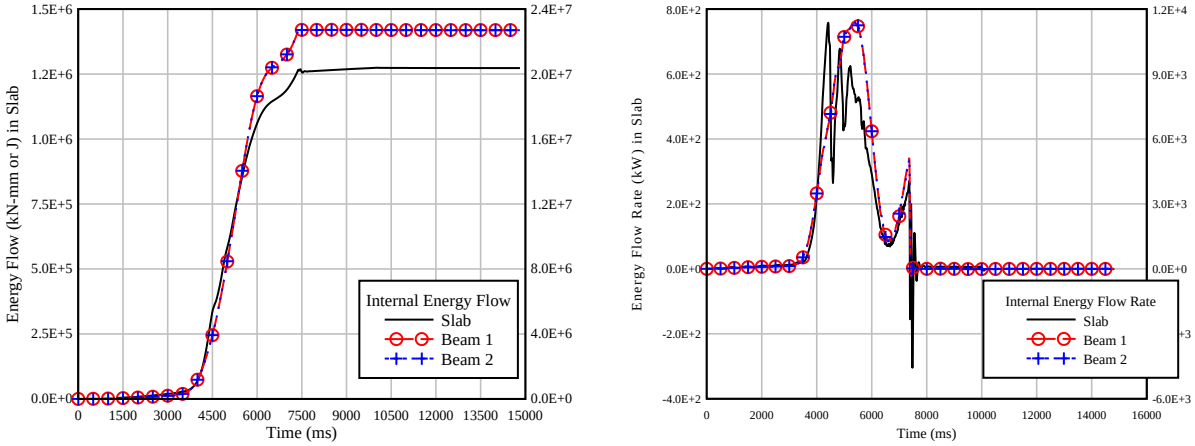

A) B)

Figure A-14. Internal energy-time histories of slab and failed beams. A) Energy flow as reported. B) Energy flow rate from differentiation

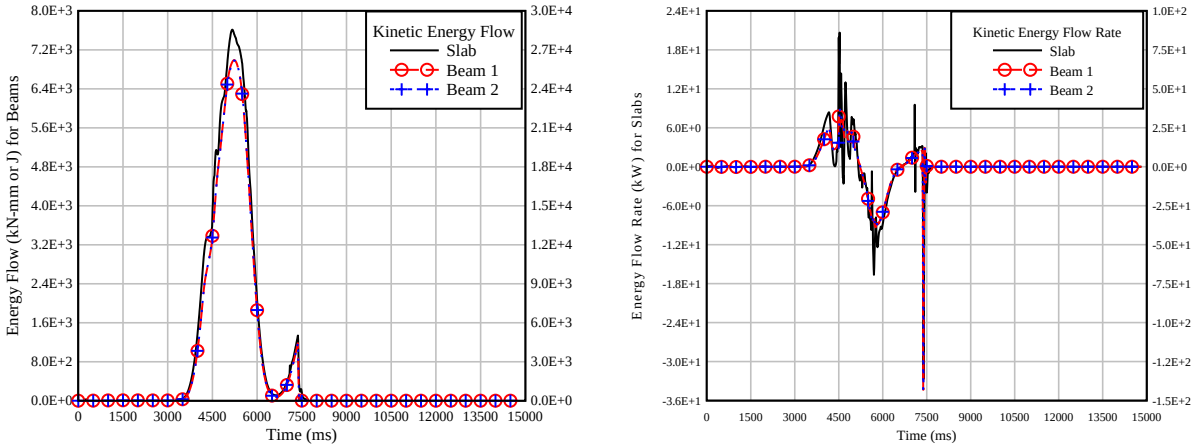

A B

Figure A-15. Kinetic energy-time histories of slab and failed beams. A) Energy flow as reported. B) Energy flow rate from differentiation

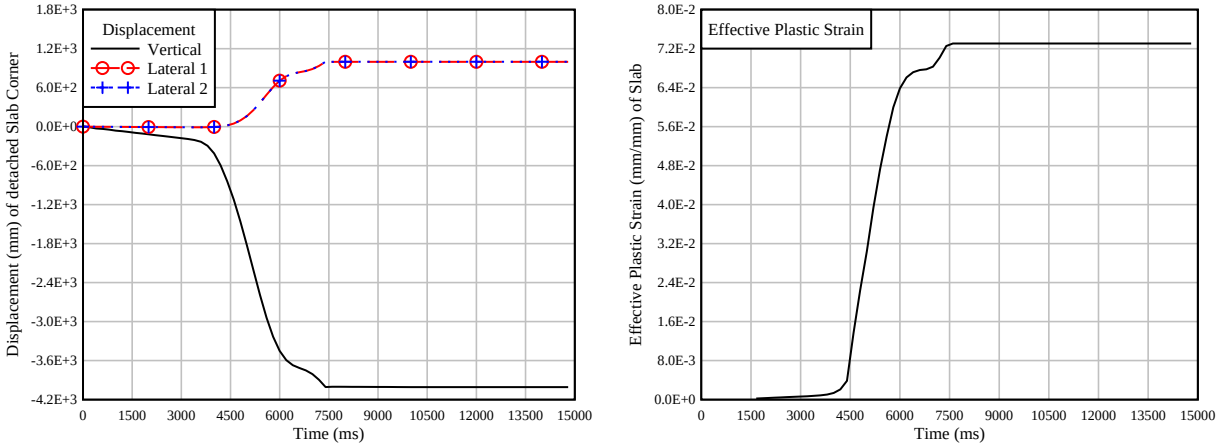

A B

Figure A-16. Example failure indicating criteria-time histories. A) Vertical displacement of the connection at the top of removed column. B) Plastic-strain at the center of slab adjoining the removed column

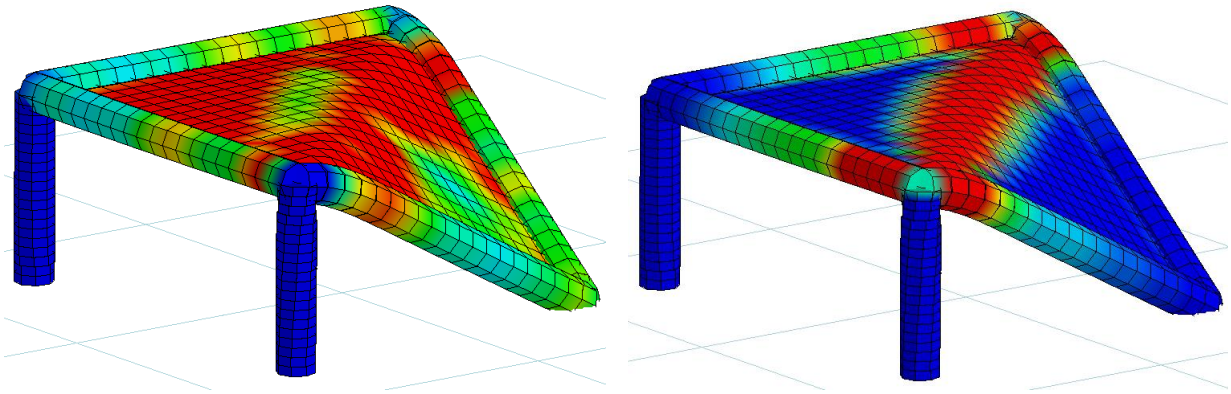

A B

Figure A-17. Stress and strain contours at the end of collapse. A) Effective (Von-Mises) stress. B) Effective plastic strain.

APPENDIX B
MID-RISE BUILDING DETAILS

B.1 Introduction

For potential reference, the following is provided to supplement the introduction of the ten-story, or nine-story with a single-story basement, SAC-commissioned building in Boston introduced in § 2.4. The structural system under consideration is a ten-story moment resisting frame established for seismic design research in response to the 1994 Northridge earthquake (FEMA, 2000). The structure is a typical moment resisting steel frame, with both shear and moment-resisting connections. Specifically, this building contains WUF-B type moment connections and single plate (shear tab) connections. This frame is considered representative of typical mid-rise steel moment resisting office buildings. The ten-story mid-rise or nine-story structural frame with single-story basement is presented below.

B.2 FEMA Specifications for the Mid-Rise Building in Boston

The following was extracted directly from Appendix B in "State of the Art Report on Systems Performance of Steel Moment Frames Subject to Earthquake Ground Shaking" (FEMA, 2000). The following description of the ten-story building in Boston is included along with the referenced figures and tables:

B.1 Description of Buildings and Basic Loading Conditions

As part of the SAC steel project, three consulting firms were commissioned to perform code designs for 3-, 9-, and 20-story model buildings, following the local code requirements for the following three cities: Los Angeles (UBC, 1994), Seattle (UBC, 1994), and Boston (BOCA, 1993). All prevailing code requirements for gravity, wind, and seismic design needed to be considered. The buildings were to be designed as standard office buildings situated on stiff soil (soil type S2 as per UBC '94 and BOCA '93 definitions).

The floor plans and elevations for the buildings were preset, as shown in Figure B-1. The shaded area indicates the penthouse location. Gravity frame columns are located only below the penthouse in the 20-story buildings, resulting in two bays of 40 feet bounding a 20-foot bay in the gravity frames. The column bases in the 3-story buildings are considered as fixed. The 9-story buildings have a single-level basement, and the 20-story buildings have a 2-level basement. The buildings were required to conform to a

drift limit of h/400, where "h" is the story height. The loading information provided was the following:

Steel framing:	as designed
Floors and Roof:	3 inch metal decking with 2.5 inches of normal weight concrete fill and fireproofing
Roofing:	7 psf average
Ceilings/Flooring:	3 psf average, including fireproofing
Mech./Electrical:	7 psf average for all floors, additionally 40 psf over penthouse area for equipment
Partitions:	as per code requirements (10 psf for seismic load, 20 psf for gravity design)
Exterior Wall:	25 psf of wall surface average, including any penthouses. Assume 2 feet from perimeter column lines to edge of building envelope. Include 42 inch parapet at main roof level, none at penthouse roof.
Live Load:	typical code values for office occupancy (50 psf everywhere)
Wind Load:	as per code requirements, assuming congested area (exposure B as per UBC '94 definition)
Seismic Load:	as per code requirements.

Based on this basic information, the consulting firms were asked to carry out three types of structural designs:

1. Pre-Northridge Designs: These designs were based on design practices prevalent before the Northridge earthquake, i.e., without consideration of the FEMA 267 (1995) document.
These designs had the standard beam-to-column welded connection details.

2. Post-Northridge Designs: These designs were to additionally conform to the provisions of FEMA 267 (1995). The designers decided on the use of cover-plated beam flanges in order to move the location of the plastic hinge in the beam away from the face of the column.

3. Special Designs: Two types of special designs were carried out for the 9-story post-Northridge structures in all three geographic locations. The first special design involved the use of reduced beam sections, while the other design involved the use of a higher strength steel (A913) for the columns.

Thus, the basic definitions for the buildings were kept constant between the different regions, but no other constraints concerning the design of the buildings (e.g., number of moment-resisting connections, choice of member sections, etc.) were imposed. The buildings so designed can be considered as being representative of typical steel moment frame structures in the three geographic locations, designed according to either pre- or post-Northridge design practice.

All three design offices selected perimeter moment-resisting frames as the structural system. In all cases the design of the moment frames in the two orthogonal directions was either identical or very similar, thus, only half of the structure is considered in the analysis. The ordinary difference between the NS and East-West (EW) direction comes from the difference in gravity load effects on account of the orientation of the gravity beams and sub-beams. Both the beams and sub-beams are oriented in the NS direction. However, as the gravity loading on the girders of the perimeter WSMFs is small and has almost negligible effect on the seismic response, the decision to analyze the structure only in the NS direction is justified.

The loading used for the analysis of the frames is based on the details given before, which result in the following floor load distribution (steel weight is assumed as 13 psf for all designs):

Floor dead load for weight calculations: 96 psf
Floor dead load for mass calculations: 86 psf
Roof dead load excluding penthouse: 83 psf
Penthouse dead load: 116 psf
Reduced live load per floor and for roof: 20 psf

Cladding and parapet loads are based on the surface area of the structures. Based on these loading definitions, the seismic mass for the structures is as follows (the values are for the entire structure):

…
9-story Structures:
Roof: 73.10 kips-sec^2/ft.
Floor 9 to Floor 3: 67.86 kips-sec^2/ft.
Floor 2: 69.04 kips-sec^2/ft.
…

The design details (member sections, doubler plates, design basis, etc.) for the different structures are summarized in the following sections.
…

B.4 Boston (BO) Structures

The placement of the MR connections in the 9-story structure is identical to the placement in the LA 9-story structure (see Figure B-2). The strong axis of the gravity frame columns is oriented in the NS direction. The design of … the 9- and 20-story structures are wind controlled designs. The member sections for the pre- and post-Northridge designs are given in Table B-7. A572 Gr. 50 steel has been used for both beams and columns in the Boston designs.

The dimensions for the cover plates used in the Boston post-Northridge designs are given in Table B-8. “T” stands for the thickness of the plates, and “L” for the length of the plates. The top cover plates have a width equal to “W1” at the face of the column, maintain this width for 2 inches from the column face, and then taper uniformly to a

width of “W2.” The bottom cover plate has a rectangular cross section with a width of “W.”

There are striking differences between the pre- and post-Northridge designs for Boston. Boston lies in seismic Zone 2A, thus the pre-Northridge designs are not required to comply with specific panel zone strength requirements or the strong column criterion, which are binding in seismic Zones 3 and 4. The post-Northridge designs, however, have to comply with both a minimum panel zone shear strength requirement as well as the strong column concept, in accordance with FEMA 267 (1995), thereby resulting in the use of significantly heavier column sections and extensive use of doubler plates.

Table B-7

PRE-NORTHRIDGE DESIGNS

NS Moment Resiting Frame

NS Gravity Frames

9-story Building

Story/Floor	COLUMNS		DOUBLER PLATES (in)	GIRDER	COLUMNS		BEAMS
	Exterior	Interior			Below penthouse	Others	
-1/1	W14X211	W14X283	0,0	W24X68	4-W14X145 & 2-W14X159	W14X145	W16X26
1/2	W14X211	W14X283	0,0	W36X135	4-W14X145 & 2-W14X159	W14X145	W16X26
2/3	W14X211, W14X159	W14X283, W14X233	0,0	W33X118	see note 3	W14X145, W12X120	W16X26
3/4	W14X159	W14X233	0,0	W30X116	4-W14X120 & 2-W14X132	W12X120	W16X26
4/5	W14X159, W14X132	W14X233, W14X211	0,0	W30X116	see note 4	W12X120, W14X90	W16X26
5/6	W14X132	W14X211	0,0	W30X108	4-W14X99 & 2-W12X106	W14X90	W16X26
6/7	W14X132, W14X99	W14X211, W14X176	0,0	W30X99	see note 5	W14X90, W12X65	W16X26
7/8	W14X99	W14X176	0,0	W27X94	6-W12X79	W12X65	W16X26
8/9	W14X99, W14X61	W14X176, W14X120	0,0	W24X76	see note 6	W12X65, W8X48	W16X26
9/Roof	W14X61	W14X120	0,0	W18X40	4-W12X53 & 2-W12X58	W8X48	W14X22

Notes:

1. Column line A has exterior column sections oriented about strong axis,
   Column line F has exterior column sections oriented about weak axis; W14X61 changes to W14X68
   Column lines B,C,D, and E have interior column sections
2. For the bay with only 1 MR connection the girder sections are (from Floor 1 to Roof) the following:
   W24X68, W27X94, W27X84, W27X84, W24X76, W24X76, W24X68, W24X62, W24X55, and W18X40
3. 4-W14X145 change at splice to 4-W14X120, 2-W14X159 change at splice to 2-W14X132
4. 4-W14X120 change at splice to 4-W14X99, 2-W14X132 change at splice to 2-W12X106
5. 4-W14X99 change at splice to 4-W12X79, 2-W12X106 change at splice to 2-W12X79
6. 4-W12X79 change at splice to 4-12X53, 2-W12X79 change at splice to 2-W12X58

General Notes

1. There are a total of 6 column lines below the penthouse for the 3- and 9-story buildings
2. For doubler plate thickess, the first number signifies the value for the exterior columns, the second for the interior columns
3. Splices are located 6 feet above the floor centerline in stories where 2 column sections are given (below splice, above splice)
4. 4-W14X99, 2-W12X106 signfies four columns of W14X99 and 2 columns of W12X106 below the penthouse

A

POST-NORTHRIDGE DESIGNS

NS Moment Resiting Frame

NS Gravity Frames

9-story Building

Story/Floor	COLUMNS		DOUBLER PLATES (in)	GIRDER	COLUMNS		BEAMS
	Exterior	Interior			Below penthouse	Others	
-1/1	W14X283	W14X500	0,0	W12X53	4-W14X145 & 2-W14X159	W14X145	W16X26
1/2	W14X283	W14X500	3/8,0	W33X141	4-W14X145 & 2-W14X159	W14X145	W16X26
2/3	W14X283, W14X257	W14X500, W14X455	3/8,3/8	W33X141	see note 3	W14X145, W12X120	W16X26
3/4	W14X257	W14X455	0,0	W21X101	4-W14X120 & 2-W14X132	W12X120	W16X26
4/5	W14X257, W14X211	W14X455, W14X398	3/8,0	W21X101	see note 4	W12X120, W14X90	W16X26
5/6	W14X211	W14X398	3/8,0	W21X101	4-W14X99 & 2-W12X106	W14X90	W16X26
6/7	W14X211, W14X159	W14X398, W14X311	1/2,7/16	W21X101	see note 5	W14X90, W12X65	W16X26
7/8	W14X159	W14X311	7/16,3/8	W18X97	6-W12X79	W12X65	W16X26
8/9	W14X159, W14X109	W14X311, W14X193	3/8,9/16	W16X67	see note 6	W12X65, W8X48	W16X26
9/Roof	W14X109	W14X193	3/8,3/8	W12X53	4-W12X53 & 2-W12X58	W8X48	W14X22

Notes:

1. Column line A has exterior column sections oriented about strong axis,
   Column line F has exterior column sections oriented about weak axis
   Column lines B,C,D, and E have interior column sections
2. For the bay with only 1 MR connection the girder sections are (from Floor 1 to Roof) the following:
   W12X53, W16X67, W16X67, W16X67, W16X67, W14X61, W12X58, W12X58, W12X53, W12X53
3. 4-W14X145 change at splice to 4-W14X120, 2-W14X159 change at splice to 2-W14X132
4. 4-W14X120 change at splice to 4-W14X99, 2-W14X132 change at splice to 2-W12X106
5. 4-W14X99 change at splice to 4-W12X79, 2-W12X106 change at splice to 2-W12X79
6. 4-W12X79 change at splice to 4-12X53, 2-W12X79 change at splice to 2-W12X58

General Notes

1. There are a total of 6 column lines below the penthouse for the 3- and 9-story buildings
2. For doubler plate thickess, the first number signifies the value for the exterior columns, the second for the interior columns
3. Splices are located 6 feet above the floor centerline in stories where 2 column sections are given (below splice, above splice)
4. 4-W14X99, 2-W12X106 signfies four columns of W14X99 and 2 columns of W12X106 below the penthouse

B

Figure B-1. Beam, sections, column sections, and doubler plates for three-story building in Boston. A) Pre-Northridge design. B) Post-Northridge design

Table B-8

TOP AND BOTTOM FLANGE COVER PLATE DETAILS

9-story Building

Girder Section		W33X141	W21X101	W18X97
Top Plate	T x W1 x W2 x L	1 x 11-1/2 x 5-1/2 x 20	13/16 x 12 x 6 x 14	7/8 x 11 x 5 x 12
Bottom Plate	T x W x L	1 x 13-1/2 x 20	11/16 x 14 x 14	3/4 x 13 x 12

Girder Section		W16X67	W12X58	W12X53
Top Plate	T x W1 x W2 x L	11/16 x 10 x 4 x 11	11/16 x 9-1/2 x 3-1/2 x 9	11/16 x 9-1/2 x 3-1/3 x 9
Bottom Plate	T x W x L	9/16 x 11-1/2 x 11	9/16 x 11-1/2 x 9	9/16 x 11-1/2 x 9

Figure B-2. Cover plate details for ten-story Boston building post-Northridge design

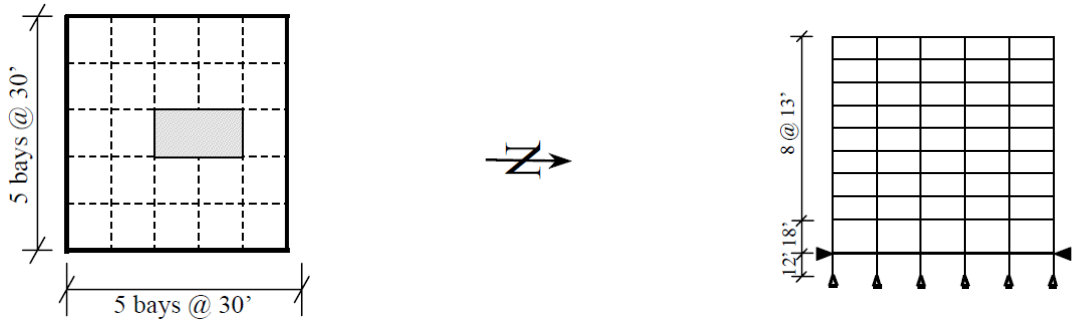

Figure B-3. Floor plan and elevation for ten-story Boston building

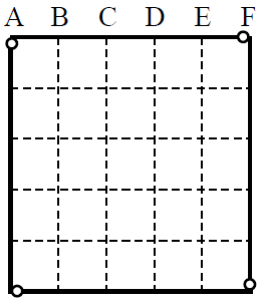

Figure B-4. Layout of moment-resisting connections in ten-story building

LIST OF REFERENCES

Adhikary, Satadru Das, Li, Bing, and Fujikake, Kazunori. (2013). "Strength and behavior in shear of reinforced concrete deep beams under dynamic loading conditions", *Nuclear Engineering and Design*, Vol. 259, pp. 14 – 28.

Allen, D. E., and Schriever, W. R. (1973). "Progressive Collapse, Abnormal Loads, and Building Codes", *National Research Council Canada*, Reprinted from ASCE National Meeting on Structural Engineering Proceedings, Cleveland, OH, (April 1972), pp. 21 – 47.

ACI. (2004). "Building Code Requirements for Structural Concrete (ACI 318-05) and Commentary", Farmington Hills, MI.

ASCE. (2002). "Minimum Design Loads for Buildings and Other Structures", *ASCE 7-02*, Reston, VA: ASCE.

ASCE. (2005). "Minimum Design Loads for Buildings and Other Structures", *ASCE 7-05*, Reston, VA: ASCE.

ASCE. (2008). *ASCE-31 and ASCE-41: What Good Are They?*, Structures 2008: Crossing Borders, 8 p. Reston, Virginia: ASCE.

ASCE. (2010). *Design of Blast-Resistant Buildings in Petrochemical Facilities 2nd Edition*, ASCE Task Committee on Blast-Resistant Design, Reston, VA: ASCE, 158 p.

ASCE. (2011a). Blast Protection of Buildings, *SEI/ASCE 59-11*, Reston, VA: ASCE.

ASCE. (April 2011b). *Recommendations for Design and Disproportionate Collapse of Structures* Draft, Terminology and Procedures Sub-Committee, Disproportionate Collapse Standards and Guidance Committee, Structural Engineering Institute (SEI) ASCE Standard 59-11, Reston, VA: ASCE.

Arup (2011). *Review of International Research on Structural Robustness and Disproportionate Collapse*, Department for Communities and Local Government (DCLG) and Centre for the National Protection of Infrastructure (CPNI) 200 p.

Astarlioglu S., and Krauthammer T., (2012). *Dynamic Structural Analysis Suite (DSAS) User Manual Version 4*, Center for Infrastructure Protection and Physical Security (CIPPS), University of Florida, Gainesville, Fla, 37 p.

Azimi, Mohammadamin, Bin Adnan, Azlan, Osman, Mohd Hanim, Bin Mohd Sam, Abdul Rahman, Faridmehr, Iman, and Hodjati, Reza. (2014). "Energy Absorption Capacity of Reinforced Concrete Beam-Column Connections, with Ductility Classes Low", *American Journal of Civil Engineering and Architecture*, Vol. 2, No. 1, pp. 42 – 52.

Baker, John Fleetwood, Williams, Edward Leader, and Lax, Douglas. (1948). "The Design of Framed Buildings against High-Explosive Bombs", The Civil Engineer in War, 3, pp. 80 – 112.

British Steel plc. (1999). The Behaviour of Multi-Storey Steel Framed Buildings in Fire, Swinden Technology Centre (STC), South Yorkshire, UK: British Steel plc STC, 82 p.

Burnett, E. F. P. and Leyendecker, E. V. (1973). Residential Buildings and Gas-Related Explosions, NBSIR 73-208, Center for Building Technology, NBS, Washington, D.C.

Byfield, Michael, Mudalige, Wsesundara, Morison, Colin, and Stoddart, Euan. (August 2014). *A review of progressive collapse research and regulations*, Proceedings of the Institute of Civil Engineers (ICE) Structures and Buildings 167, Issue SBB, pp. 447 – 456.

Committee, F. O., Board, O. I. S., & Commission, O. E. S. (2000). Blast Mitigation for Structures: 1999 Status Report on the DTRA/TSWG Program, Washington, DC, USA: National Academies Press, retrieved from http://www.ebrary.com.

Corley, W. G., Mlakar Sr., P. F., Sozen, M. A., and Thornton, C. H. (1998). "The Oklahoma City Bombing: Summary and Recommendations for Multi-hazard Mitigation", *Journal of Performance of Constructed Facilities*, Vol. 12, No. 3, August, pp. 100 – 112, Reston, VA: ASCE.

Corley, W. Gene. (2002). Applicability of Seismic Design in Mitigating Progressive Collapse, National Institute of Standards and Technology (NIST) Workshop, 13 p, Skokie, IL: Construction Technology Laboratories (CTL).

Cormie, David, Geoff, Mays, and Smith, Peter. (2009). *Blast Effects on Buildings 2nd Edition*, 40 Marsh Wall, London E14 9TP: Thomas Telford Limited.

Crawford, J. E., Malvar, L. J., Morrill, K. B., and Ferritto, J. M. (May 2001a). Composite Retrofits to increase the blast resistance of reinforced concrete buildings, Proceedings of the 10th International Symposium on Interaction of the Effects of Munitions with Structures, San Diego, CA.

Crawford, John E. (2001b). Retrofit Methods to Mitigate Progressive Collapse, Karagozian & Case (K&C) Structural Engineers, 55 p, Glendale, CA: K&C.

Crowder, Brian. (2005). Progressive Collapse – Historical Perspective, Naval Facilities Engineering Command (NAVFAC), Seminar Presentation, 30 slides.

Culver, Charles G. (1976). Live-Load Survey Results for Office Buildings, Journal of the Structural Division, Vol. 102, Issue 12, pp. 2269 – 2284, Washington D.C.: ASCE, National Bureau of Standards (NBS), Center for Building Technology, Disaster Research Program.

Daily Mail Pictures. (2011). Photo: A view of the Kansallis House in Bishopsgate in the City of London which was damaged when an IRA bomb rocked the city, Daily Mail, Archived Images Picture Collection, http://mailpictures.newsprints.co.uk/view/19064000/elib_assc-mmglpict000005171717_jpg.

DOD. (2000). *DOD Minimum Antiterrorism Standards for Buildings UFC 4-010-01 Interim*, DOD, Washington, D.C.

DOD. (2001). *Interim Antiterrorism/Force Protection Construction Standards – Progressive Collapse Design Guidance*, Department of Defense (DOD) Washington, DC.

DOD. (2003). *Design of Buildings to Resist Progressive Collapse - Unified Facilities Criteria UFC 4-023-03*, DOD, 176 p.

DOD. (2007). *DOD Minimum Antiterrorism Standards for Buildings UFC 4-010-01*, DOD, Washington, D.C., 71 p.

DOD. (2009). *Design of Buildings to Resist Progressive Collapse - Unified Facilities Criteria UFC 4-023-03*, DOD, 181 p.

DOD. (2013a). *DOD Minimum Antiterrorism Standards for Buildings UFC 4-010-01*, DOD, Washington, DC, 111 p.

DOD. (2013b). *Design of Buildings to Resist Progressive Collapse - Unified Facilities Criteria UFC 4-023-03*, DOD, 245 p.

Dusenberry, Donald O., and Juneja, Gunjeet. (2003). Review of Existing Guidelines and Provisions Related to Progressive Collapse, Multi-hazard Mitigation Council of the National Institute of Building Standards, Washington, D.C. p. 1 – 31.

Dusenberry, D. O., and Hamburger, R. O. (2006). Practical means for energy- and power-based Analysis of Disproportionate Collapse Potential, *Journal of Performance of Constructed Facilities*, Vol. 20, No. 4, pp. 336 – 348.

Dusenberry, Donald O. (2010). *Handbook for Blast-Resistant Design of Buildings*, John Wiley & Sons, Inc., Hoboken, New Jersey, 484 p.

Ellingwood, B. R., and Culver, C. G. (August 1977). Analysis of Live Loads in Office Buildings, Journal of the Structural Division, Volume 103, Issue 8, pp. 1551 – 1560, Reston, VA: ASCE.

Ellingwood, B. R. and Dusenberry, D. O. (2005). Building Design for Abnormal Loads and Progressive Collapse, *Computer-Aided Civil and Infrastructure Engineering*, Vol. 20, pp. 194 – 205.

Ellingwood, Bruce R. (2006). Mitigating Risk from Abnormal Loads and Progressive Collapse, *Journal of Performance of Constructed Facilities*, Vol. 20, pp. 315 – 323, Reston, VA: ASCE.

Ellingwood, Bruce R. (September, 18, 2007). Assessment and Mitigation of Risk from Competing Low-Probability, High-Consequence Hazards, Symposium on Emerging Developments in Multi-Hazard Engineering, 4 p, Atlanta, GA: Georgia Institute of Technology.

Ellingwood, Bruce R., Smilowitz, Robert, Dusenberry, Donald O., Duthinh, Dat, and Carino, Nicholas J. (2007). Best Practices for Reducing the Potential for Progressive Collapse in Buildings, National Institute of Standards and Technology (NIST), NISTIR 7396, 216 p.

Engelhardt, M. D. and Sabol, T. A. (1994). "Testing of Welded Steel Moment Connections in Response to the Northridge Earthquake", Progress Report to the AISC Advisory Subcommittee on Special Moment Resisting Frame Research, Austin, Texas: University of Texas, Austin.

Ettouney, Mohammed. (04-05 December 2003). Assessing and Mitigating Threats to Buildings, Steel Building Symposium: Blast and Progressive Collapse Resistance, AISC and The Steel Institute of New York (SINY), AISC: United States of America (US), pp. 87 – 95, 114 p.

FEMA and ASCE. (1996). "The Oklahoma City Bombing: Improving Building Performance through Multi-Hazard Mitigation", *FEMA Rep. 277*, ASCE and FEMA, Washington, D.C.

FEMA. (September 2000). FEMA-355C, State of the Art Report on Systems Performance of Steel Moment Frames Subject to Earthquake Ground Shaking, SEAOC, ATC, and CUREe Joint Venture (SAC JV) and FEMA, Washington DC: 344 p.

FEMA. (December 2003a). FEMA 426, Reference Manual to Mitigate Potential Terrorist Attacks Against Buildings, Risk Management Series, Washington, D.C.: FEMA, 420 p.

FEMA. (December 2003b). FEMA 427, Primer for Design of Commercial Buildings to Mitigate Terrorist Attacks, Risk Management Series, Washington, D.C.: FEMA, 108 p.

FEMA and DHS. (November 2010). "Blast-Resistance Benefits of Seismic Design – Phase 2 Study: Performance Analysis of Structural Steel Strengthening Systems", National Earthquake Hazards Red Program, *FEMA P-439B*, DHS and FEMA, Washington, D.C.

Foley, C.M., Schneeman, C., and Barnes, K. (2008). Quantifying and Enhancing the Robustness in Steel Structures: Part I—Moment-Resisting Frames, Engineering Journal, Fourth Quarter, pp. 247 – 266.

GSA. (2000). *Progressive Collapse Analysis and Design Guidelines for New Federal Office Buildings and Major Modernization Projects*, Office of Chief Architect, General Services Administration, Washington, D. C.

GSA. (2003). *Progressive Collapse Analysis and Design Guidelines for New Federal Office Buildings and Major Modernization Projects*, Office of Chief Architect, General Services Administration, Washington, D. C., 119 p.

GSA. (24 October 2013). *Alternate Path Analysis & Design Guidelines for Progressive Collapse Resistance*, General Services Administration, Washington, D. C., 143 p.

Ghosh, S. K. (2014). Treatment of Progressive Collapse in US Codes and Standards – Part 2/2: An overview about fib and PCI strategies, Precast Concrete Elements, Concrete Plant International (CPI), www.cpi-worldwide.com, pp. 138 – 150.

Gupta, A., and Krawinkler, H. (2000). "Behavior of ductile SMRFs at various seismic hazard levels", Journal of Structural Engineering Vol. 126, No. 1, pp. 98 – 107.

Haberland, Marco, and Starossek, Uwe. (2009). Progressive Collapse Nomenclature, Structures 2009: Don't Mess with Structural Engineers, ASCE, pp. 1886 – 1895.

Hallquist, John O. (17 May 2014). *LS-DYNA® Keyword User's Manual: Volumes I, II, and III LS-DYNA R7.1*, Livermore Software Technology Corporation, Livermore (LSTC), Livermore, California, 2281 p., 1265 p., and 183 p.

Hyde, David. (1988). User's Guide for Microcomputer Program ConWep, Applications on TM 5-855-1, Fundamentals of Protective Design for Conventional Weapons, Revised February 22, 1993, Instruction Report SL-88-1, Structures Laboratory, Waterways Experiment Station, Corps of Engineers, Department of The Army, Vicksburg, MS: Dept. of The Army, 30 p.

Jones, Norman. (1997). Structural Impact, Cambridge, U.K.: Cambridge University Press, 573 p.

Kirby, B. R. (1997). Large Scale Fire Tests: the British Steel European Collaborative Research Programme on the BRE 8-Storey Frame, British Steel PLC, Swinden Technology Centre, International Association for Fire Safety Science (IAFSS), Fire Safety Science – Proceedings of the Fifth International Symposium, England, UK: IAFSS, pp. 1129 – 1140.

Koh, Y. H., Krauthammer, T., and Bui, L. (2011). "Characterizing A Reinforced Concrete Beam-Column-Slab connection and its Implementation for Progressive Collapse Assessment", Final Report to U.S. Army ERDC, CIPPS-TR-0111-2011, CIPPS, UF, Gainesville, FL: UF Press, 212 p.

Krauthammer, T., Lim, J., Choi, H. J., and Elfahal, M. (2004a). *Evaluation of Computational Approaches for Progressive Collapse and Integrated Munitions Effects Assessment*, Protective Technology Center, Pennsylvania State University, PTC-TR-002-2004.

Krauthammer, Theodor, Lim, Joonhong, Yim, Hyun Chang, and Elfahal, Motaz. (2004b). *Three Dimensional Steel Connections Under Blast Loads*, Protective Technology Center, Penn State University, PTC-TR-004-2004.

Krauthammer, T. and Cipolla, J. (2007a). Building Blast Simulation and Progressive Collapse Analysis, National Agency for Finite Element Methods and Standards (NAFEMS) World Conference Proceedings, 11 p.

Krauthammer, Theodor, Yim, Hyun Chang, Astarlioglu, Serdar, Starr, Craig, and Lim, Joonhong. (2007b). "Blast-Induced Response of Moment Connections," ASCE Structures Congress, Structural Engineering Research Frontiers, 15 p.

Lennon, T. (February 2004). Client Report: Results and observations from full-scale fire test at Building Research Establishment (BRE) Cardington, 16 January 2003, Client report number 215-741, Cardington, UK: BRE Ltd., 63 p.

Lim, J., and Krauthammer, T. (2006). "Progressive Collapse of 2-D Steel-Framed Structures with Different Connection Models", *Engineering Journal* (Third Quarter) pp. 201 – 215.

Loizeaux, Mark, and Osborn, Andrew E. N. (2007). "Progressive Collapse—An Implosion Contractor's Stock in Trade", *Journal of Performance of Constructed Facilities*, pp 391 – 402, Reston, VA: ASCE.

Longinow, A., and Ellingwood, B. R. (1998). *The Impact of The Ronan Point Collapse—25 years after*, Structural Engineering World Wide 1998, Paper Reference Elsevier Science, New York, pp 312 – 2.

Malvar, L. J. (1998). "Review of static and dynamic properties of steel reinforcing bars", *ACI Materials Journal*, Vol. 95, No. 5, pp. 609 – 616.

Malvar, L. J., and Ross, C. J. (1998). "Review of static and dynamic properties of concrete in tension", *ACI Materials Journal*, Vol. 95, No. 6, pp. 735 – 739.

Marchand, K., Williamson, E., and Stevens, D. (2008a). "SEI pre-standard and commentary on disproportionate collapse: Part I – risk and applicability determination for disproportionate collapse", IABSE Congress Chicago.

Marchand, K., Williamson, E., and Stevens, D. (2008b). "SEI pre-standard and commentary on disproportionate collapse: Part II – prescriptive approaches to provide robustness", IABSE Congress Chicago.

Marjanishvili, S. M. (2004). "Progressive Analysis Procedure for Progressive Collapse", *Journal of Performance of Constructed Facilities*, Vol. 18, No. 2, pp. 79 – 85.

Marjanishvili, S. M., and Agnew, Elizabeth. (2006). "Comparison of Various Procedures for Progressive Collapse Analysis", *Journal of Performance of Constructed Facilities*, Vol. 20, No. 4, pp. 365 – 374.

Martin, Rachel and Delatte, Norbert J. (2000). *Another Look at the L'Ambiance Plaza Collapse*, A, Vol. 19, No. 2, pp. 172 – 177.

McGuire, R. K., and Cornell, C. A. (July 1974). "Live Load Effects in Office Buildings", *Journal of the Structural Division*, Volume 100, Issue 7, pp. 1351 – 1366, Washington D.C.: ASCE.

McKay, Aldo, Marchand, Kirk, and Diaz, Manuel. (2012). "Alternate Path Method in Progressive Collapse Analysis: Variation of Dynamic and Nonlinear Load Increase Factors", *Practice Periodical on Structural Design and Construction*, Vol. 17, pp. 152 – 160, Reston, VA: ASCE.

Mitchell, G. R., and Woodgate, R. W. (1971). Floor Loadings in Office Buildings—the results of a survey current paper 3/71, Watford, England: Building Research Station.

Mlakar Sr., P. F., Corley, W. G., Sozen, M. A., and Thornton, C. H. (1998). "The Oklahoma City Bombing: Analysis of Blast Damage to the Murrah Building", *Journal of Performance of Constructed Facilities*, Vol. 12, No. 3, August, pp. 113 – 119, Reston, VA: ASCE.

Nair, R. Shankar. (2004). "Progressive Collapse Basics", *Modern Steel Construction*, Vol. 44, No. 3, March, pp. 37 – 42.

Nair, R. Shankar. (2006). "Preventing Disproportionate Collapse", *Journal of Performance of Constructed Facilities*, Vol. 20, pp. 309 – 314.

Nassr, Amr A., Razaqpur, A. Ghani, Tait, Michael J., Campidelli, Manuel, and Foo, Simon. (2013). "Strength and stability of steel beam columns under blast load", *International Journal of Impact Engineering*, Vol. 55, pp. 34 – 48.

NBCC. (1970). Canadian Structural Design Manual, Supplement No. 4 Publication Number NRC 11530 of the National Research Council of Canada, Ottawa, Canada.

NBCC. (1975). Canadian Structural Design Manual, Supplement No. 4 Publication No. NRC 13989 of the National Research Council of Canada, Ottawa, Canada.

NIST. (September 2005). Final report on the collapse of the World Trade Center Towers, NIST, Gaithersburg, MD.

Osteraas, J. D. (2006). "Murrah Building Bombing Revisited: A Qualitative Assessment of Blast Damage and Collapse Patterns", *Journal of Performance of Constructed Facilities*, Vol. 20, No. 4, pp. 330 – 335.

Ožbolt, Joško, Sharma, Akanshu, and Reinhardt, Hans-Wolf. (2011). "Dynamic fracture of concrete – compact tension specimen", *International Journal of Solids and Structures*, Vol. 48, pp. 1534 – 1543.

Pearson, C. and Delatte, N. (2005). Ronan Point Apartment Tower Collapse and its Effect on Building Codes, Civil and Environmental Engineering Faculty Publications, Cleveland State University and *Journal of Performance of Constructed Facilities*, Reston, VA: ASCE, Vol. 19, No. 2, pp. 172 – 177.

Polman, Dick. (18 April 18 2013). Boston Bombing: Memories of London From Early 1990s, The Contributor, Cagle Cartoons, Philadelphia, PA: NewsWorks/WHYY.

Robertson, Leslie E., and Naka, Takeo. (1980). Tall Building Criteria and Loading, American Society of Civil Engineers (ASCE), Monograph on the Planning and Design of Tall Buildings, Committee 5 (Gravity Loads and Temperature Effects) of the Council on Tall Buildings and Urban Habitat, New York, NY: ASCE, Vol. CL, 900 p.

Smith, P. P., Byfield, M. P., Goode, D. J. (2010). "Building Robustness Research during World War II", *Journal of Performance of Constructed Facilities*, Vol. 24, pp. 529 – 535, ASCE: Reston, VA.

Smythe, Andrew W., and Gjelsvik, Atle. (2006). "Energy Capacity Criterion for the Design of Columns against Collapse", *Journal of Engineering Mechanics*, Vol. 132, ASCE: Reston VA, pp. 594 – 599.

Starossek, Uwe, and Haberland, Marco. (11 March 2010). "Approaches to measures of structural robustness", *Structure and Infrastructure Engineering, First* article pp. 1 – 7.

Stevens, David, Martin, Eric, Williamson, Eric, McKay, Aldo, and Marchand, Kirk. (2012). Recent Developments in Progressive Collapse Design, Protection Engineering Consultants, San Antonio, TX, 10 p.

Surahman, Adang. (2007). "Earthquake-resistant structural design through energy demand and capacity", *Earthquake Engineering and Structural Dynamics*, 19 p. John Wiley and Sons, Ltd.

Systems. (May 1968). "Systems Built Apartments Collapse" *Engineering News-Record*, May 23, 1968, p. 23.

Szyniszewski, S. (2009). "Progressive Collapse of Moment Resisting Steel Framed Buildings Quantitative Based Energy Approach", PhD Dissertation, 291 p, Civil and Coastal Engineering, ESSIE, School of Engineering, UF: Gainesville, FL: UF Press.

Szyniszewski, S., and Krauthammer, T. (2012). "Energy flow in progressive collapse of steel framed buildings", *Engineering Structures*, Vol. 42, pp. 142 – 153.

Tavakoli, H. R., and Alashti, A. Rashidi. (2012). "Evaluation of progressive collapse potential of multi-story moment resisting steel frame buildings under lateral loading", *Scientia Iranica Transactions A: Civil Engineering*, Sharif University of Technology, Vol. 20, No. 1, pp. 77 – 86.

Taylor, D. A. (1975). Progressive Collapse, Building Structures Section, Division of Building Research, National Research Council of Canada, Ottawa, Canada, pp 517 – 529.

Tsai, Ying-kuan. (2015). Energy Based Load-Impulse Diagrams for Structural Elements, PhD Dissertation, 200 p, Civil and Coastal Engineering, ESSIE, School of Engineering, UF: Gainesville, FL: UF Press.

Tsai, Ying-kuan, and Krauthammer, Ted. (2015). Energy- and power-based Load-Impulse Diagrams for Structural Elements, Fifth International Conference on Design and Analysis of Protective Structures (DAPS2015) Furama Riverfront, Singapore, CIPPS, UF.

UFC. (01 June 2013). UFC 4-023-03 Design of Buildings to Resist Progressive Collapse, Department of Defense, 245 p.

Unknown. (02 November 1966). 12 Missing in Rubble: Building Collapse Traps Scot Workers, *Saint Petersburg Times*, Saint Petersburg, FL, p. 11-A, http://news.google.com/newspapers?id=DfxRAAAAIBAJ&sjid=QnQDAAAAIBAJ&pg=3564%2C493197.

Wilkes, John. (2002). Development of a Low-Profile Barrier for Curved Alignments Using Impact Finite Element Simulation, Master of Engineering Thesis, UF, School of Engineering, Civil and Coastal Engineering, UF: Gainesville, FL: UF Press, 41 p.

Wilkes, John R., and Smith, M. (September 2015) Progressive Collapse of a Ten Story Reinforced Concrete Building, Center for Infrastructure Protection and Physical Security (CIPPS), CIPPS-TR-003-2015, University of Florida, 83 p.

Wilkes, John R., and Krauthammer, Theodor. (2016) An Energy Flow Methodology for Progressive Collapse, Center for Infrastructure Protection and Physical Security (CIPPS), CIPPS-TR-003-2016, University of Florida.

Wright, Richard, Kramer, Samuel, and Culver, Charles. (1973). Building Practices for Disaster Mitigation, U.S. Department of Commerce, NBS, Building Science Series (46) 474 p.

Yim, Hyun Chang. (2007). A Study of Steel Moment Connections for Structures Under Blast and Progressive Collapse Loading Rates, PhD Dissertation, 156 p, Civil and Coastal Engineering, ESSIE, School of Engineering, UF: Gainesville, FL: UF Press.

Yim, H.C., and Krauthammer, T. (January 2007). Studies of Structural Steel Moment Connections Behavior Under Blast and Progressive Collapse, and the Development of Simplified Models for their Numerical Simulation, *Final Report to U.S. Army ERDC, CIPPS-TR-001-2007*, CIPPS, UF.

Yim, H.C., and Krauthammer, T. (May 2009). Effects of Connection Behavior on Progressive Collapse of Steel Moment Frames, Proceedings of 13th International Symposium on the Interaction of the Effects of Munitions with Structures (ISIEMS), Bruehl, Germany, 17 p.

Yim, Hyun Chang, and Krauthammer, Ted. (2010). "Mathematical-Mechanical Model of WUF-B Connection Under Monotonic Load", *Engineering Journal*, 2nd quarter, pp 71 – 90.

Yim, Hyun Chang, and Krauthammer, Ted. (June 2012). Mechanical Models of Steel Connections for Progressive Collapse Analysis", Proceedings of Fourth International Conference on Design and Analysis of Protective Structures (DAPS) Jeju, South Korea.

BIOGRAPHICAL SKETCH

John Robert Wilkes has received a diploma from Palatka High School (1995), a Bachelor of Science in engineering from Tulane University (1999), and a Master of Engineering from University of Florida (2002). The author studied biomedical engineering, mechanical engineering, and kinesiology during his undergraduate tenure and structural engineering graduate tenure. His undergraduate research included a study of the effects of prophylactic knee braces on gait and the design of a lift system for an individual with 20% r.o.m. of a non-dominant arm. He graduate research during his master's studies entailed the development of a low-profile barrier for the Florida Department of Transportation using numerical simulations of vehicle-barrier impact events—resulting in U.S. Patent 6767158. After consulting as a Professional Engineer for nearly a decade in over twenty states and in several countries abroad, John returned to the University of Florida in 2011 to earn a doctorate with a research focus on the numerical modeling of events for purposes of protecting against extreme loading scenarios. Under the direction of Professor Ted Krauthammer, he has earned a certificate in Critical Infrastructure Protection and will graduate in August 2016, where he will continue his career at Sandia National Laboratories.